Planetary Bow Shocks and Foreshocks in the Solar System

Christian Mazelle

IRAP, CNRS - University Paul Sabatier – CNES, Toulouse, France

Kinetic physics of astrophysical plasmas, Paris, 18-20 June 2025

Shocks in Space

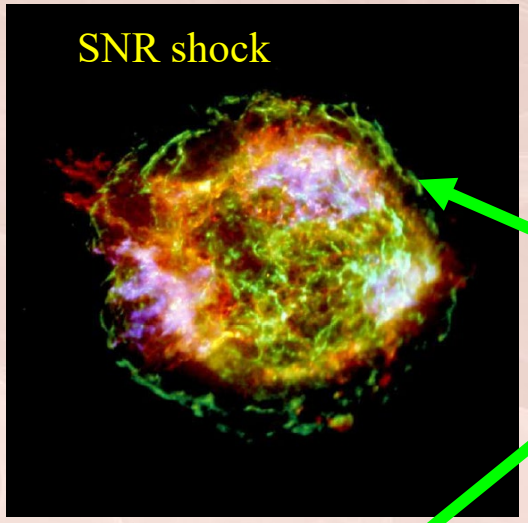

(*collisional* shocks).
fluid shocks, etc.

(*collisionless* shocks).
Supernova Remnant shock ,
interstellar bow shock,
heliospheric termination shock,
interplanetary shocks,
CME-driven shock,
planetary bow shock, etc.

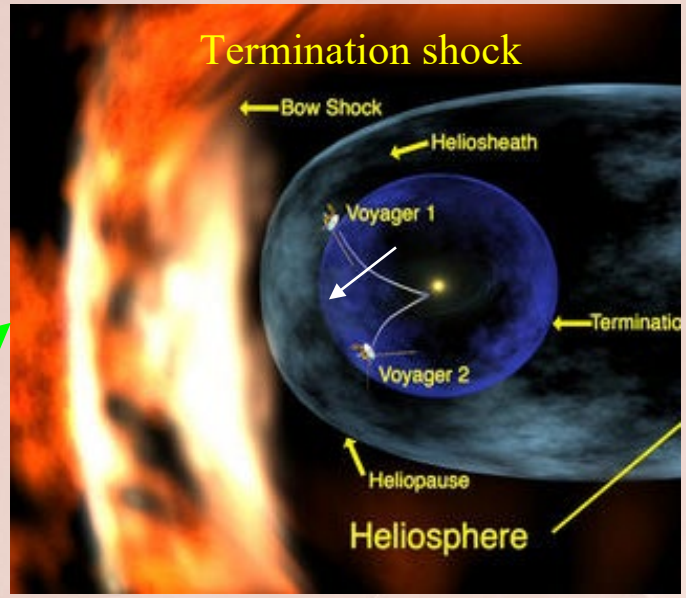

Efficient particle accelerators

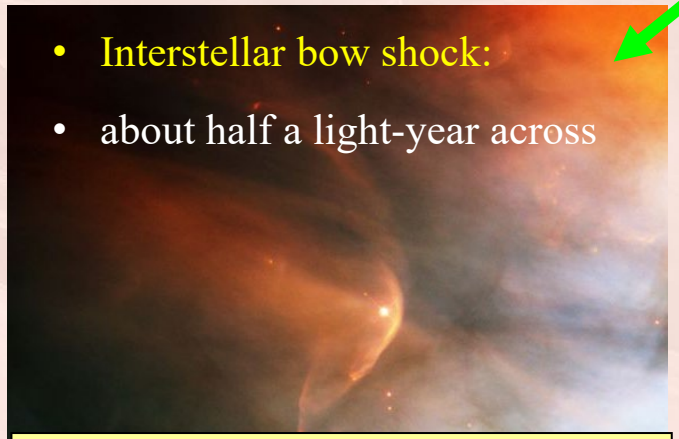

- Interstellar bow shock:
- about half a light-year across

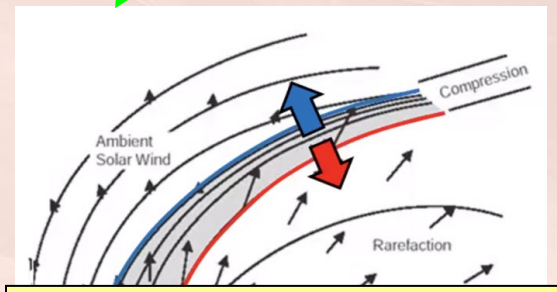

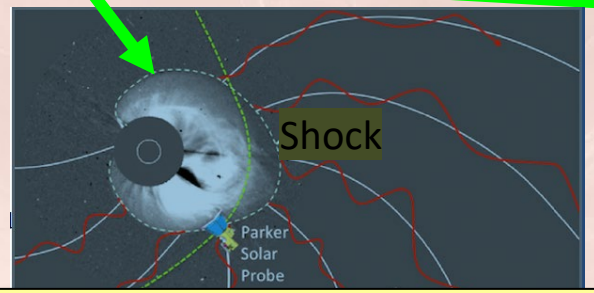

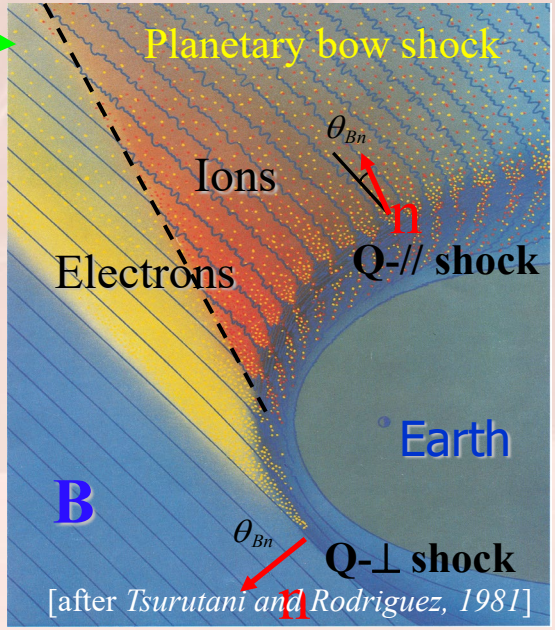

***collisionless* :**

- Highly tenuous media
- Scales much larger than collision mean free path of the particles

No sound in Space !

- But electrically charged particles (electrons, ions) and elecromagnetic fields (space plasmas): Pressures.
- Characteristic wave speed for plasma perturbations: Alfvenic and Magnetosonic (slow and fast) for compressive waves.

Shocks:

- Nonlinear steepening
- Dissipation, irreversibility (production of entropy)
- Converting flow energy to thermal (particle heating)

How to do that without collisions?

- Wave dispersion
- Instabilities
- Particle reflection
- Particle acceleration

Terrestrial bow shock

Bow shock and Foreshock: terrestrial 'paradigm'

Fast magnetosonic shock: $M_f > 1$

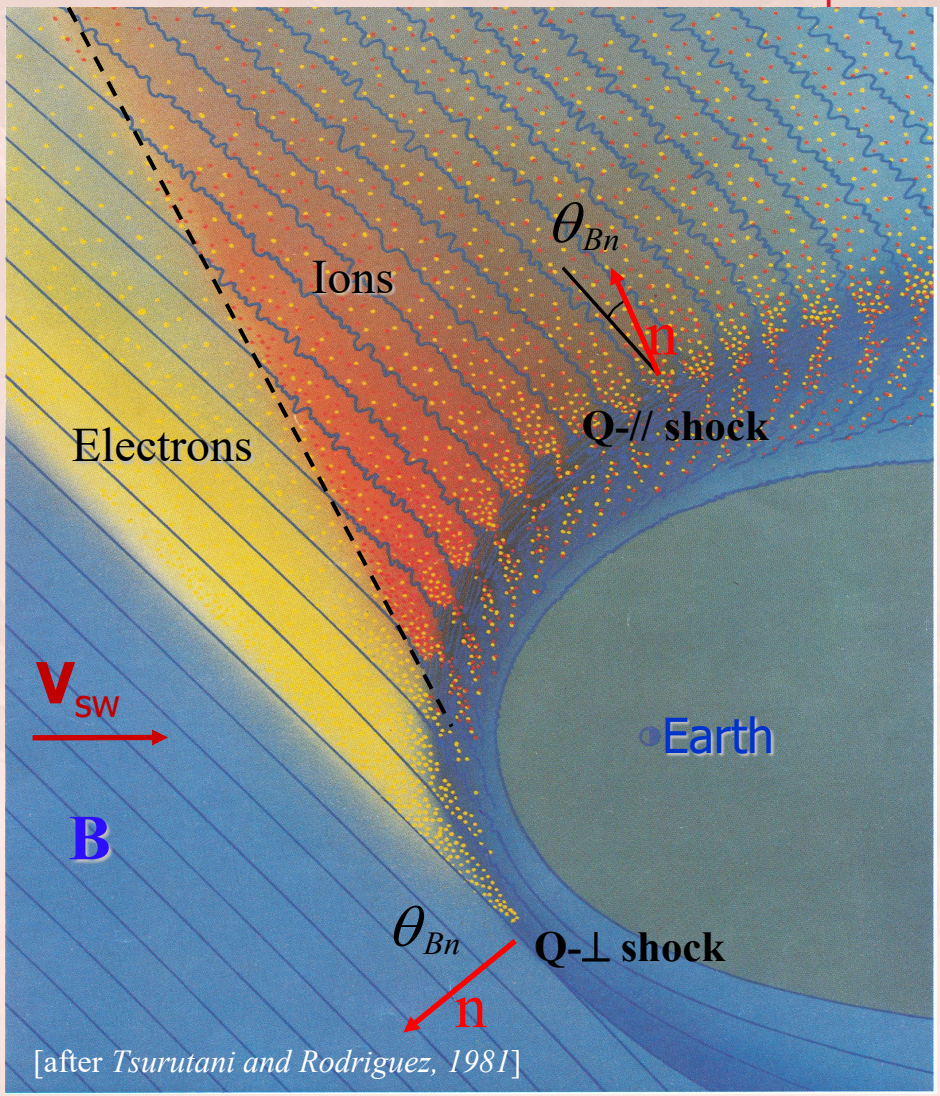

- θ_{Bn} : second main parameter after Mach number
- Q-⊥ and Q-$_{//}$: very different

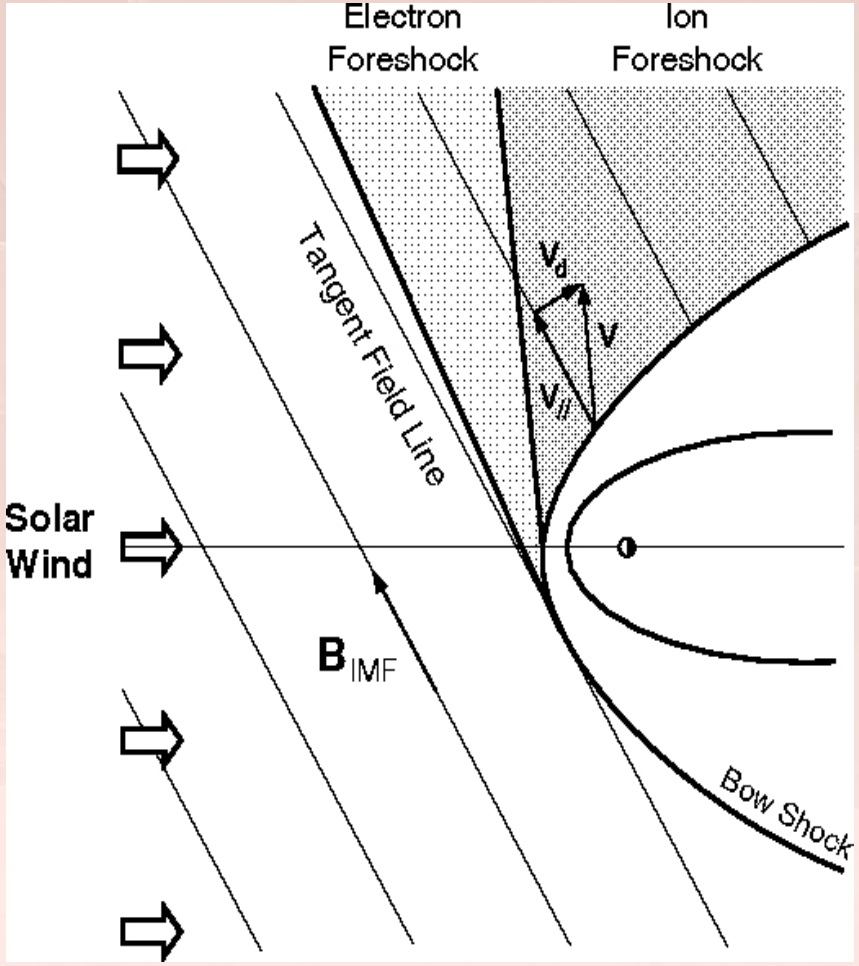

Bow shock and Foreshock: terrestrial 'paradigm'

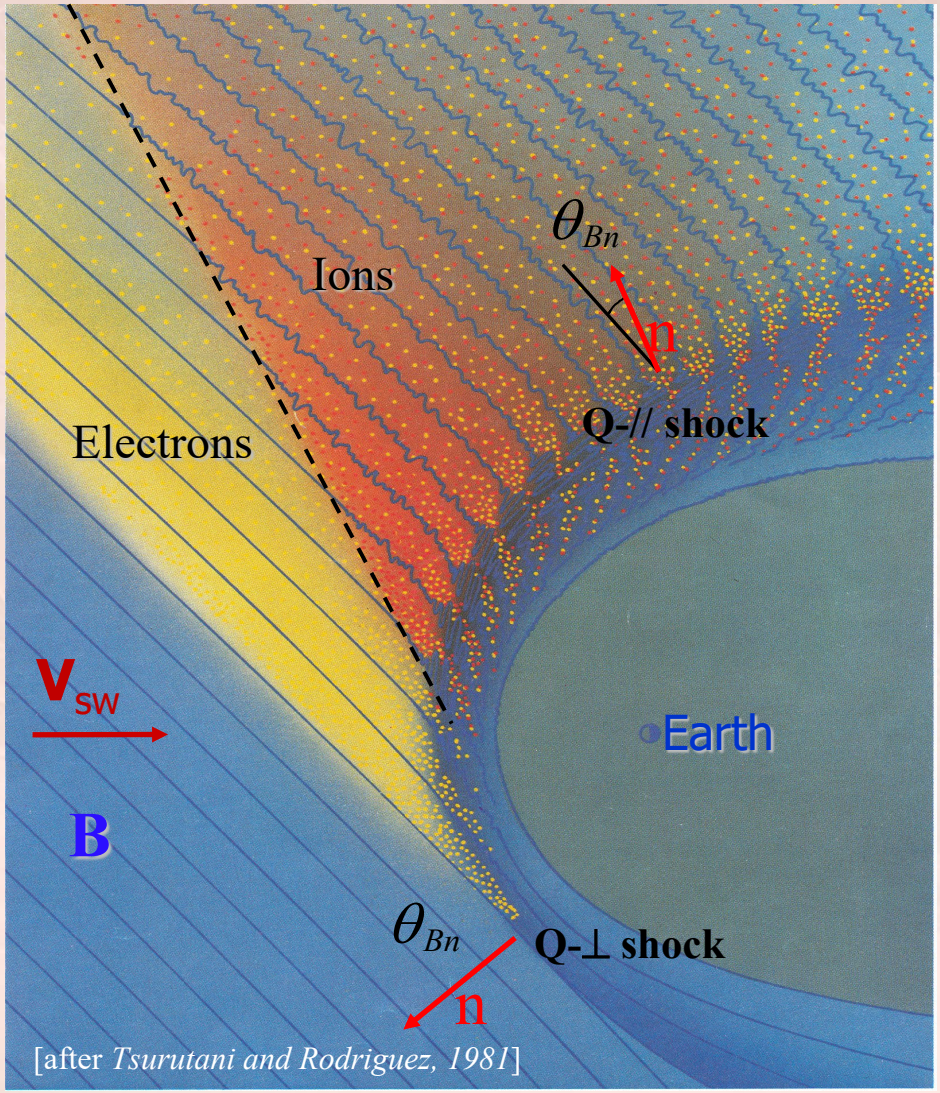

- θ_{Bn} : Q-⊥ and Q-$_{//}$: very different for ion reflection and upstream characteristics.

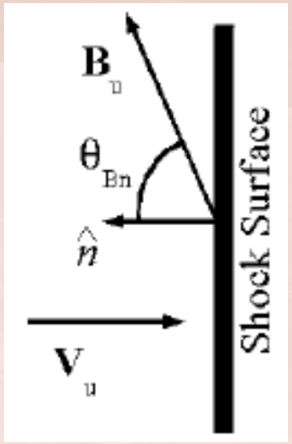

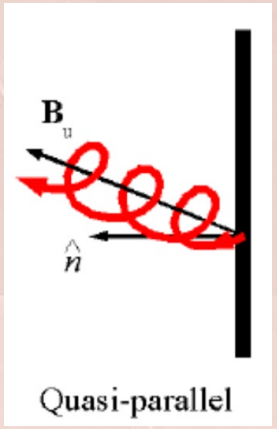

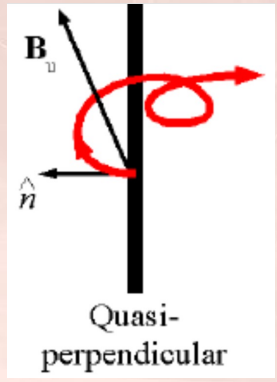

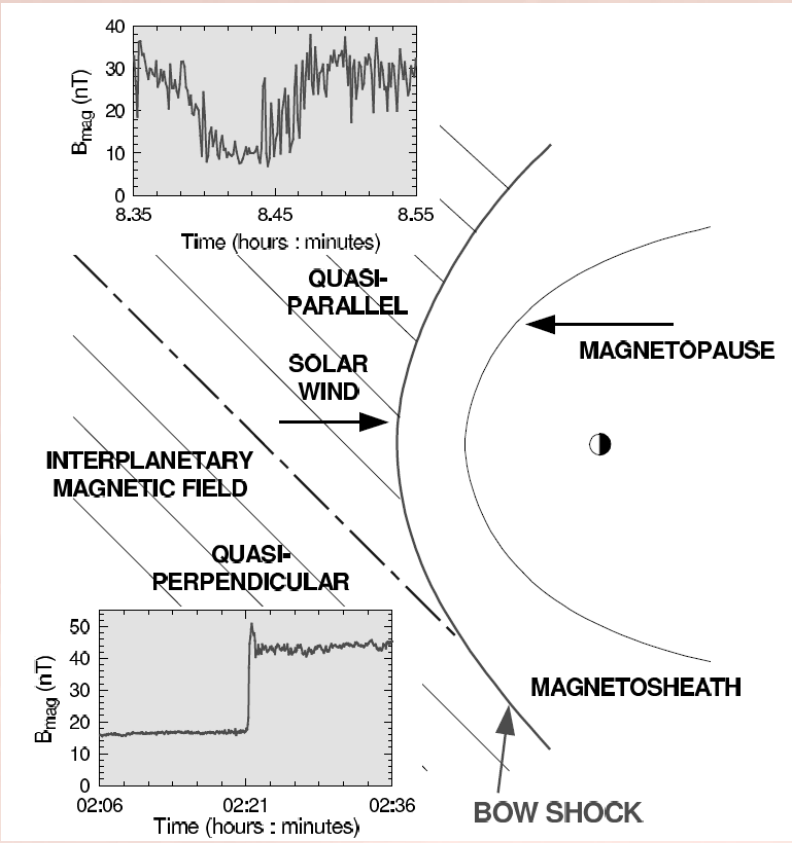

Supercritical Q-perp shocks display specific sub-structures related to necessary extra energy dissipation

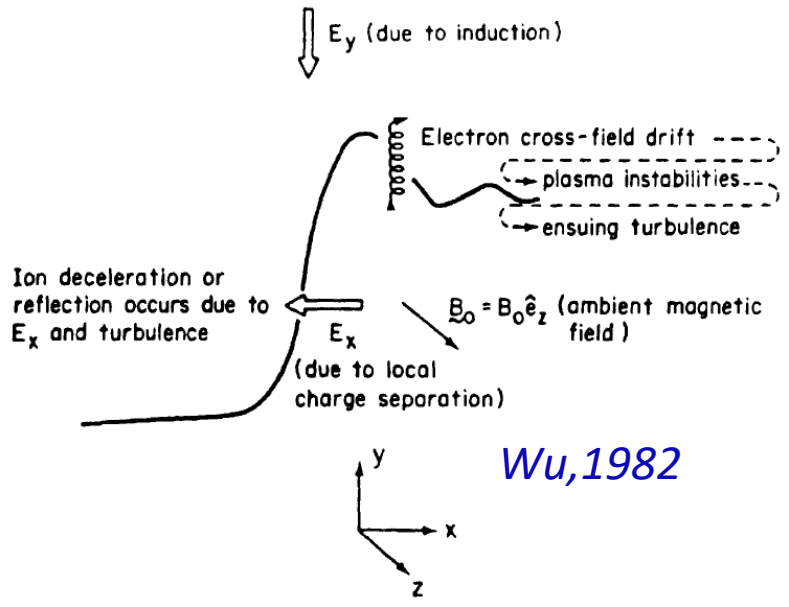

Wu,1982

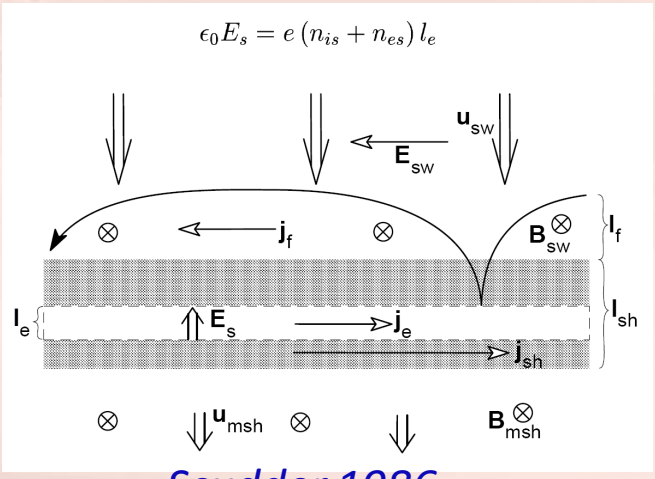

Scudder,1986

Above a critical value of M_f, dispersion is not sufficient to balance steepening via "anomalous resistive" dissipation (microinstabilities): other dissipation process by reflected ions mandatory

→ characteristics substructures:

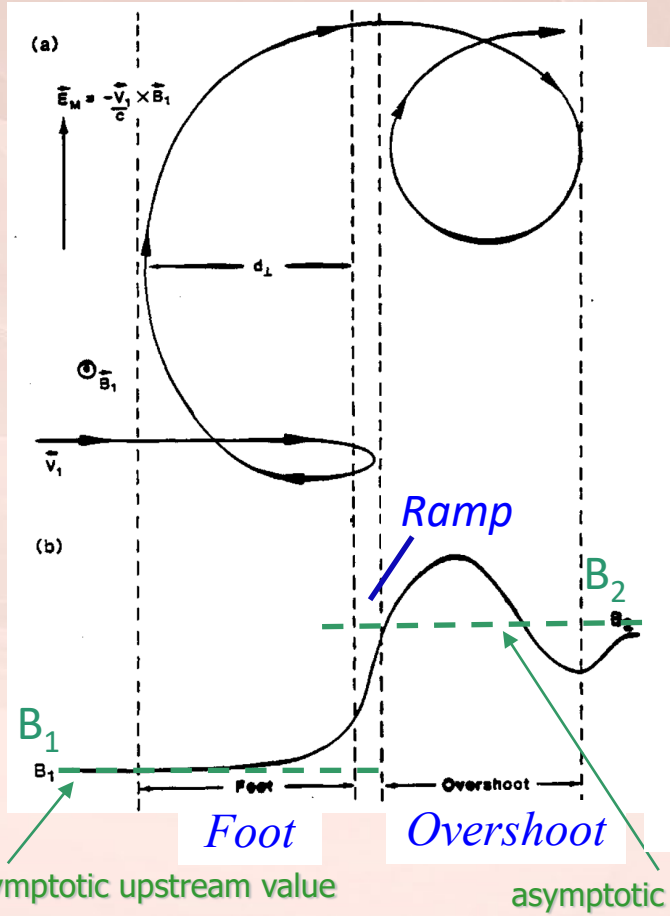

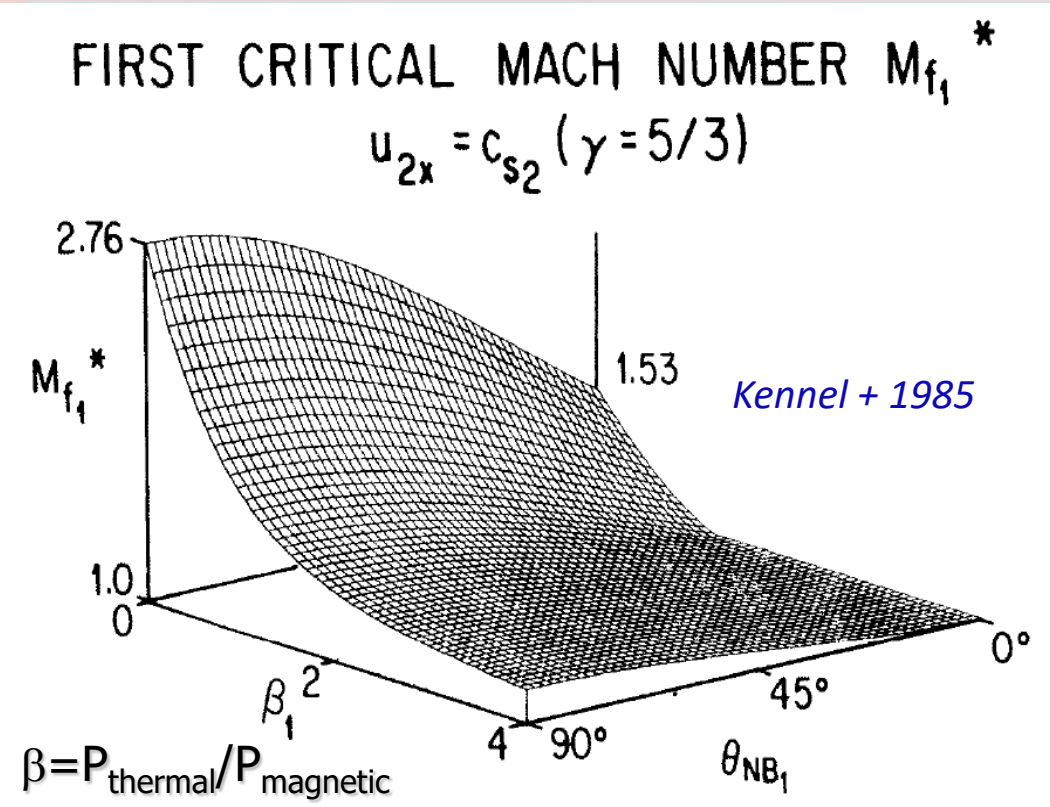

Kennel + 1985

Supercritical Q-perp shocks display specific sub-structures related to necessary extra energy dissipation

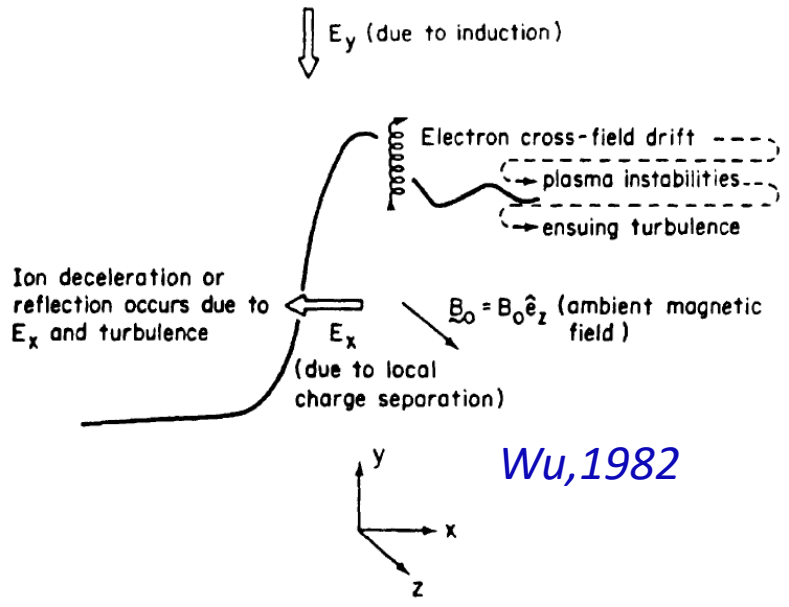

Wu,1982

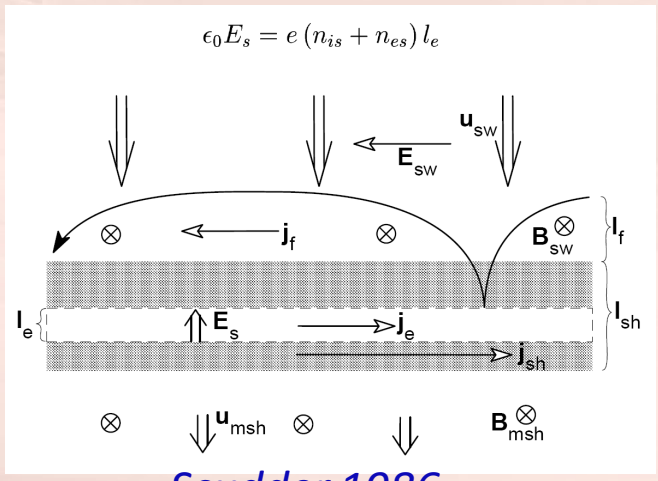

Scudder,1986

Above a critical value of M_f, dispersion is not sufficient to balance steepening via "anomalous resistive" dissipation (microinstabilities): other dissipation process by reflected ions mandatory

→ characteristics substructures:

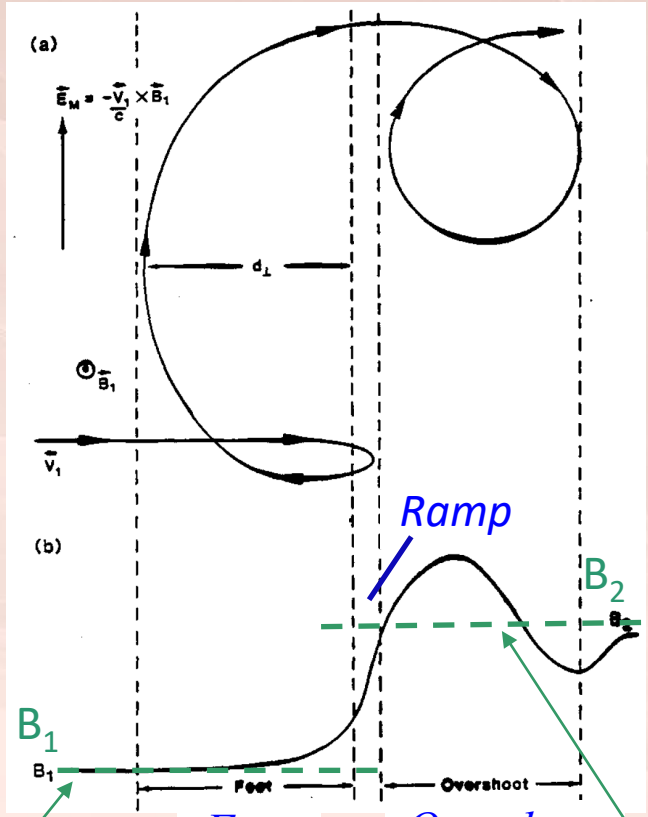

Foot *Overshoot*

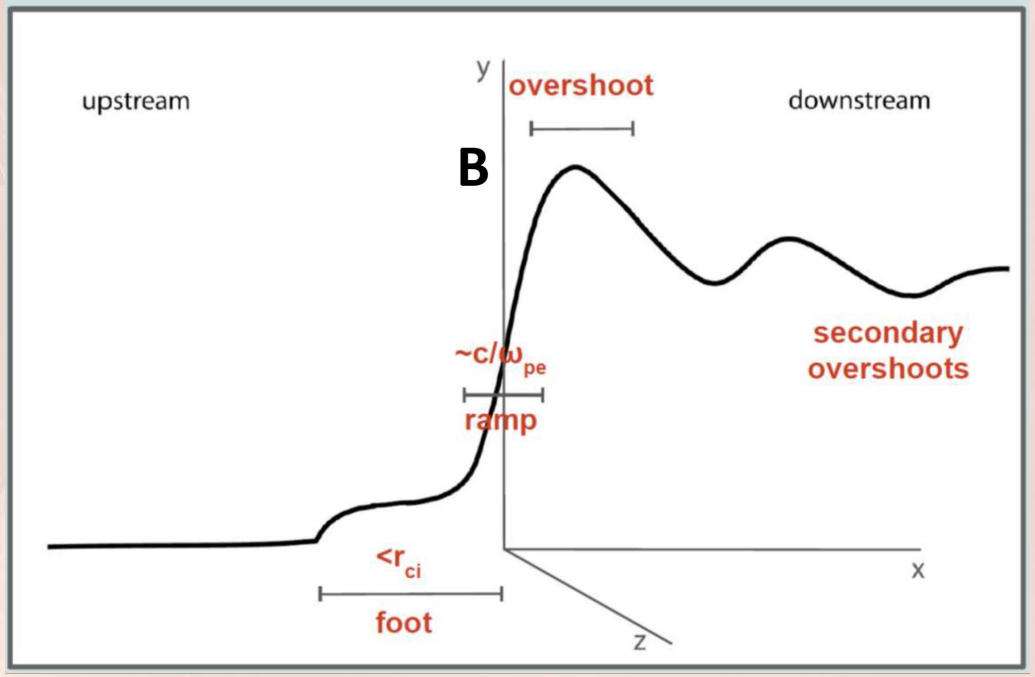

after Balogh and Treumann, 2013

Supercritical Q-perp shocks display specific sub-structures related to necessary extra energy dissipation

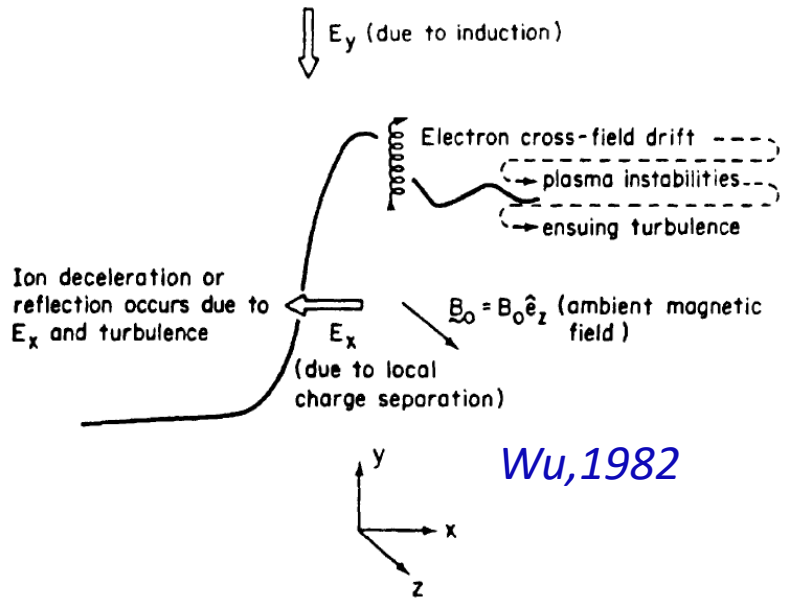

Wu,1982

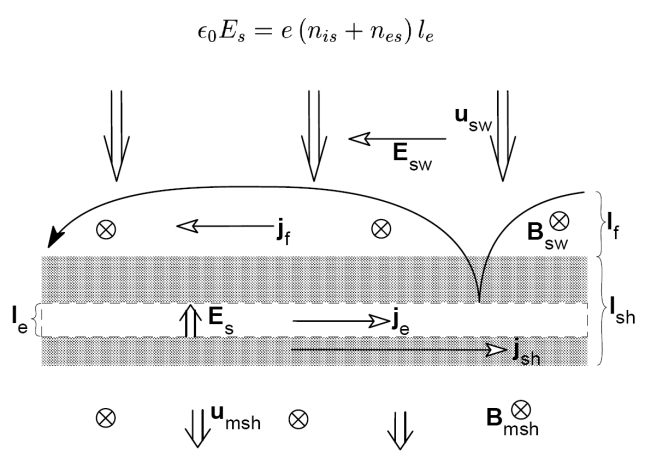

Scudder,1986

Above a critical value of M_f, dispersion is not sufficient to balance steepening via "anomalous resistive" dissipation (microinstabilities): other dissipation process by reflected ions mandatory

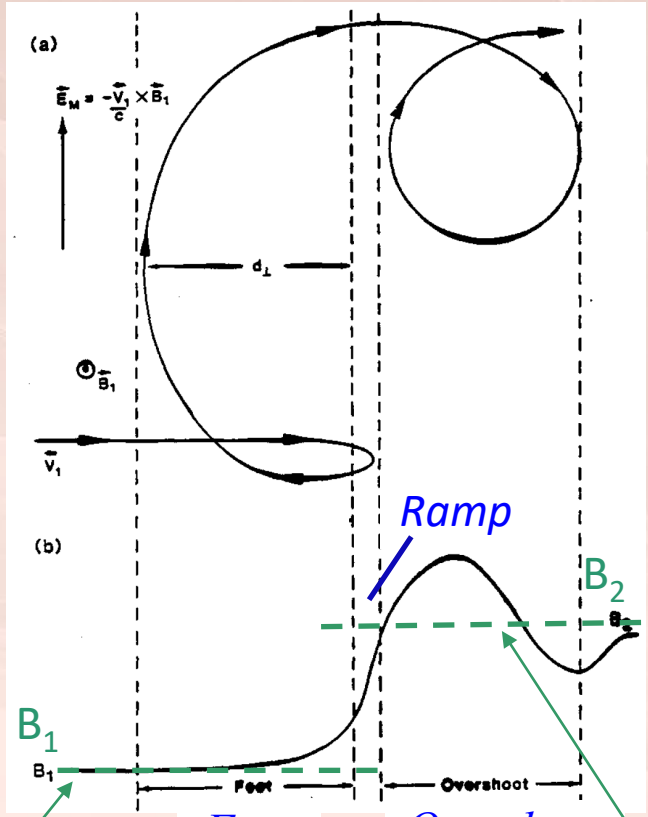

→ characteristics substructures:

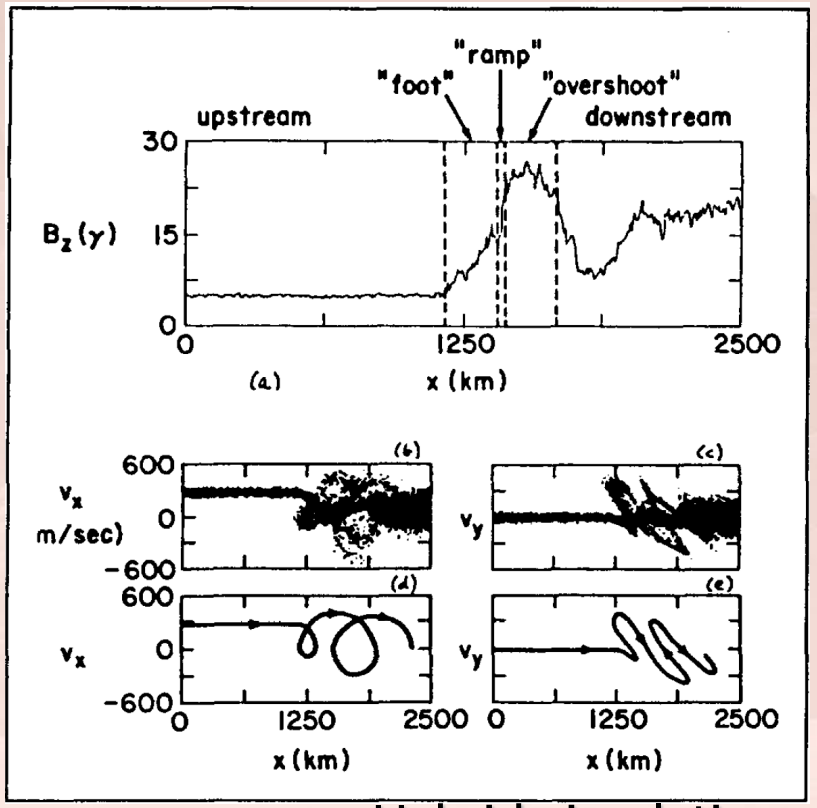

Hybrid simulation
[Leroy, 1981]

Q-perp shock nonstationarity

- Both hybrid/full particle simulations and recent experimental results have clearly evidenced that the front of a supercritical quasi-perpendicular shock can also be nonstationary.
- One responsible mechanism proposed for this nonstationarity is the self-reformation of the front itself being due to the accumulation of reflected ions.
- Important consequences of this nonstationarity are that not only the amplitude but also the spatial scales of fields components at the shock front (ramp and foot) are strongly varying within each cycle of the self-reformation.

2D PIC simulation

θ_{Bn}= 90°

M_A= 5.2

m_p/m_e=84

β_i=0.02

Yang, Lembège, and Lu, JGR, 2011

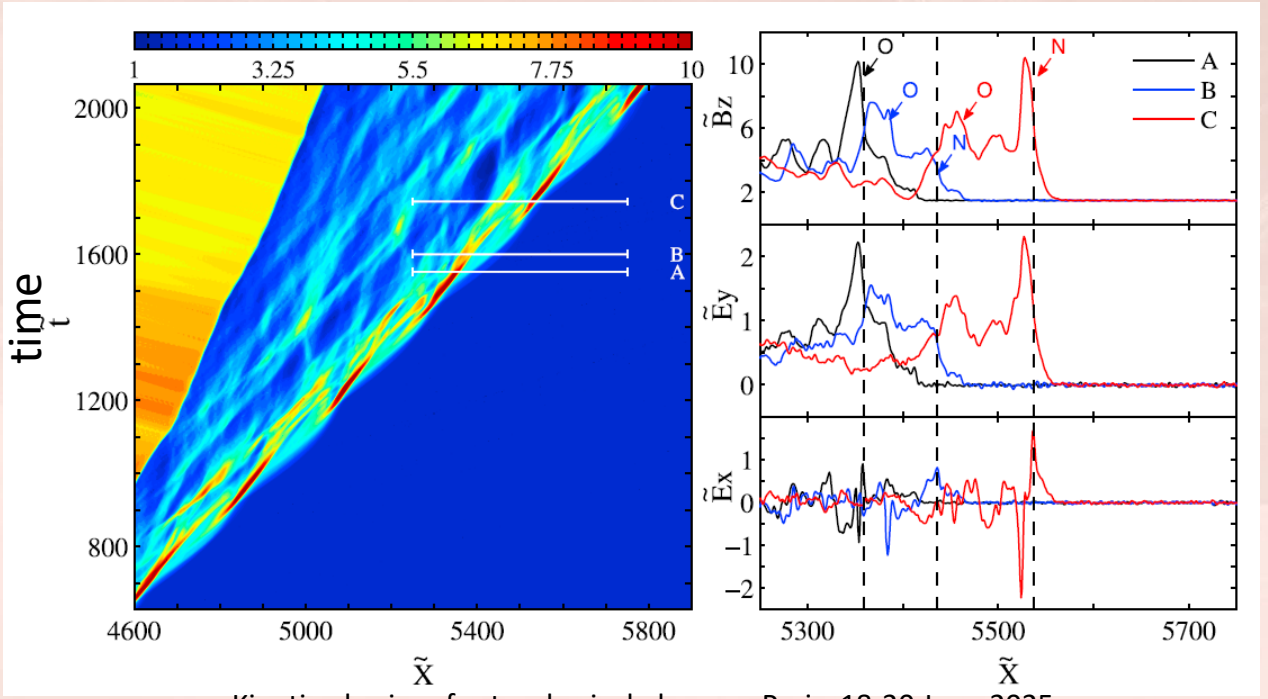

O: old ramp

N: new ramp

Foot thickness: comparison between PIC simulations and multi-spacecraft determinations

2D PIC: θ_{Bn}= 90° M_A= 5.2 m_p/m_e=84 β_i=0.02

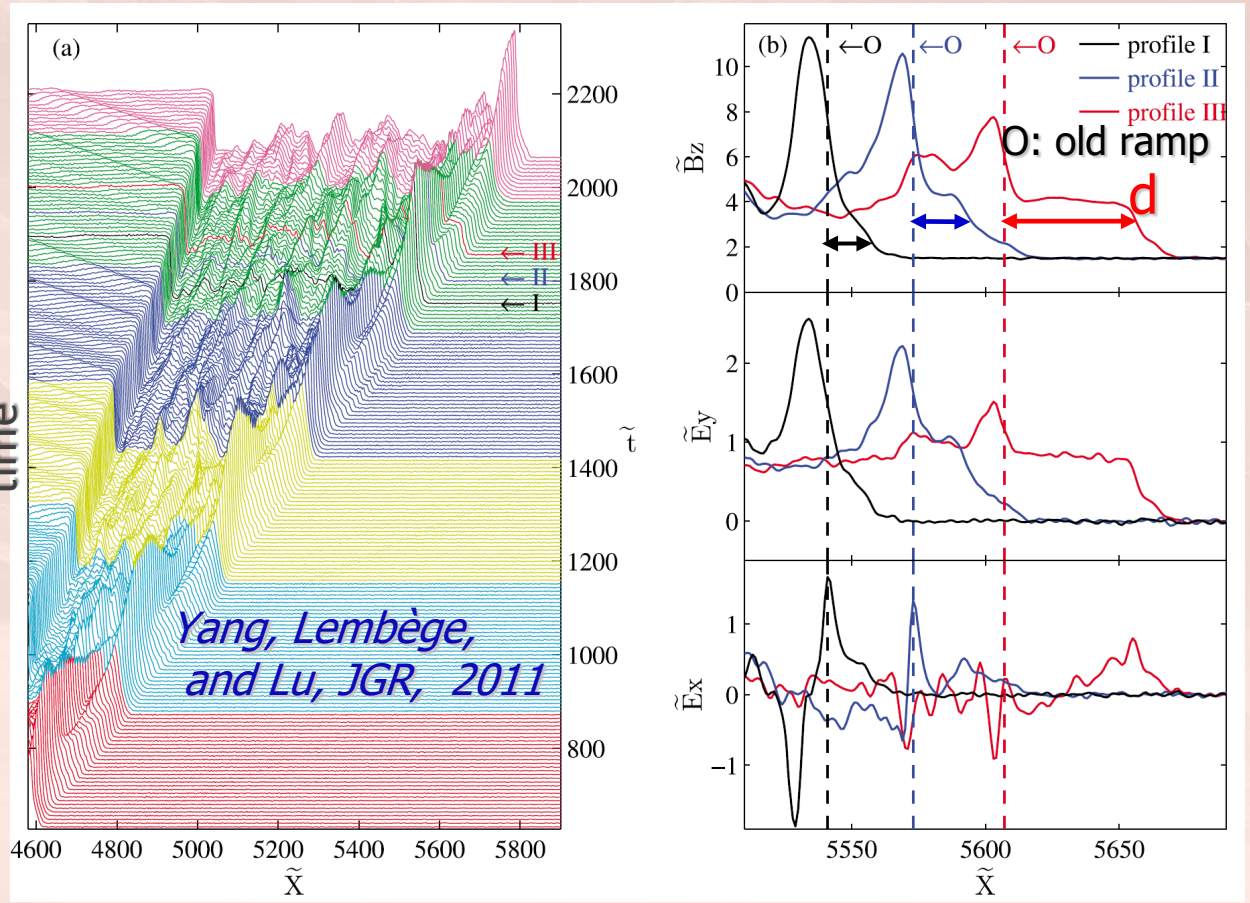

Large variation of magnetic foot thickness during one self-reformation cycle

Cluster: θ_{Bn}= 86± 2° M_A=4.1 β_i=0.05

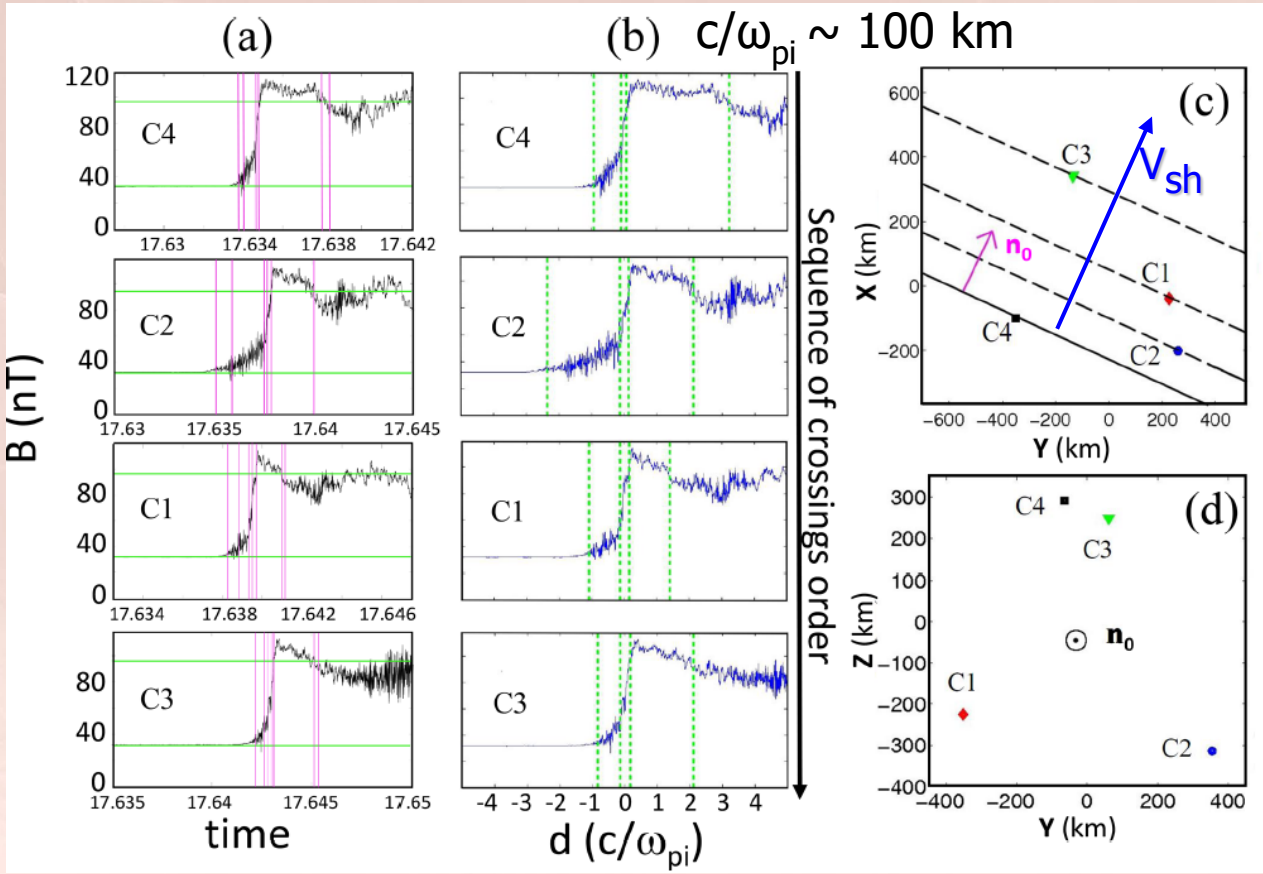

consistent with multi-spacecraft analysis

Mazelle +, 2010; Mazelle and Lembège, 2021

Foot thickness: comparison between PIC simulations and multi-spacecraft determinations

2D PIC: θ_{Bn}= 90° M_A= 5.2 m_p/m_e=84 β_i=0.02

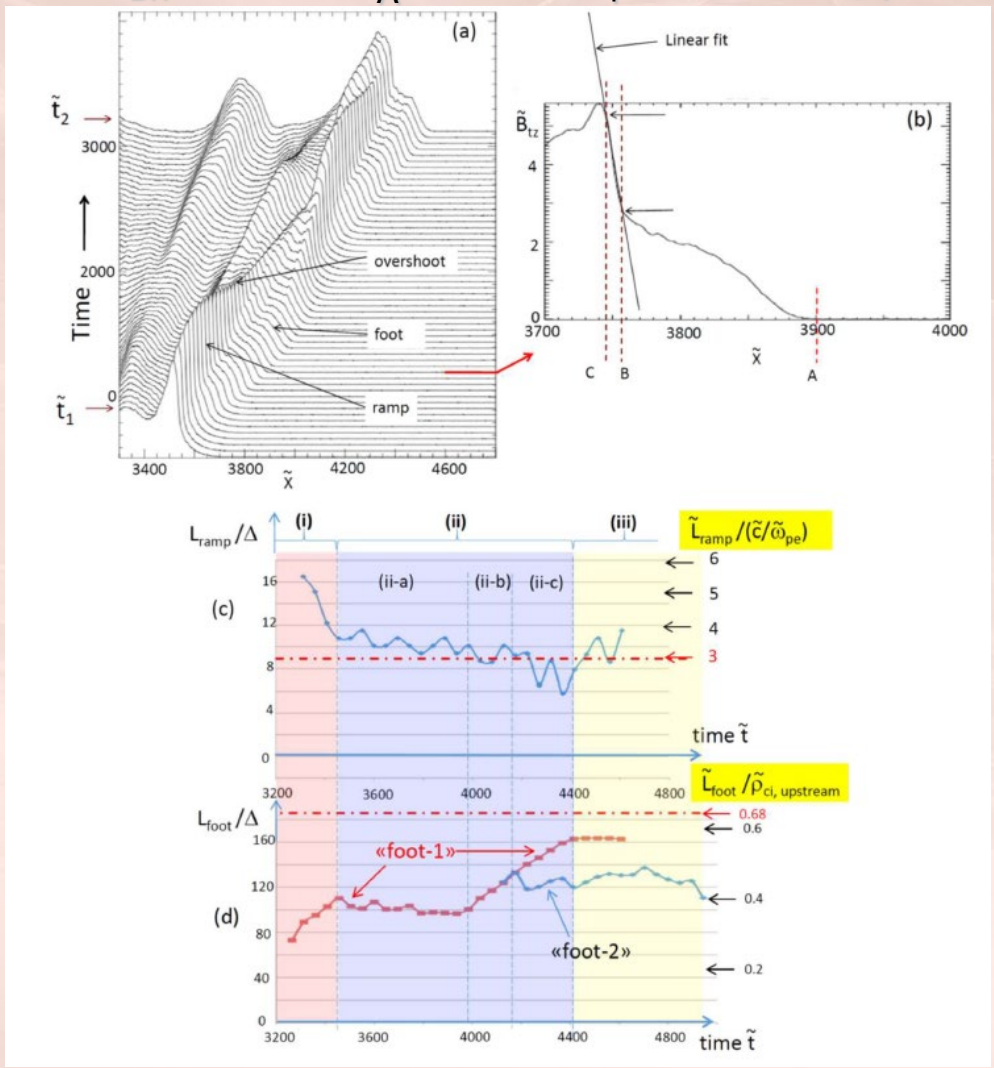

Cluster: mostly narrow ramps

thickness of a few electron inertial lengths
Could favor Shock Surfing Acceleration (SSA) ?

e.g. Zank+ 1996

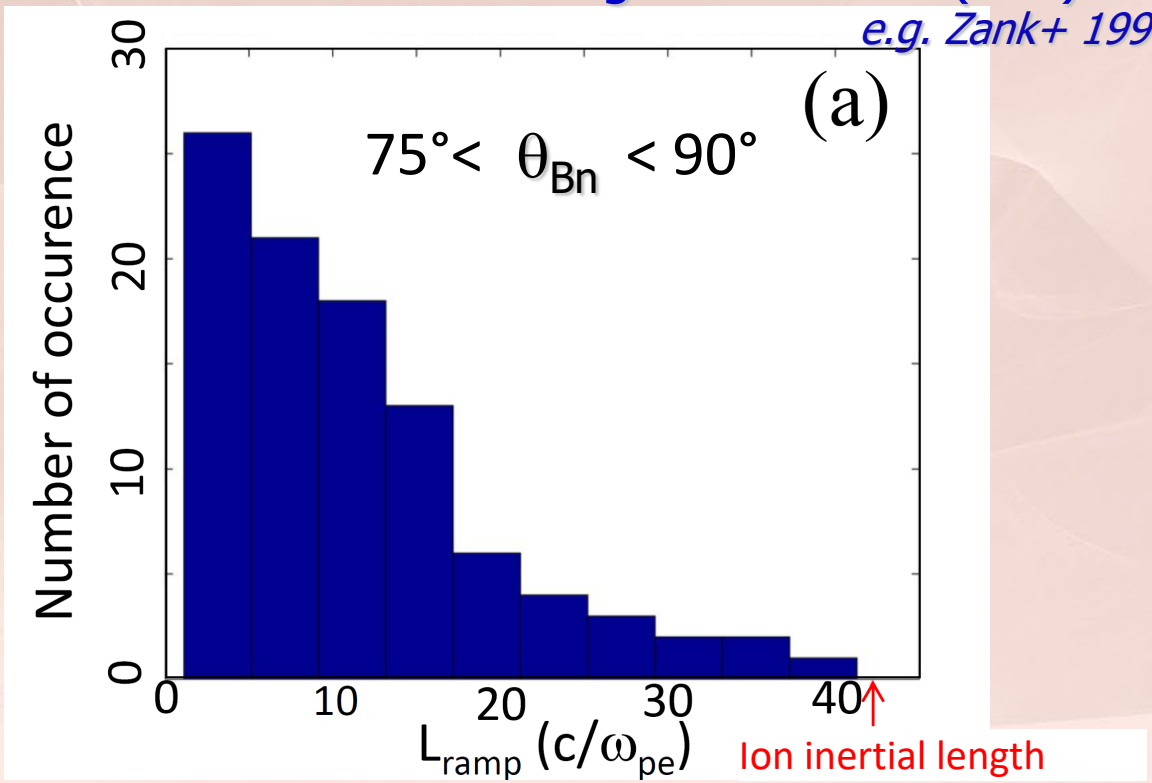

Mazelle and Lembège, 2021

Quasi-parallel shocks: θ_{Bn}~0 ($\beta \geq 1$)

$\beta = P_{thermal}/P_{magnetic}$

- Magnetic field ~ parallel to shock normal
  - Significant flux threads shock surface
- Disturbed transition in **B**: not shock motion
  - **Extended spatial transition**

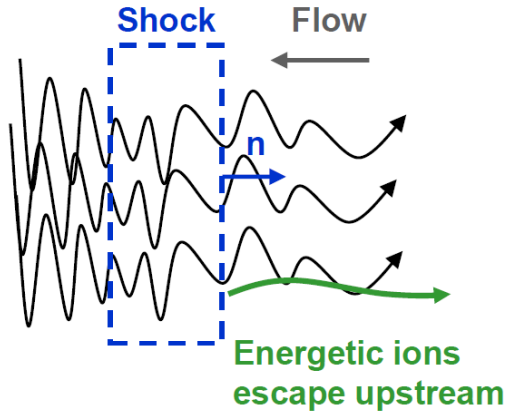

Cluster observations

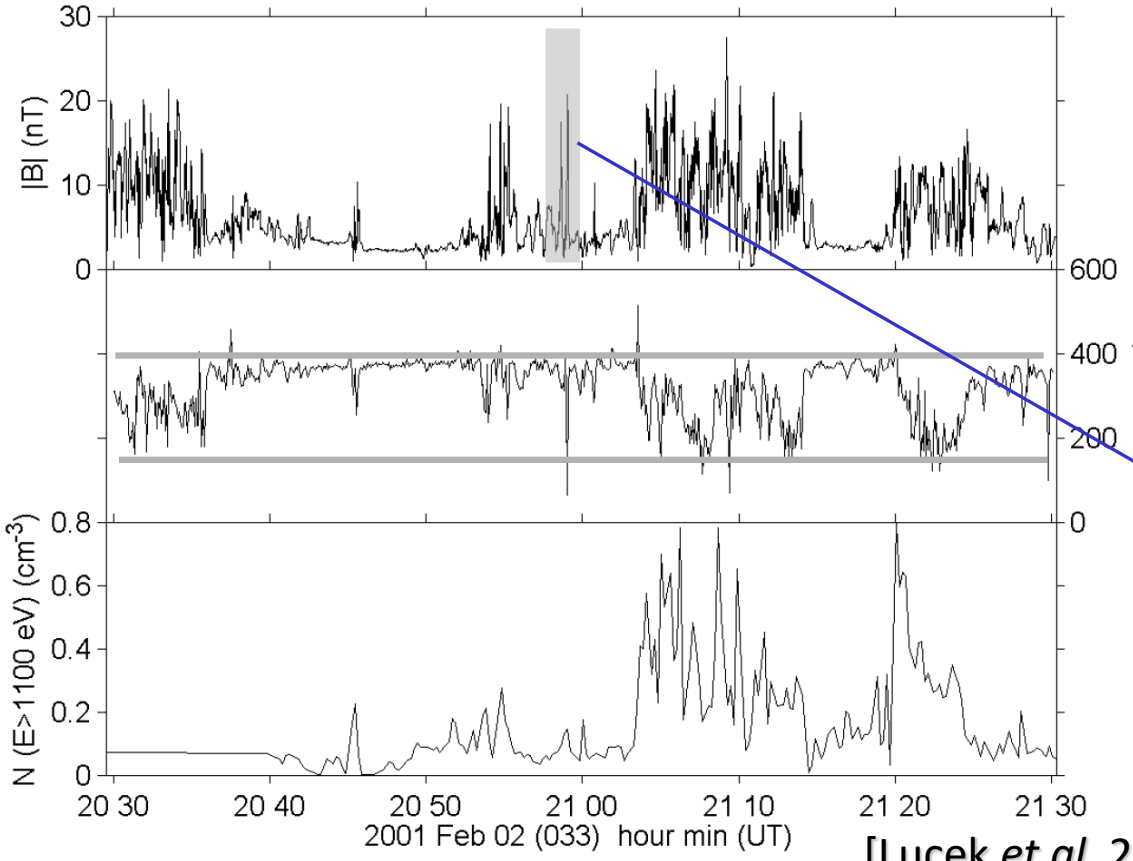

- Particles escape upstream
  - Generate ULF waves
  - Waves carried back to shock
- Pulsations (SLAMS) grow by interacting with hot ions
  - **Shock intrinsically time varying**

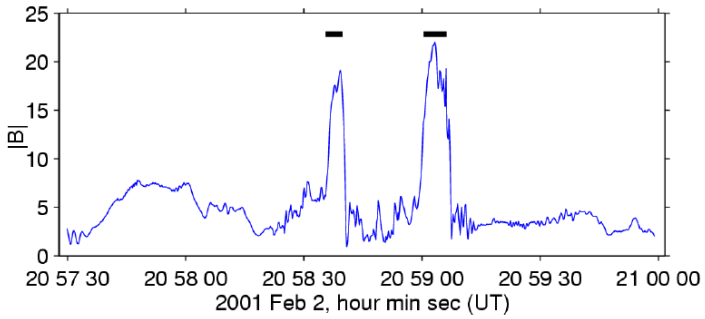

[Lucek *et al*. 2002]

Other planetary bow shocks

Other planetary bow shocks: size

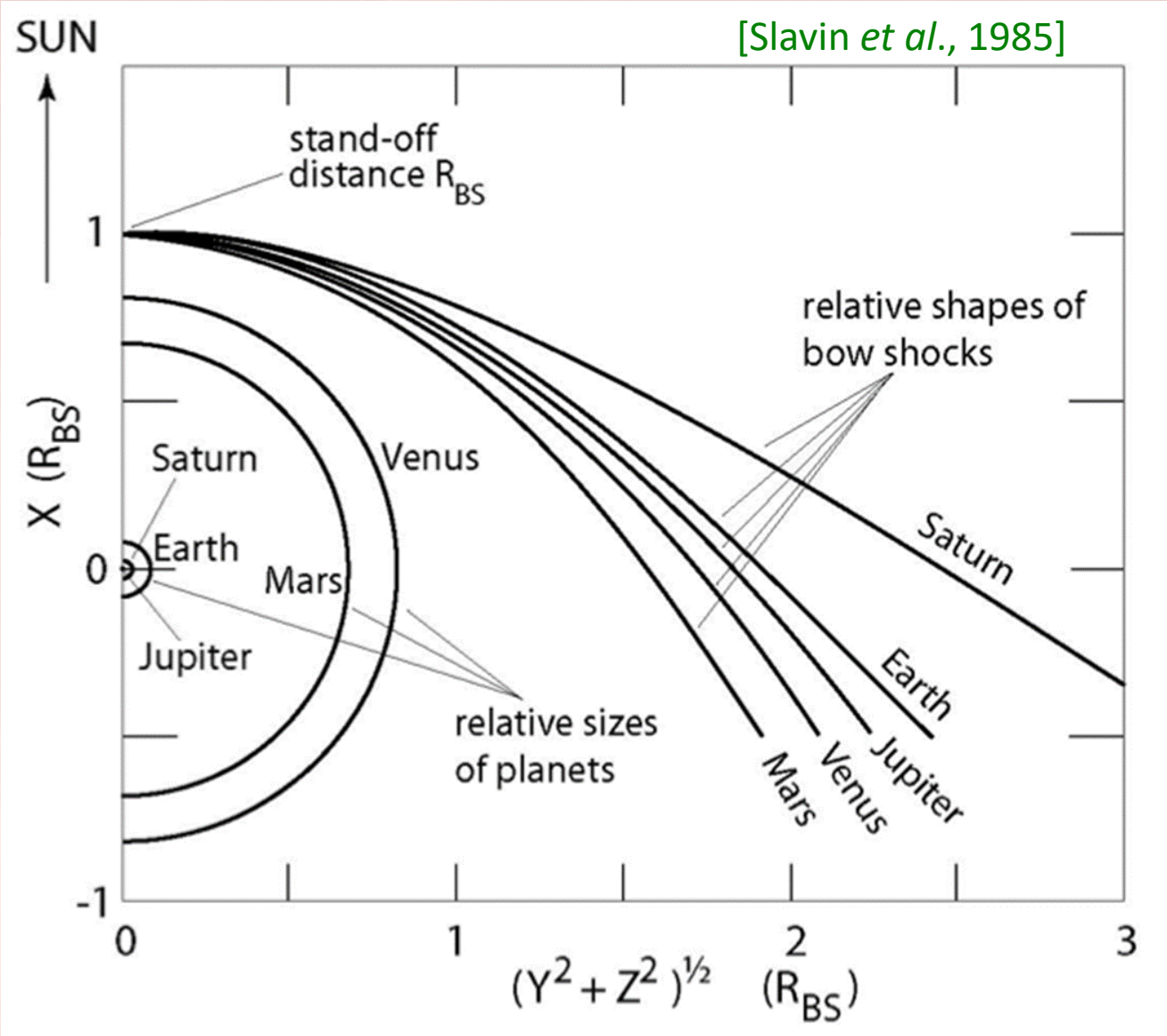

Bow shock scale and particle Larmor radius

	Planet Radius R_P/R_E	Standoff/ Scale H.	IMF B/B_E	Parker IMF θ_{BX}	Radius Curvature/ρ_i protons	θ_{Bn}= 90° Drift Length η_{90}
Earth	1	13.5	1	45°	222	1
Venus	0.95	1.4	1.7	36°	25	0.13
Mars	0.63	1.6	0.4	57°	4 [O^+: 0.25]	0.02
Saturn	9.1	26	0.04	84°	224	1.2

Shock drift acceleration efficiency comparison:

Electric field tangent to the shock

$$\mathcal{E}_t = BV\sin\theta_{BX}$$

Particle energization while drifting for a distance l

$$\Delta E = q\mathcal{E}_t l = qBVl\sin\theta_{BX}$$

For a nearly perpendicular drift

$$l \sim L\sqrt{1+\frac{X_0}{L}}, \quad L = \text{semilatus}, X_0 = \text{conic section focus}$$

Comparison with Earth bow shock

$$\eta_{90} = \frac{(\Delta E)_{Planet}}{(\Delta E)_{Earth}} \sim \frac{\left[B\sin\theta_{BX}L\sqrt{1+2X_0/L}\right]_{Planet}}{\left[B\sin\theta_{BX}L\sqrt{1+2X_0/L}\right]_{Earth}} \times \frac{R_P}{R_E}$$

Shock Drift Acceleration (SDA)

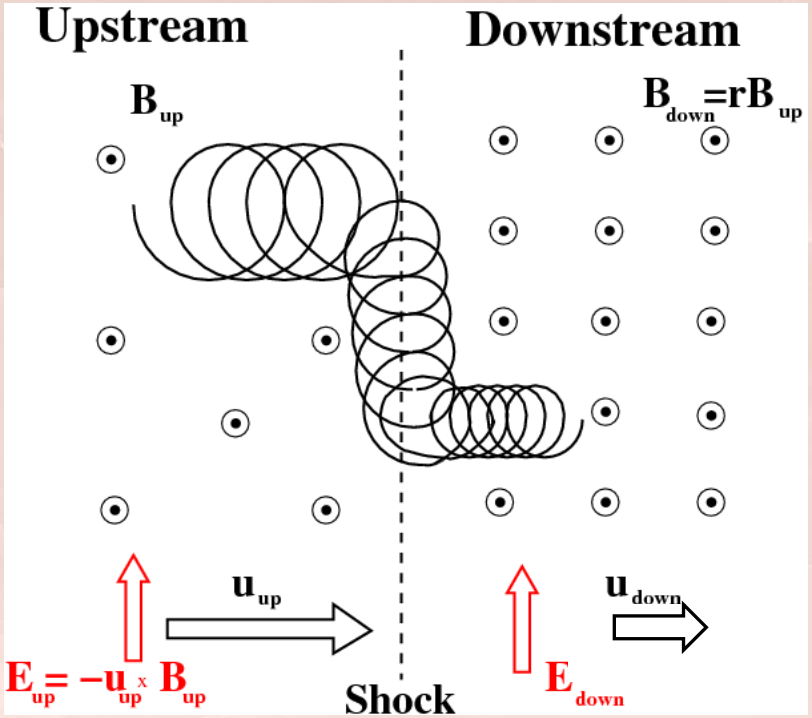

Martian Bow Shock

Martian Bow Shock: very small size

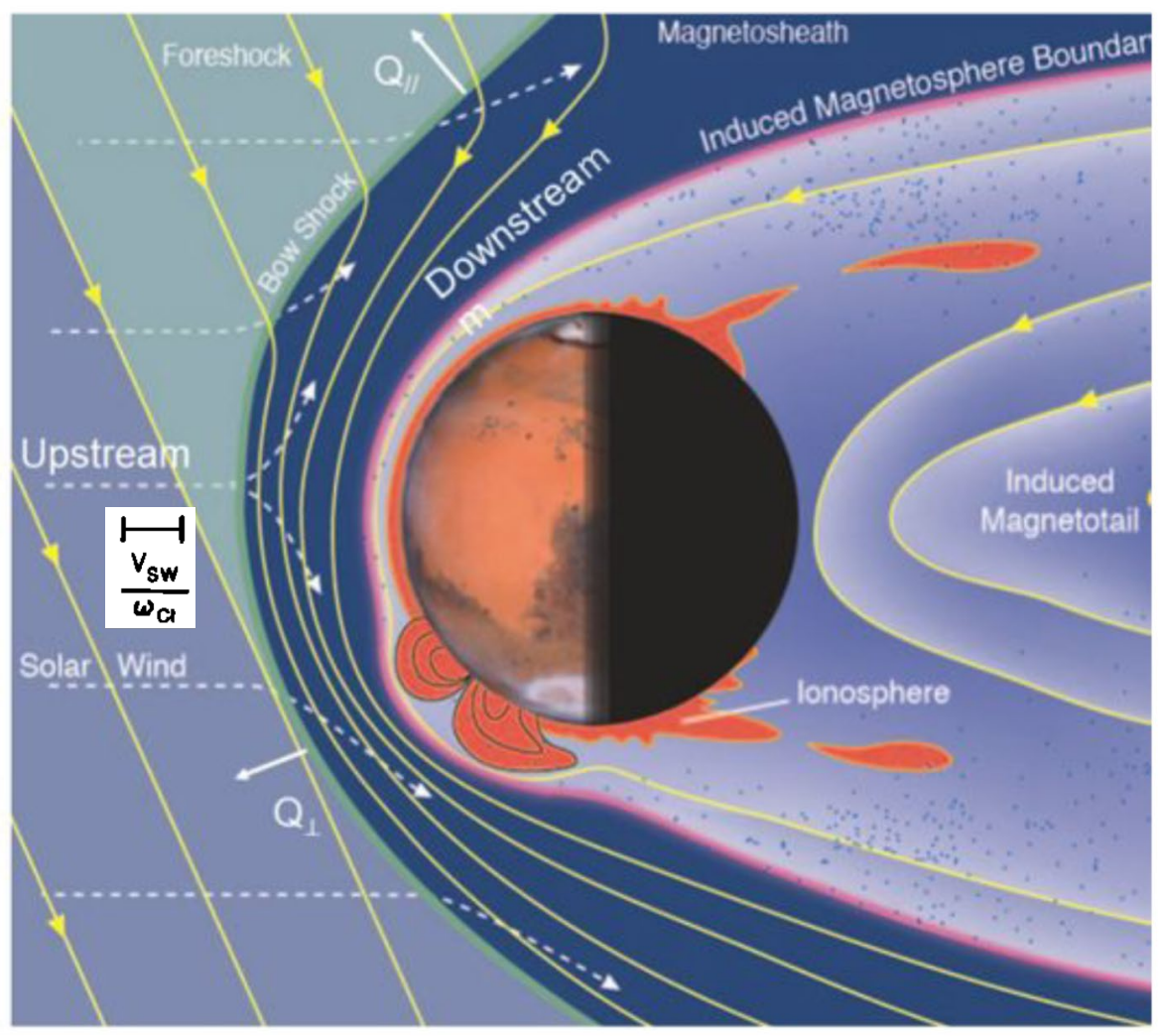

- Mars has no global intrinsic magnetic field: atmosphere, ionosphere and exosphere as obstacle to the solar wind.
- Thus it occupies most of its induced magnetosphere.
- Shock subsolar stand-off distance: order of SW proton convective gyroradius V_{sw}/Ω_{cp}.
- Kinetic effects on ion reflection (finite Larmor radius effects).

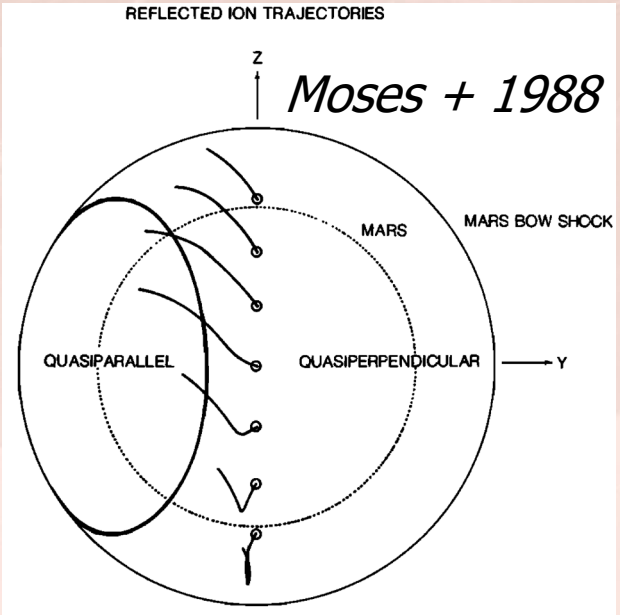

Ions reflected in the Q-perp region can be measured in the Q-// foreshock

Maven allows the first in-depth study of the Martian quasi-perpendicular bow shock

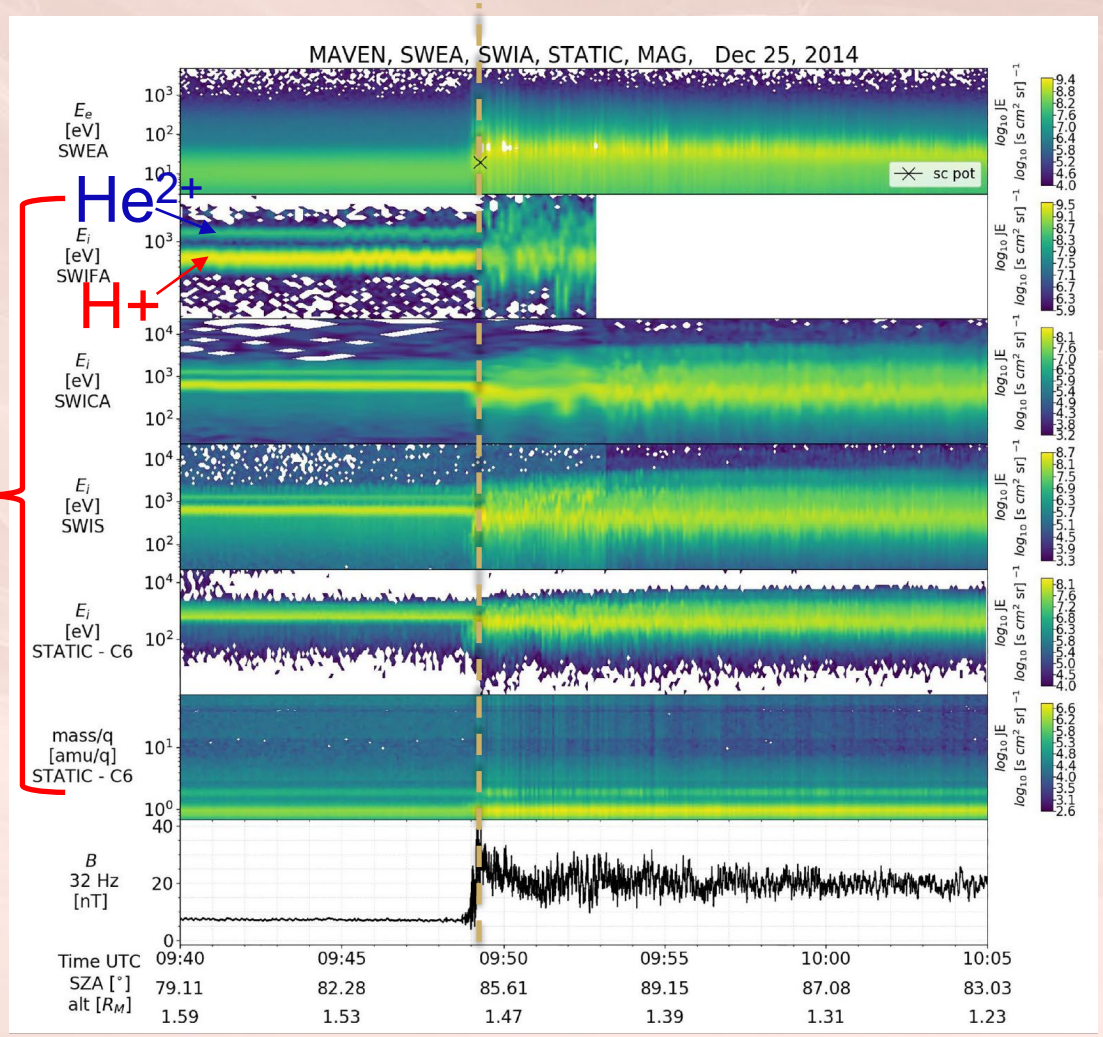

- First study @ Mars with all necessary plasma properties: electrons, ions and magnetic field.

Burne, Mazelle + 2021

Maven allows the first in-depth study of the Martian quasi-perpendicular bow shock

n

$T_{i,e}$

V

e-flux

B

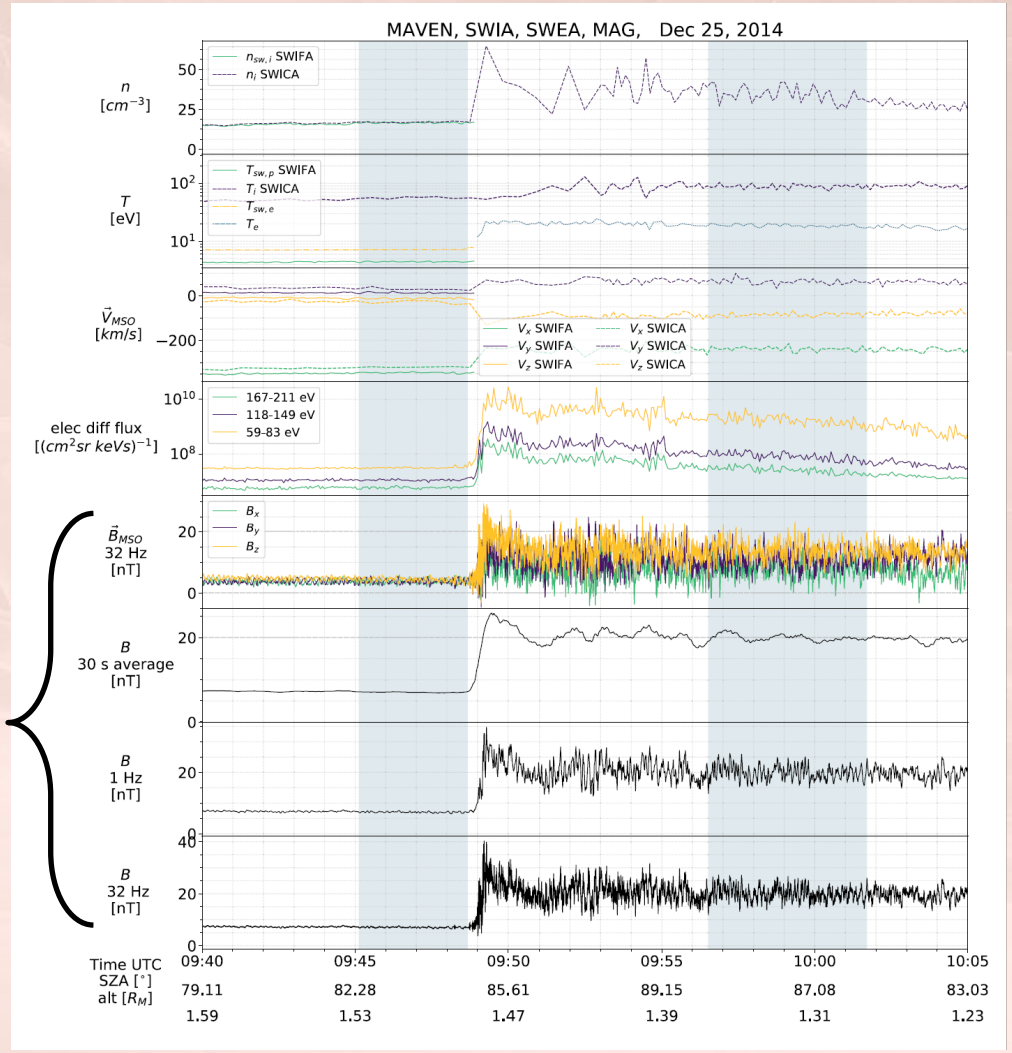

- First study @ Mars with all necessary plasma properties: electrons, ions and magnetic field.
- θ_{Bn} = 78 ± 3° from mixed coplanarity methods (Schwartz , 1998) using **B** and **V**

Shock and upstream plasma main parameters

M_f = 4.3	r_{ci} = (511 ± 16) km
β_p = 0.6	c/ω_{pi} = (55.9 ± 0.8) km
ω_{ci} = (0.68 ± 0.02) rad/s	c/ω_{pe} = (1.30 ± 0.02) km

Burne, Mazelle + 2021

Maven allows the first in-depth study of the Martian quasi-perpendicular bow shock

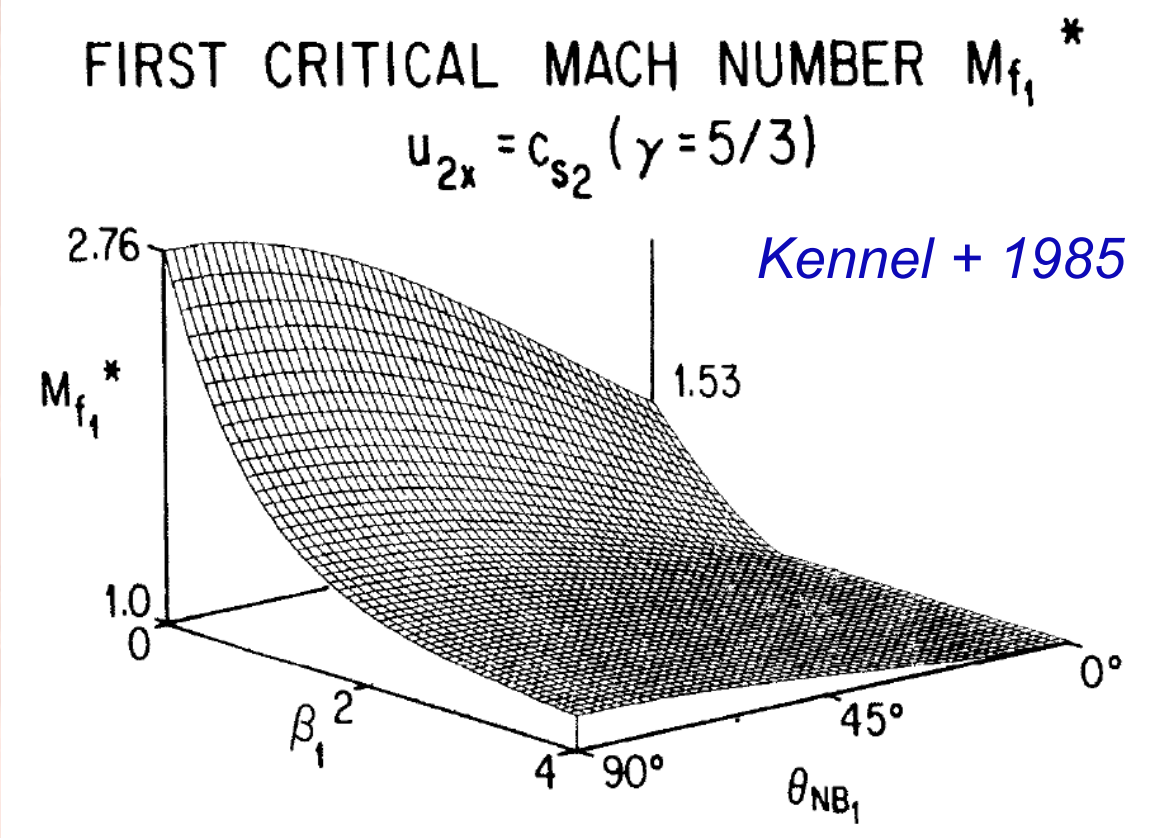

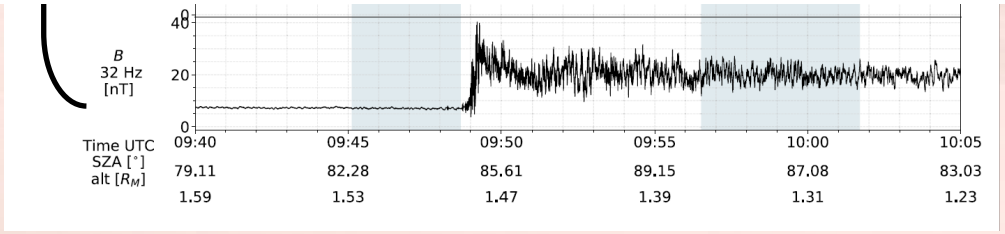

Burne, Mazelle + 2021

- First study @ Mars with all necessary plasma properties: electrons, ions and magnetic field.
- $\theta_{Bn} = 78 \pm 3°$ from mixed coplanarity methods (Schwartz , 1998) using **B** and **V**

Shock and upstream plasma main parameters

$M_f = 4.3$	$r_{ci} = (511 \pm 16)$ km
$\beta_p = 0.6$	$c/\omega_{pi} = (55.9 \pm 0.8)$ km
$\omega_{ci} = (0.68 \pm 0.02)$ rad/s	$c/\omega_{pe} = (1.30 \pm 0.02)$ km

Fast Mach number: 'supercritical'

Despite its much smaller size, the Martian q-perp bow shock displays same length scales as at Earth!

Calculation of shock velocity range from foot temporal width (*Gosling & Thomsen, 1985*):

$$V_{shock} = V_u cos(\theta_{Vn}) \frac{X_G}{1 \pm X_G} \qquad X_G = \frac{f(\theta_{Bn})}{\omega_{ci} \Delta_{foot}}$$

Shock nonstationarity: foot not necessarily fully developped. Use of percentage of formation:

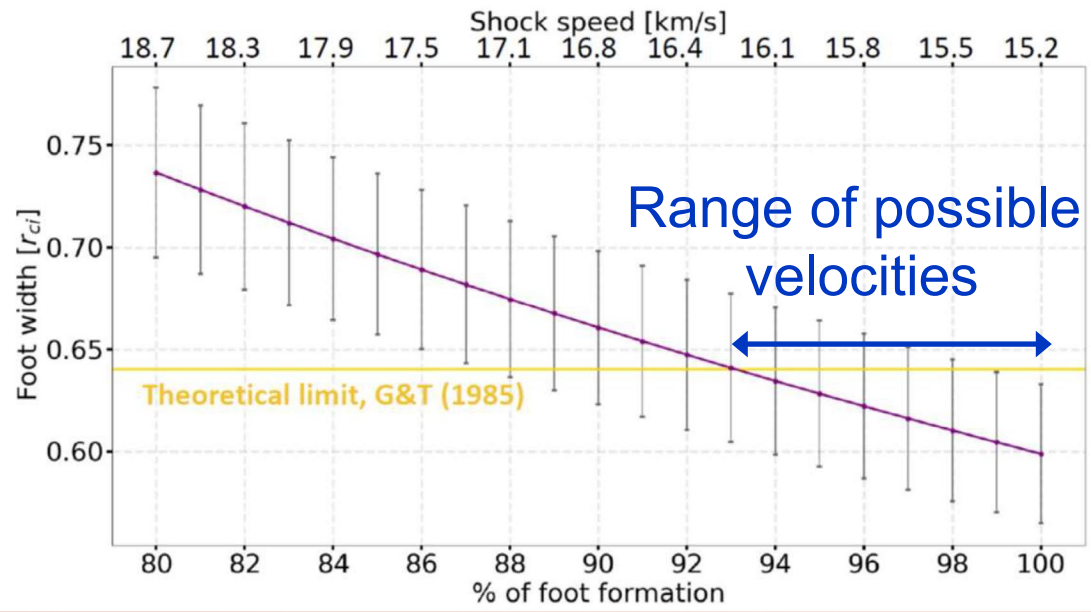

Despite its much smaller size, the Martian q-perp bow shock displays same length scales as at Earth!

Calculation of shock velocity range from foot temporal width (*Gosling & Thomsen, 1985*):

$$V_{shock} = V_u cos(\theta_{Vn}) \frac{X_G}{1 \pm X_G} \qquad X_G = \frac{f(\theta_{Bn})}{\omega_{ci} \Delta_{foot}}$$

Shock nonstationarity: foot not necessarily fully developped. Use of percentage of formation:

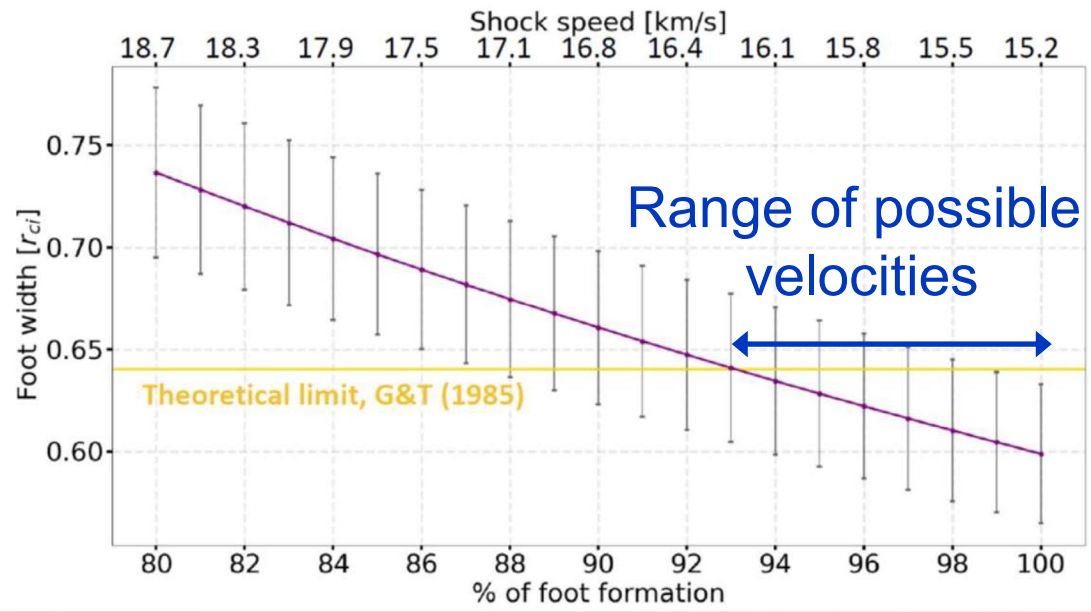

Nominal thicknesses		
FOOT	**RAMP**	**OVERSHOOT**
(308 ± 16) km	(2 ± 1) km	(1244 ± 113) km
(0.60 ± 0.04) r_{ci}	(1.5 ± 0.7) c/ω_{pe}	(2.4 ± 0.2) r_{ci}

Agrees with the **specular reflection model** (Woods, 1971; Livesey +, 1984; Gosling & Thomsen, 1985)

Agrees with Earth studies (Melott & Livesey,1987; and a study at Mars assuming static shock (Tatrallyay +, 1997)

Large statistical analysis by Fruchtman+ (2023): magnetic shock jump agrees to 1st order with Rankine-Hugoniot predictions & overshoot amplitude dependence on ion beta and Alfvén Mach number agree well with previous results.

Despite its much smaller size, the Martian q-perp bow shock displays same length scales as at Earth!

Terrestrial shock

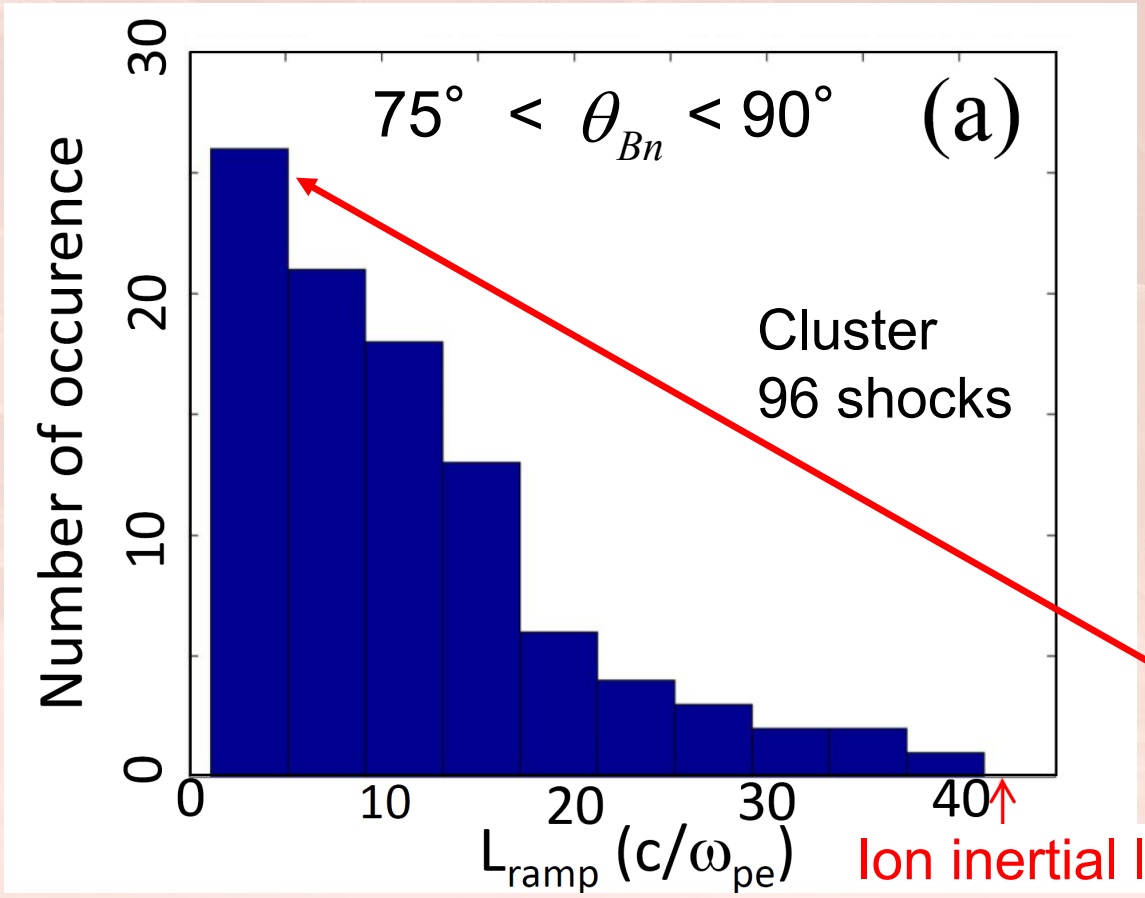

Mazelle & Lembège, 2021

Nominal thicknesses		
FOOT	**RAMP**	**OVERSHOOT**
(308 ± 16) km	(2 ± 1) km	(1244 ± 113) km
(0.60 ± 0.04) r_{ci}	(1.5 ± 0.7) c/ω_{pe}	(2.4 ± 0.2) r_{ci}

Agrees with the **specular reflection model** (Woods, 1971; Livesey +, 1984; Gosling & Thomsen, 1985)

Agrees with Earth studies (Melott & Livesey,1987; and studies at Mars assuming static shock (Tatrallyay +, 1997)

Similar to multi-spacecraft studies at Earth (Mazelle +, 2010; Mazelle & Lembège, 2021)

Importance of Martian Exosphere!

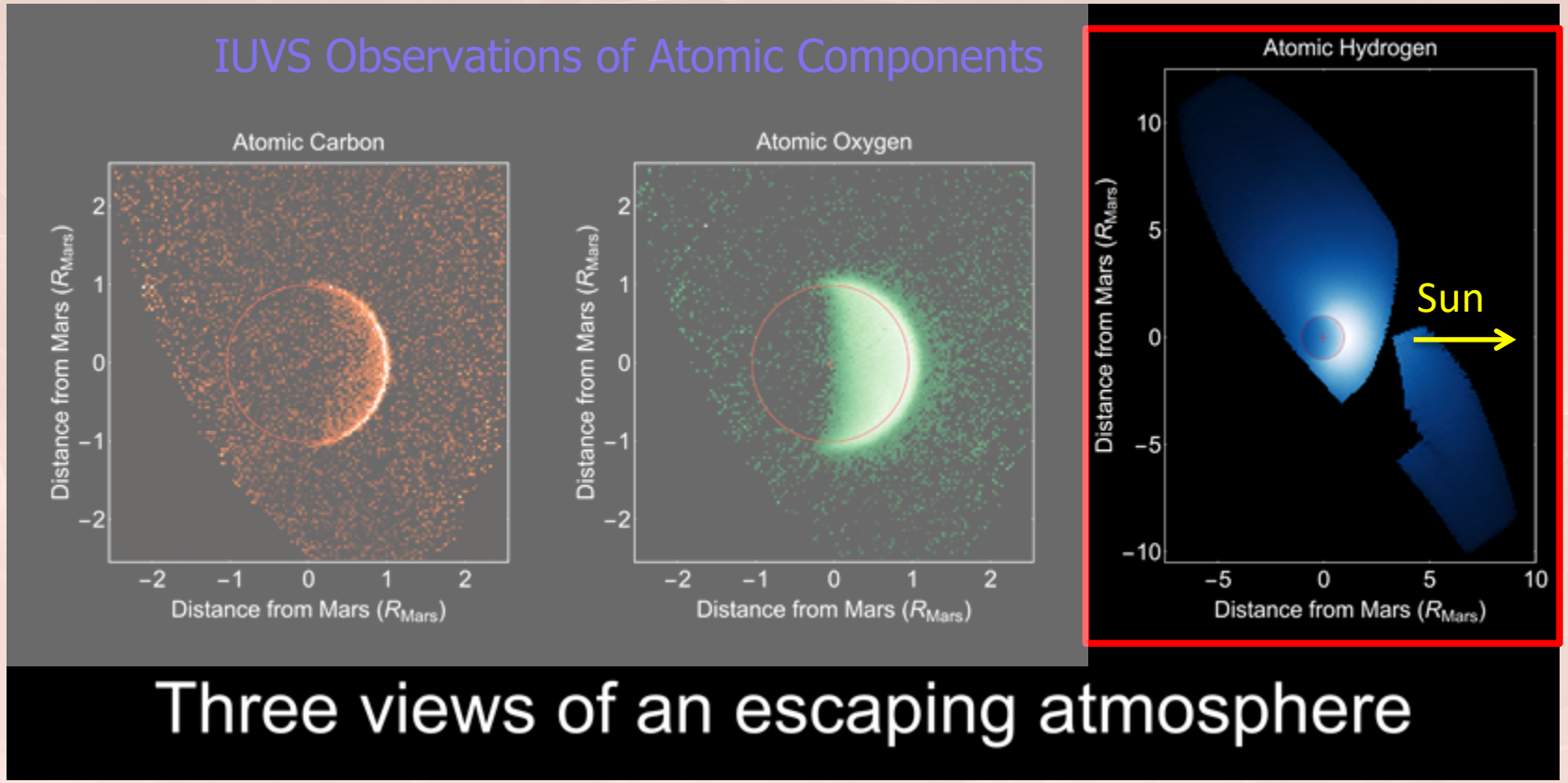

Hydrogen
Ly α
121.6 nm
brightness

[Schneider+ 2015; Chaffin+ 2015]

Mars has an extended exosphere expanding far upstream from the bow shock (in particular for H).

This is a local source of **pickup protons** from ionization of the neutrals everywhere around the planet.

These pickup protons can then produce low frequency electromagnetic waves as for comets at the local proton cyclotron frequency and often called 'Proton Cyclotron Waves' (**PCWs**)

Exospheric ion pick-up

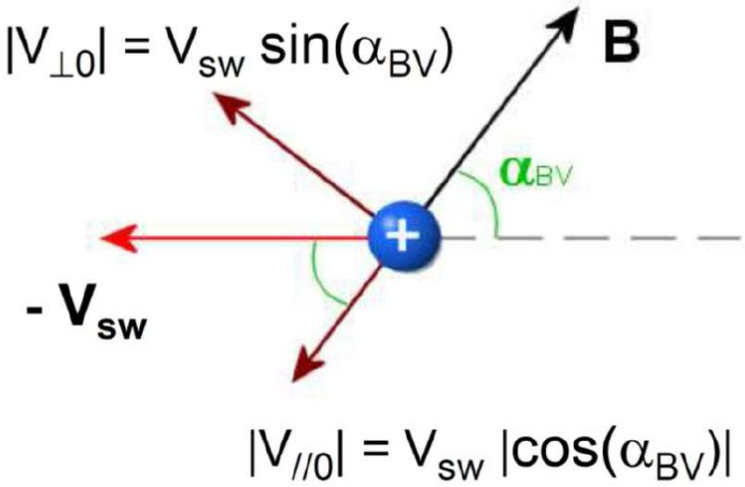

Exospheric particles are ionized far away with **negligible kinetic energy in the planetary frame**

In the SW frame they get a $-V_{sw}$ velocity initially.

So they will form a **ring-beam vdf** which is a non-thermal component unstable to the growth of **electromagnetic low frequency waves** (Wu and Davidson, 1972)

The resulting instability strongly depends on the IMF cone angle α_{BV} (Gary, 1993)

- **Small to moderate α_{BV}: electromagnetic ion–ion right-hand (RH) resonant.**
- **Large α_{BV} : the electromagnetic ion–ion left-hand (LH) mode.**
- **Maximum wave growth rates for parallel propagation.**

Exospheric ion pick-up

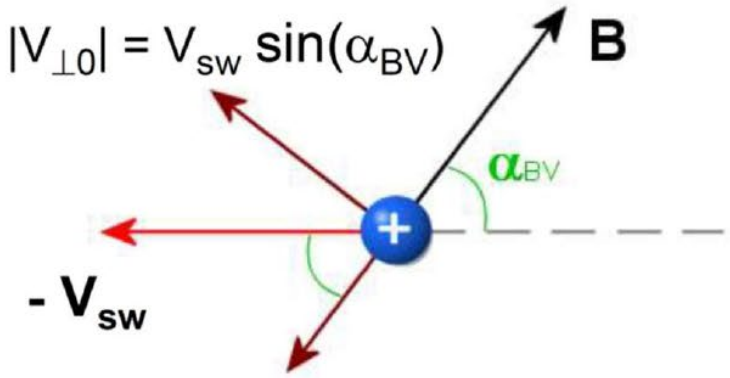

$|V_{//0}| = V_{sw} |\cos(\alpha_{BV})|$

Cyclotron resonance: $\omega - \mathbf{k}\cdot\mathbf{v}_{//} \pm n\,\Omega_i = 0\,;\; n = 0,1,2,\ldots$

n=1 fundamental most important

Doppler shift: $\omega + \mathbf{k}\cdot\mathbf{V}_{sw} = \omega_{sc}$ $\qquad \mathbf{k}\cdot\mathbf{V}_{sw} = -\mathbf{k}\cdot\mathbf{v}_{//}$

so $\omega_{sc} \cong \mp n\,\Omega_i$

For parallel propagation only n=1 $\boxed{\omega_{sc} \cong \pm \Omega_i}$ [*e.g.* Lee, 1989; Brinca, 1991]

Observed VERY CLOSE to cyclotron frequency in s/c frame (within less than 20% typically) and always left-hand polarization

\+ LH mode
\- RH mode

Example of Low Frequency Waves generated by 'freshly ionized' protons:

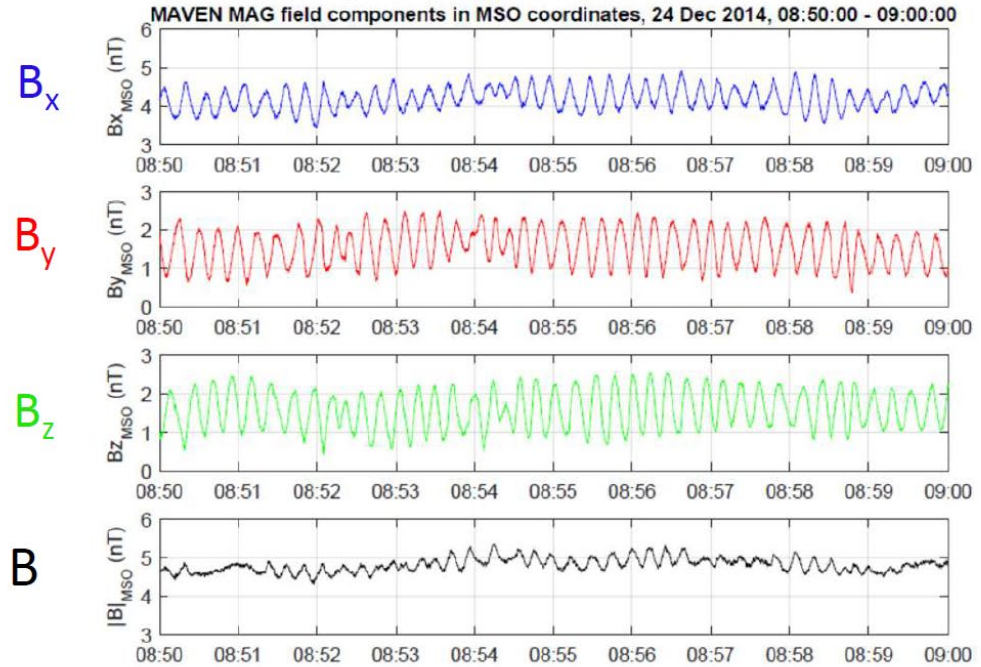

[Romanelli, Mazelle, et al., JGR, 2016]

Waves often uncorrectly called 'proton cyclotron waves': electromagnetic cyclotron-resonant mode with newly created protons from ionization of exospheric hydrogen atoms **observed at the local proton cyclotron frequency** (in s/c or planetary frame)

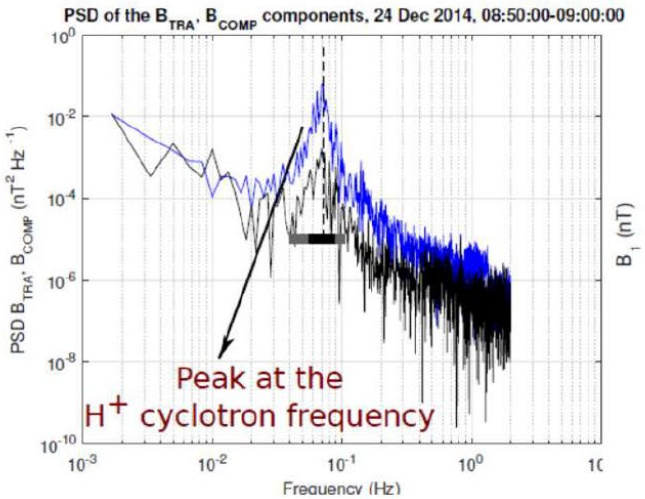

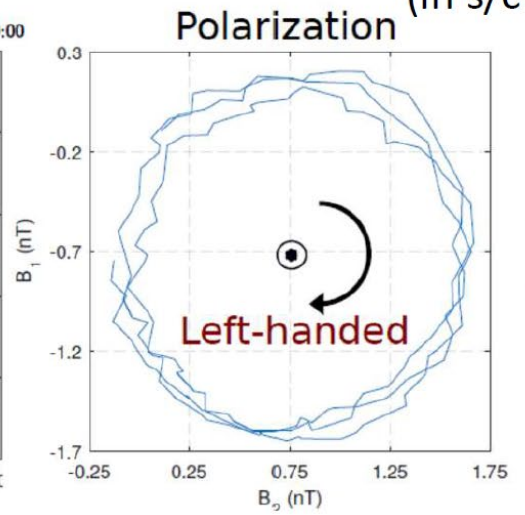

Propagation typically quasi-paralell to the ambient magnetic field

$\theta_{kB_0} < 30°$

Newly pickup protons and quasi radial IMF lead to fast shock formation at Mars as for comets

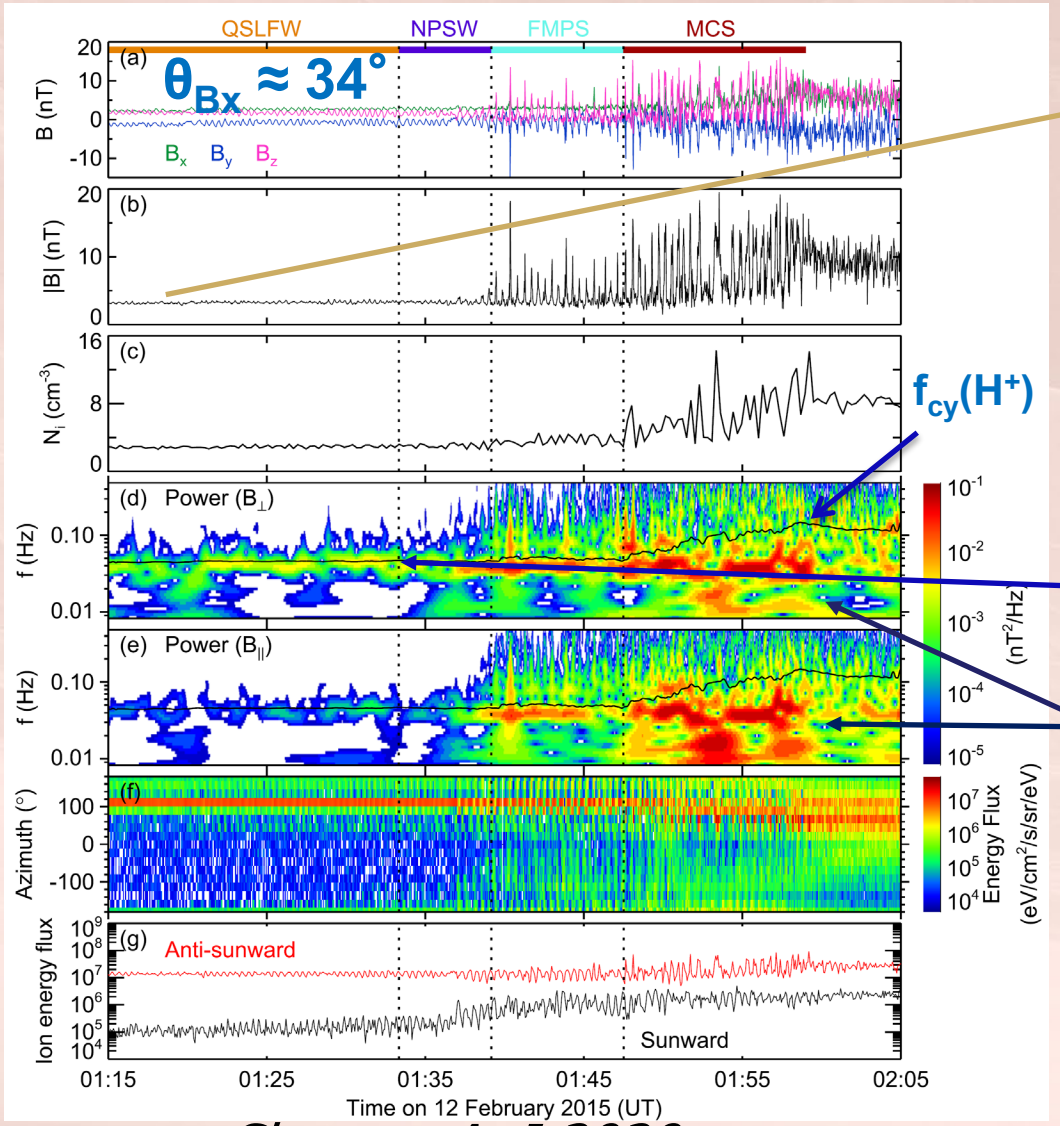

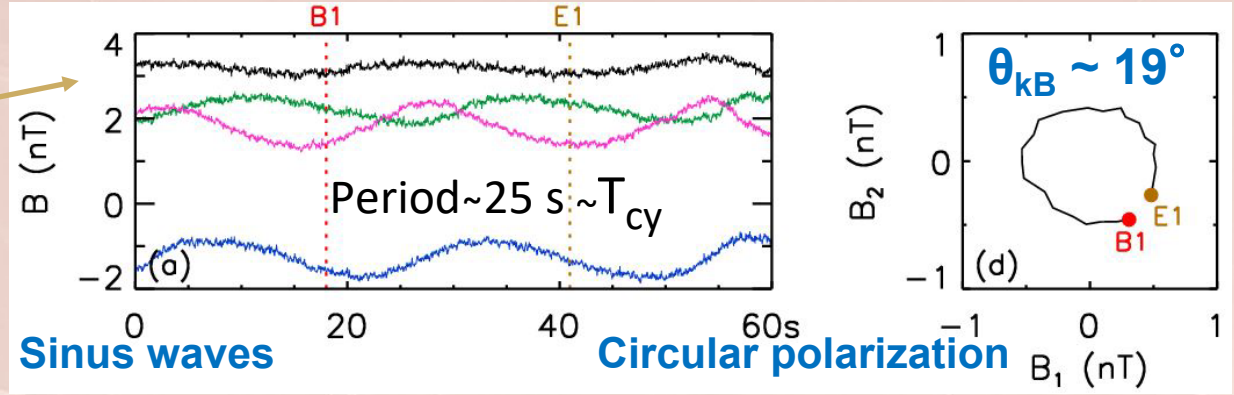

Right-hand mode waves in the plasma rest frame (fast magnetosonic mode)

Observed at the local proton cyclotron frequency in the s/c frame = generated by newly created protons (pickup)

Mostly transverse but also more and more compressive with time

Shan +, ApJ 2020a

Newly pickup protons and quasi radial IMF lead to fast shock formation at Mars as for comets

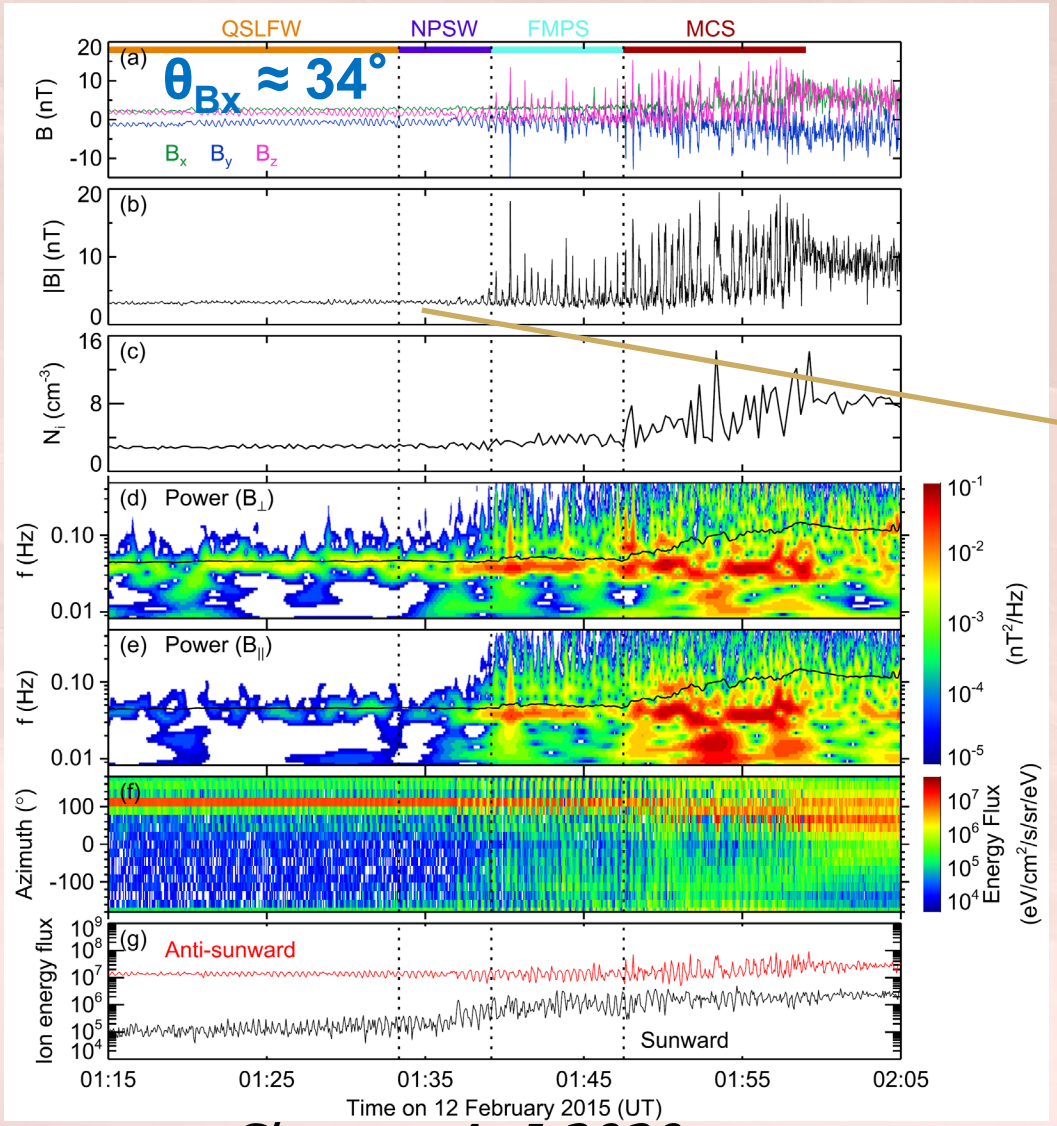

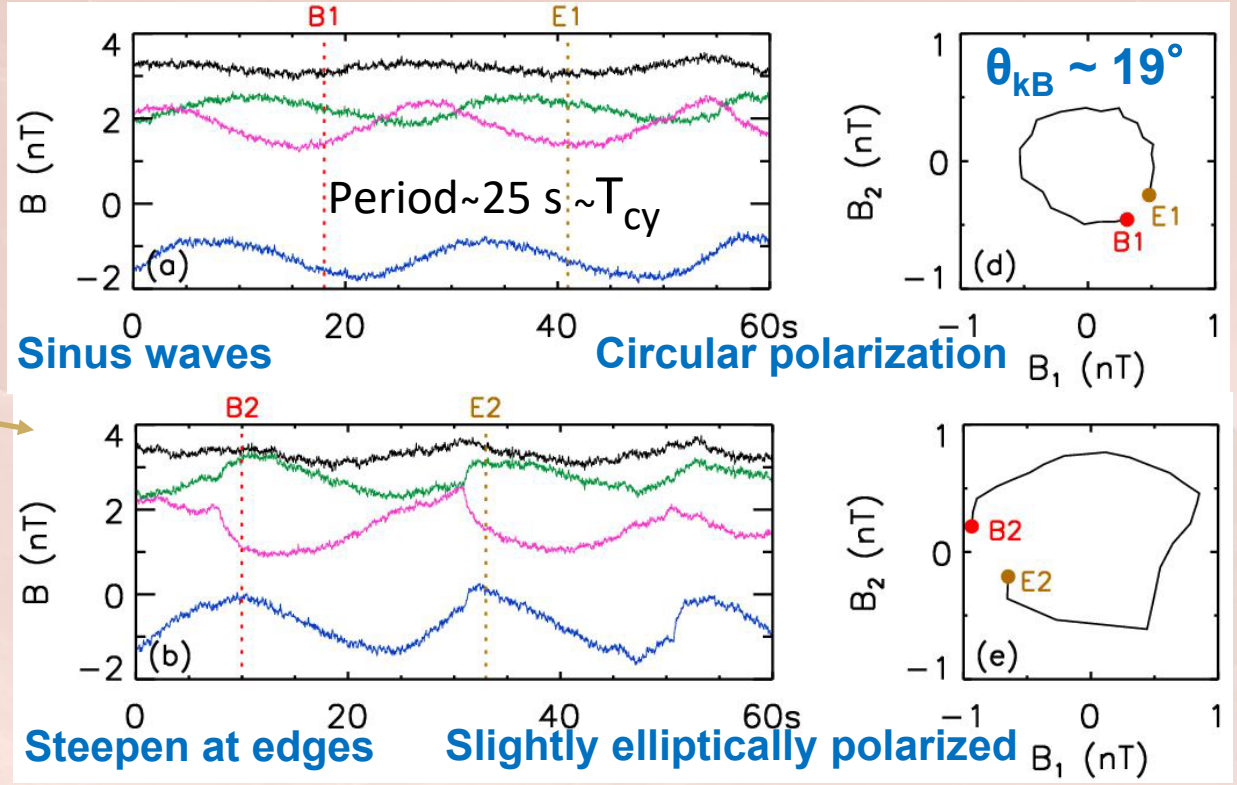

Shan +, ApJ 2020a

Newly pickup protons and quasi radial IMF lead to fast shock formation at Mars as for comets

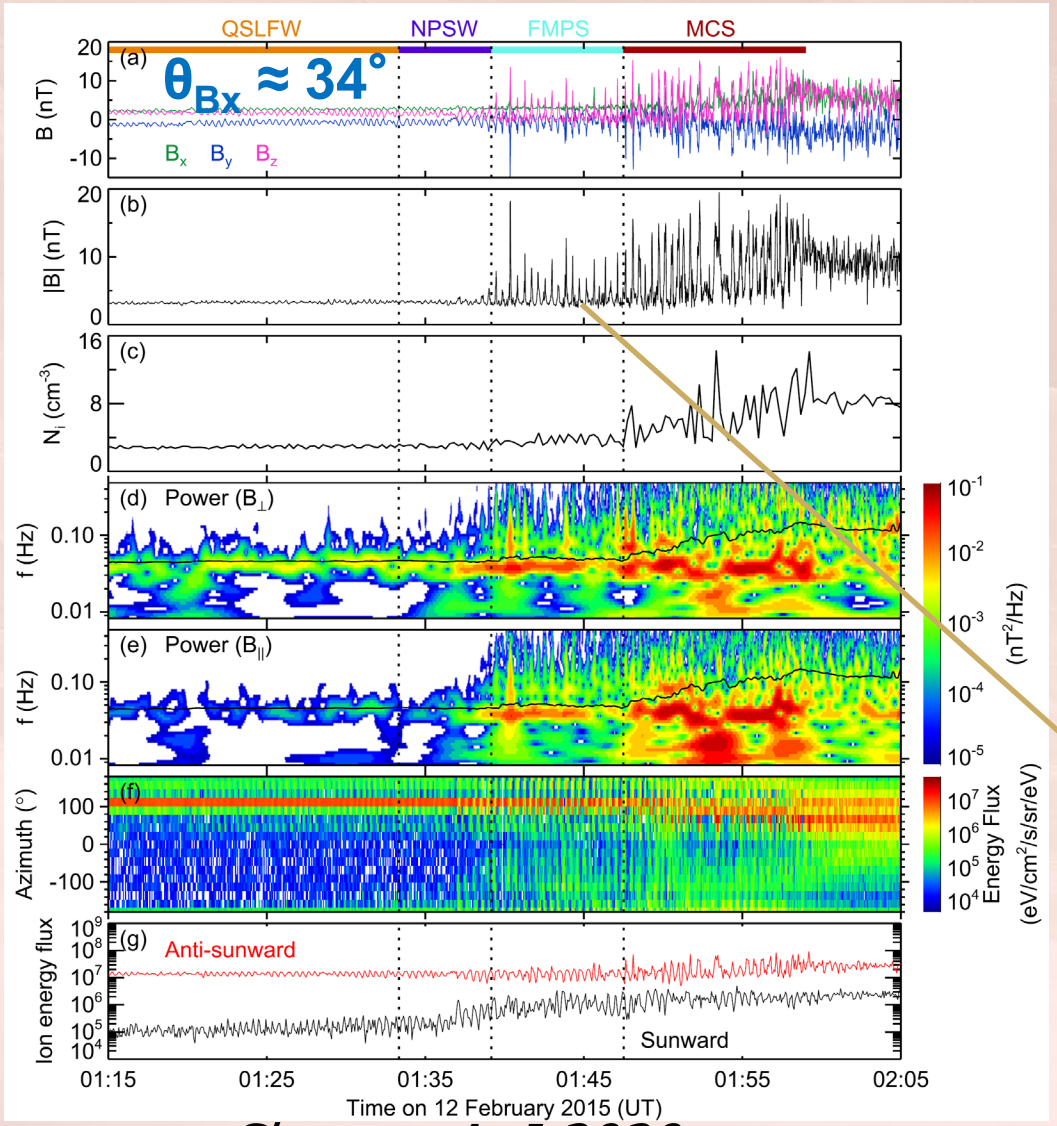

Shan +, ApJ 2020a

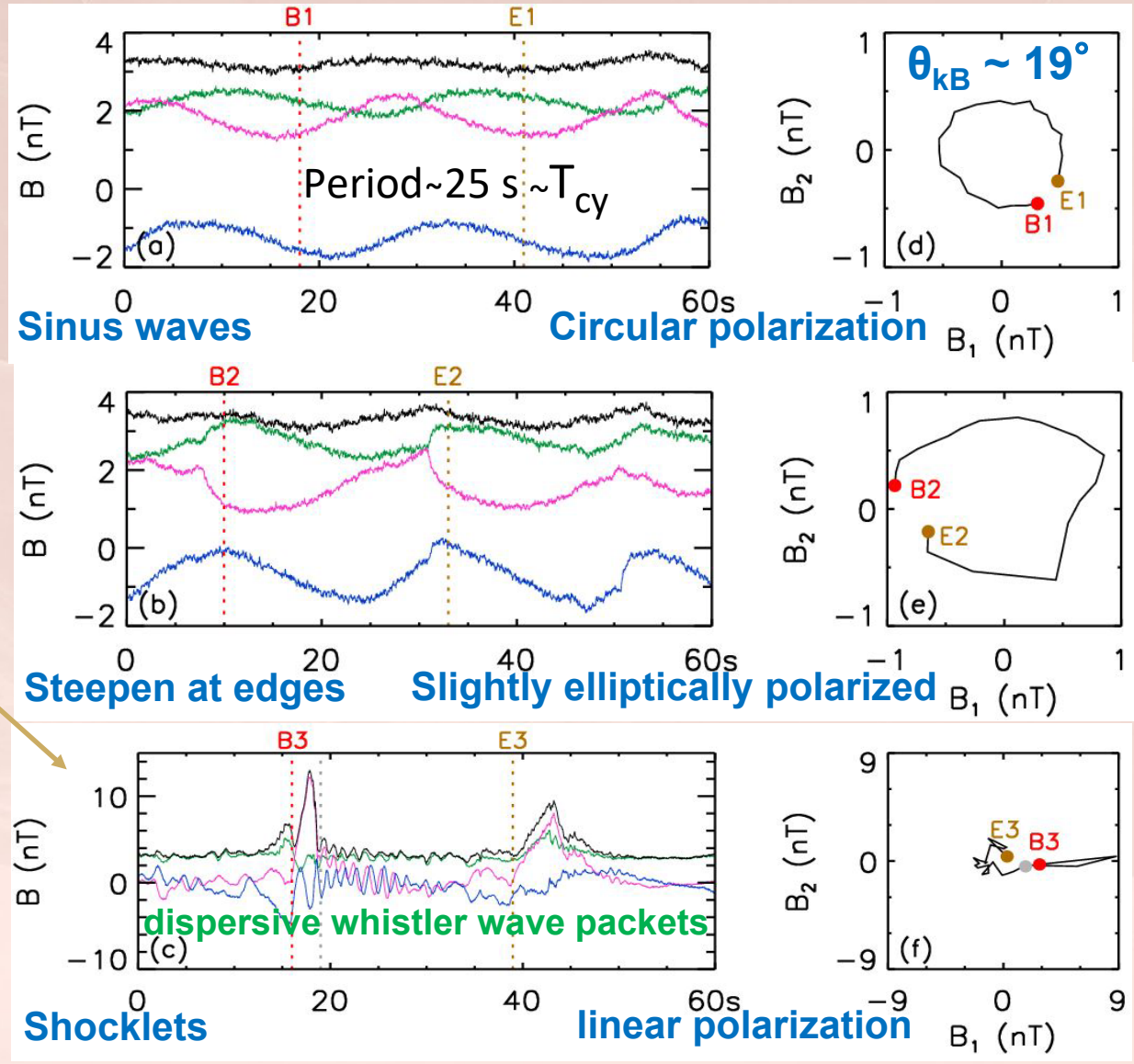

Newly pickup protons and quasi radial IMF lead to fast shock formation at Mars as for comets

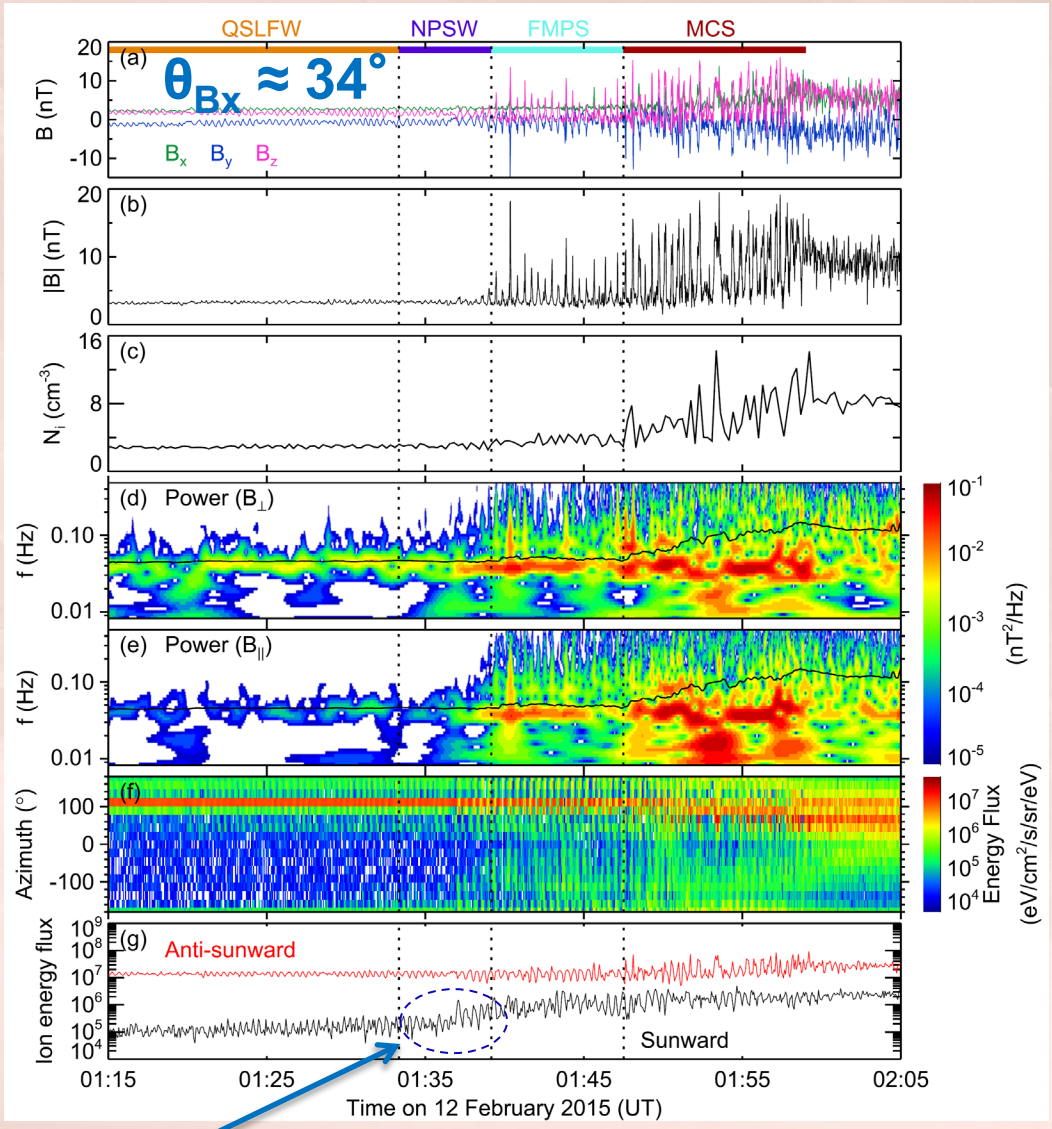

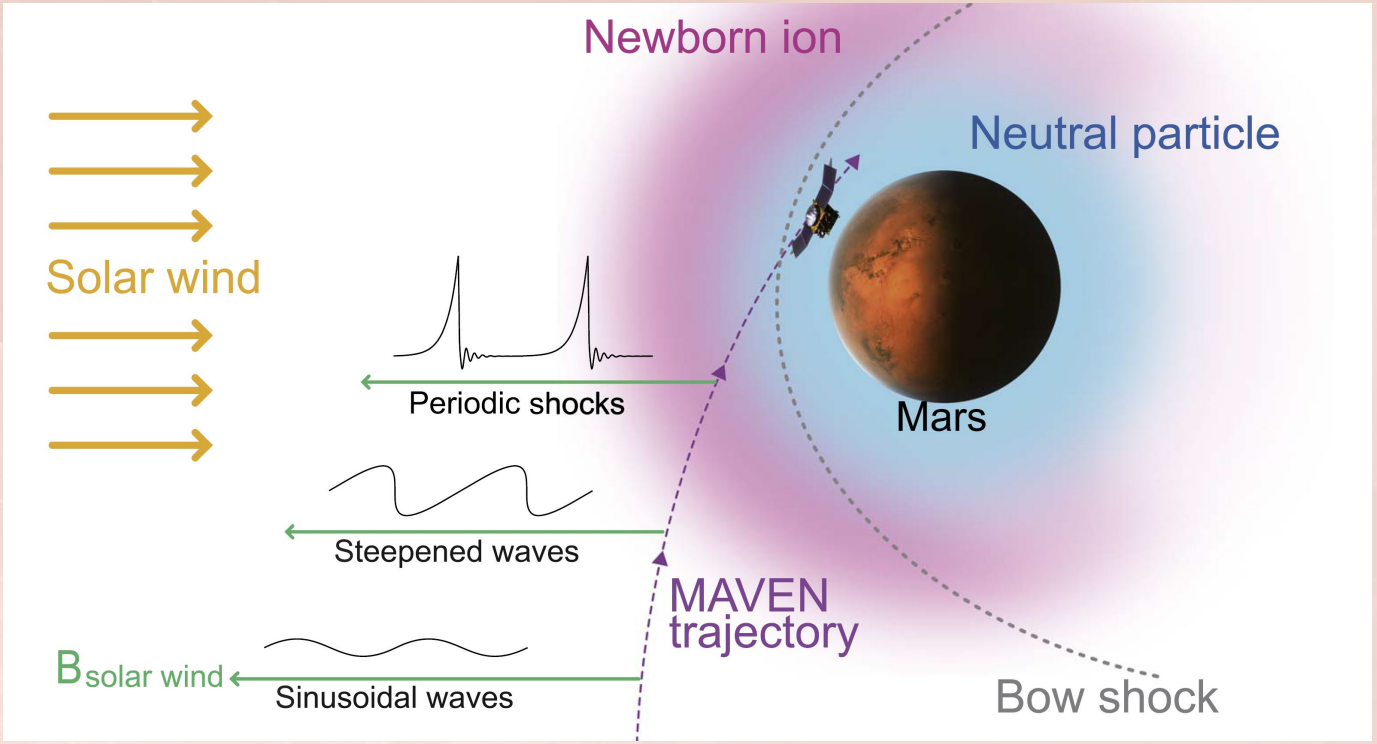

Similar properties for ULF waves @ comets
Tsurutani et al., 1987; Neubauer & Glassmeier, 1993; Mazelle +, 1995, 1997

The increasing sunward directed fluxes provided persistent energy for wave steepening. *Shan +, ApJ 2020a*

Shock with quasi-radial B-field (2)

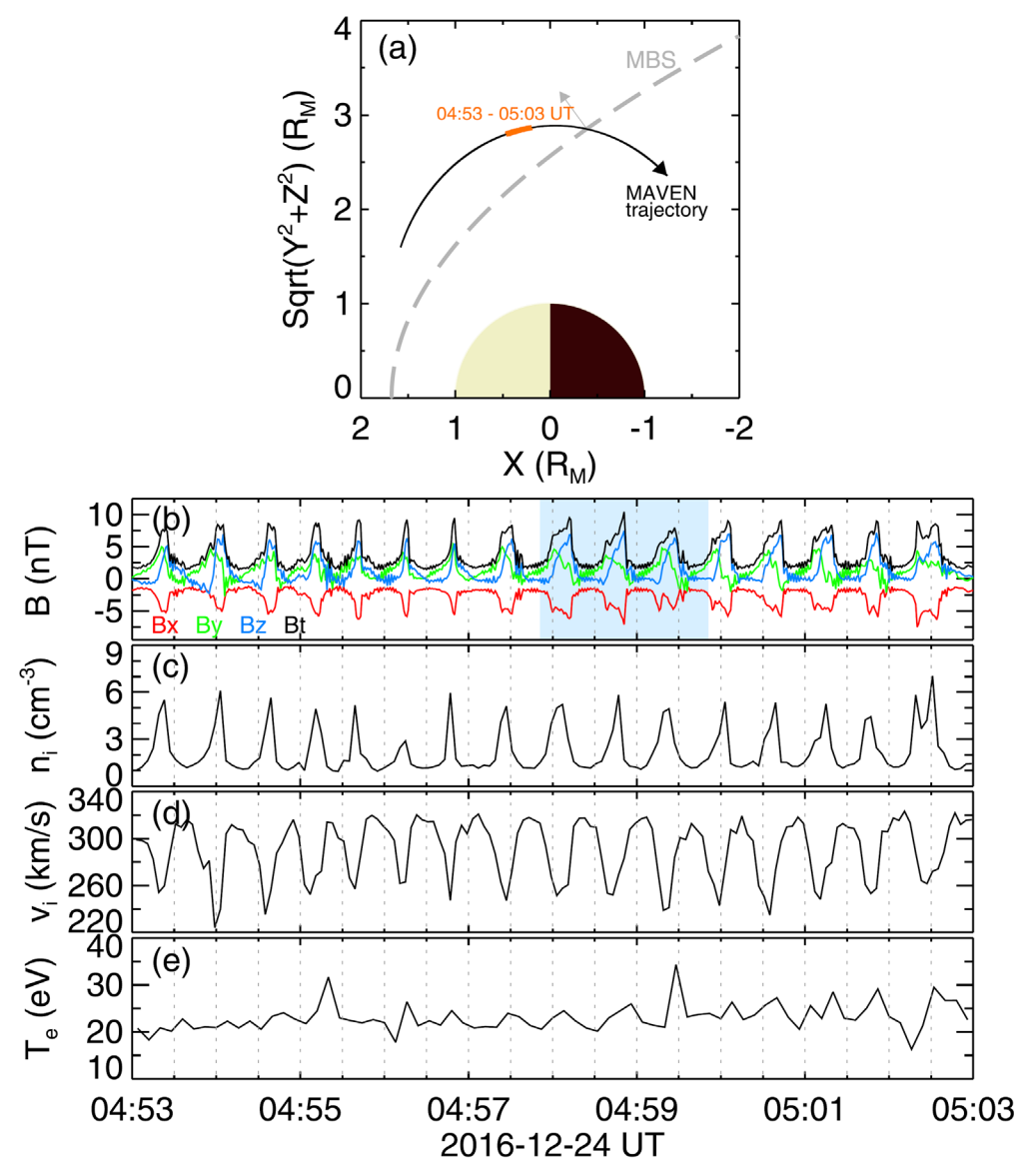

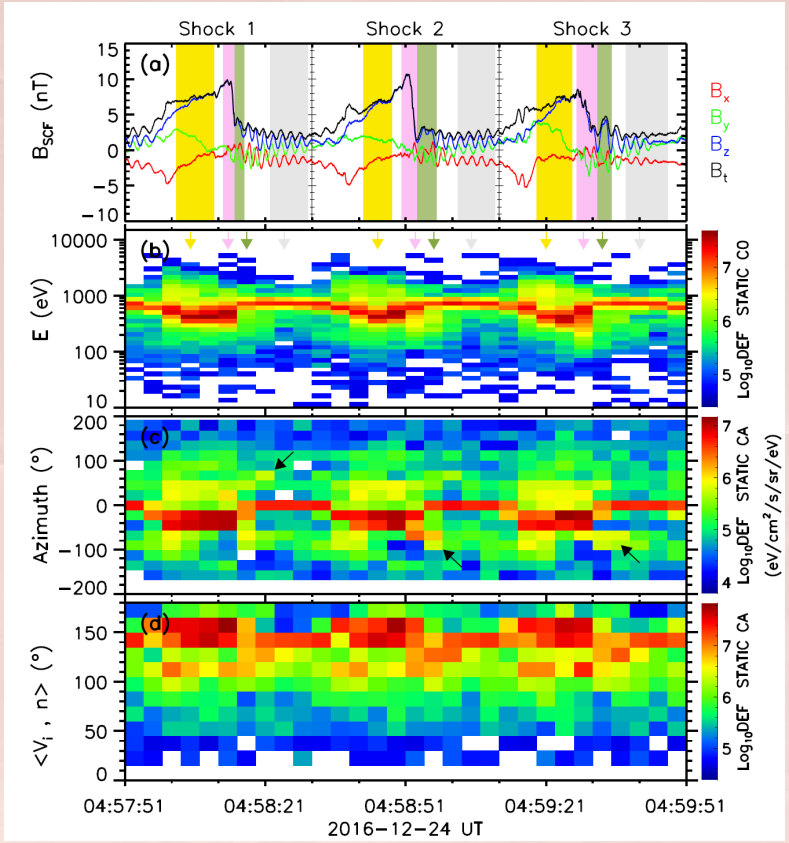

Dissipation at each ‘shocklet’ in the ion energy distribution

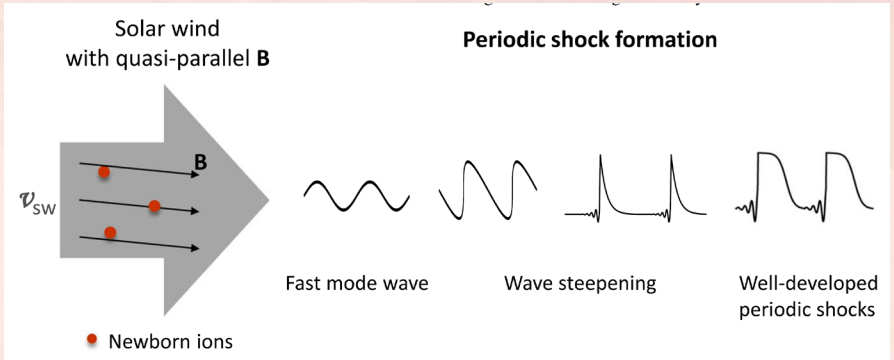

Shan + ApJ 2020b

Unusual Quasi-perpendicular bow shocks at Mars

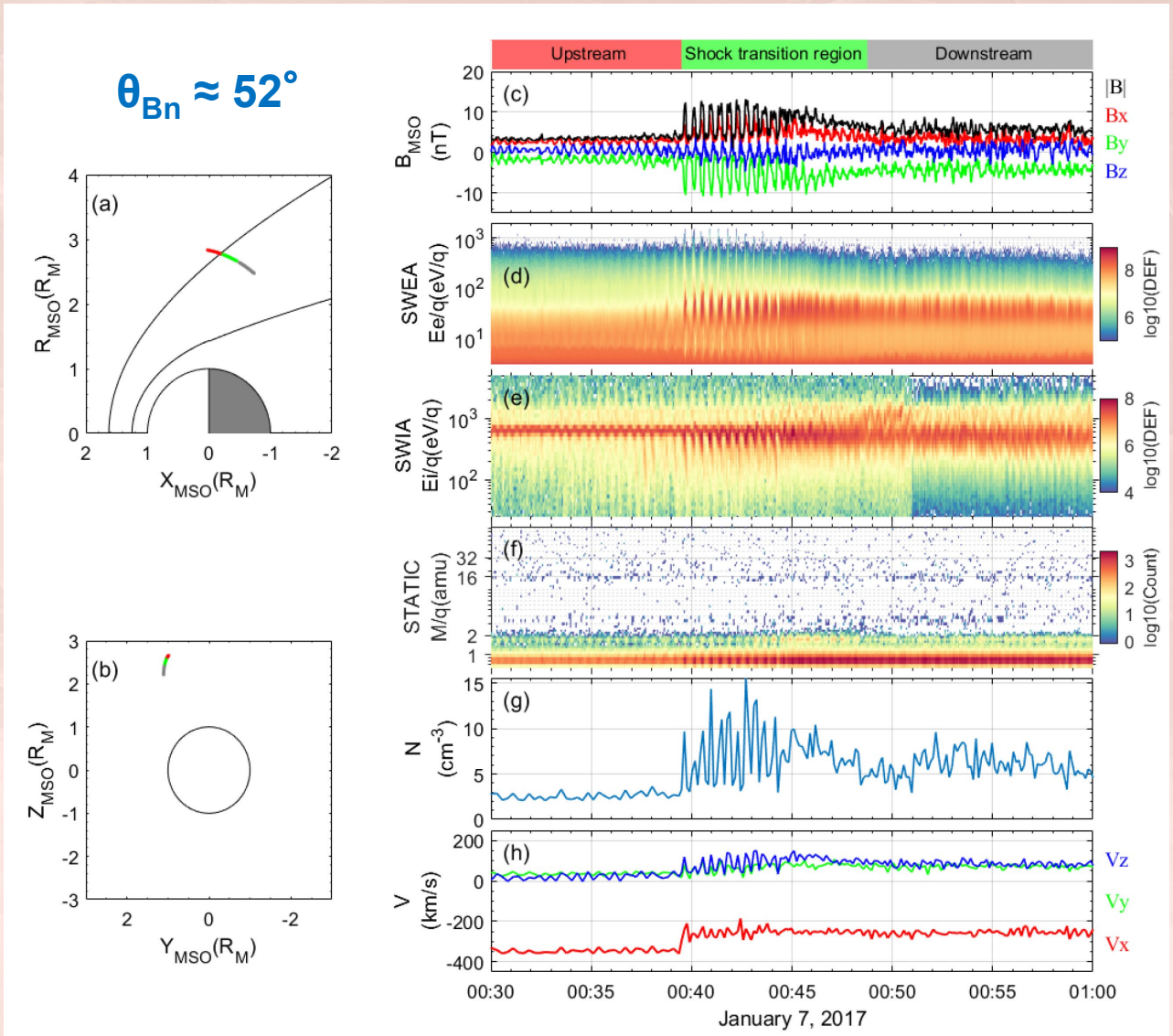

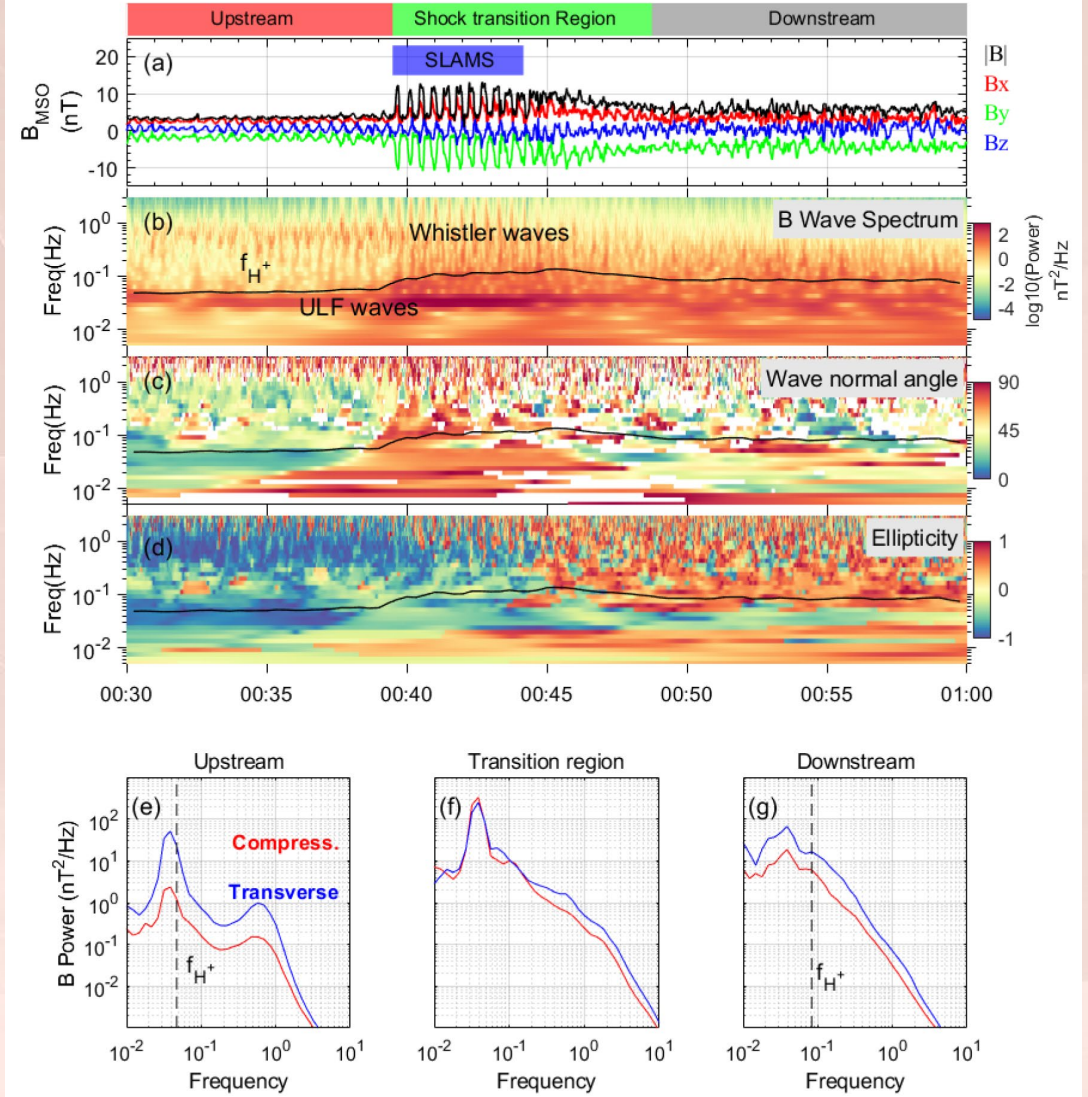

Shock reformation driven by ULF waves generated by pickup protons

Zhang+, AGU Advances 2025

Unusual HIGHLY Quasi-perp bow shocks at Mars!

Zhang+, AGU Advances 2025

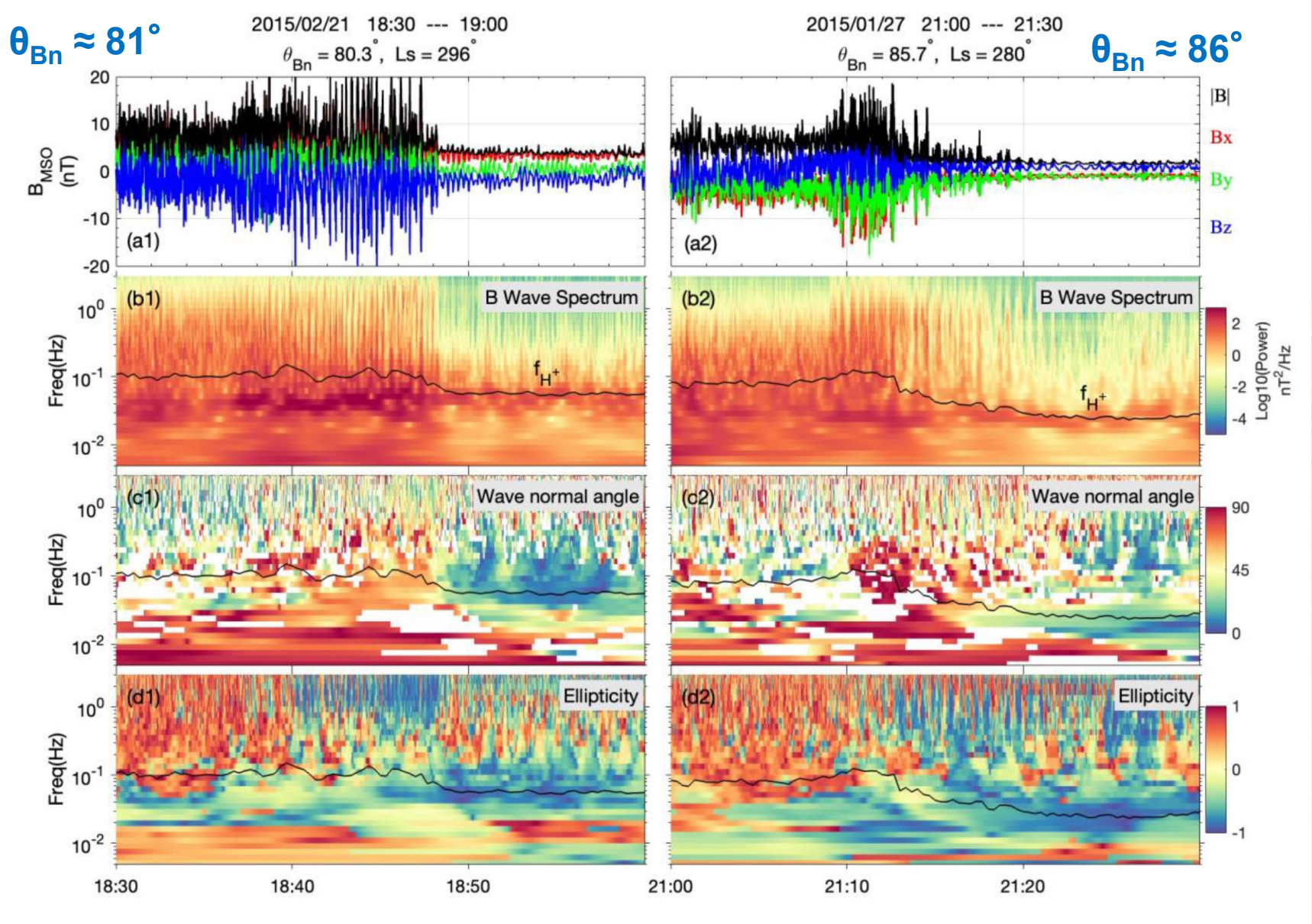

ULF waves (PCWs) upstream from nearly perp shocks!

Never for *e.g.* the terrestrial case

Open questions:

Role on the ion reflection?

Possibility of DSA?

Fermi type II?

Foreshocks

Superthermal electrons are good tracers of the magnetic connection to the bow shock

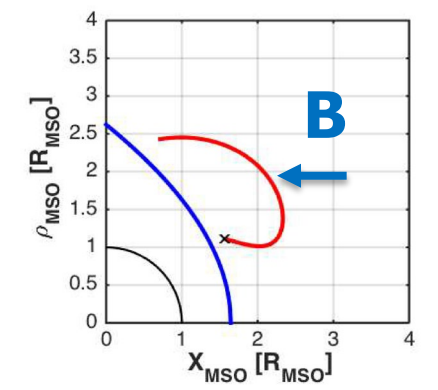

IMF ~ radial

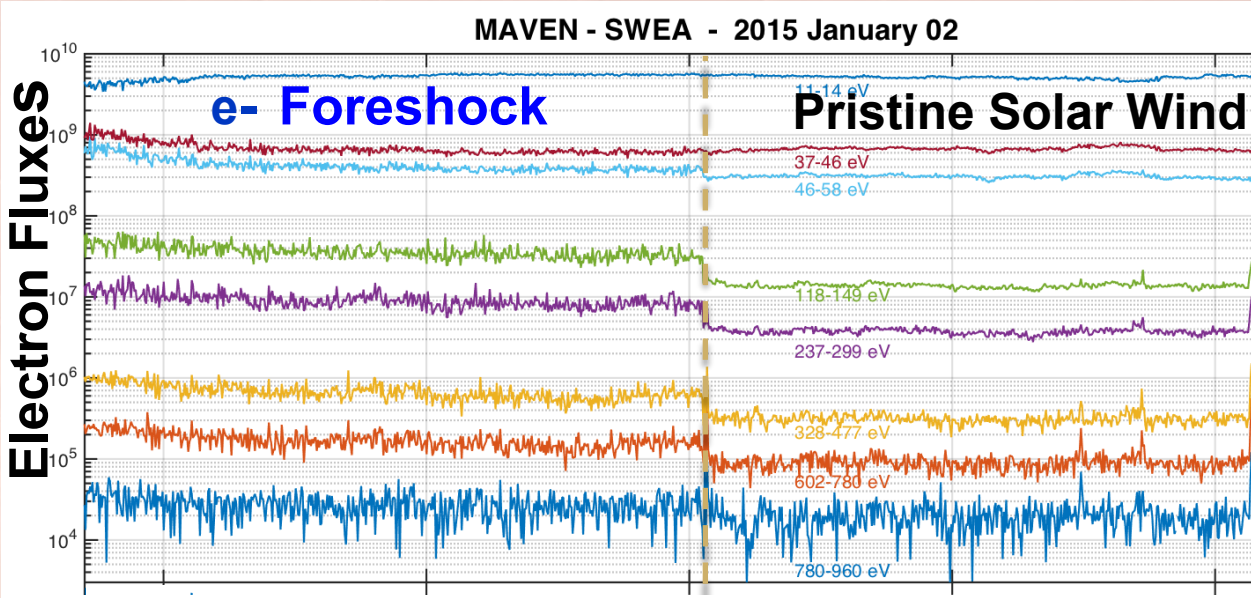

Connection model :

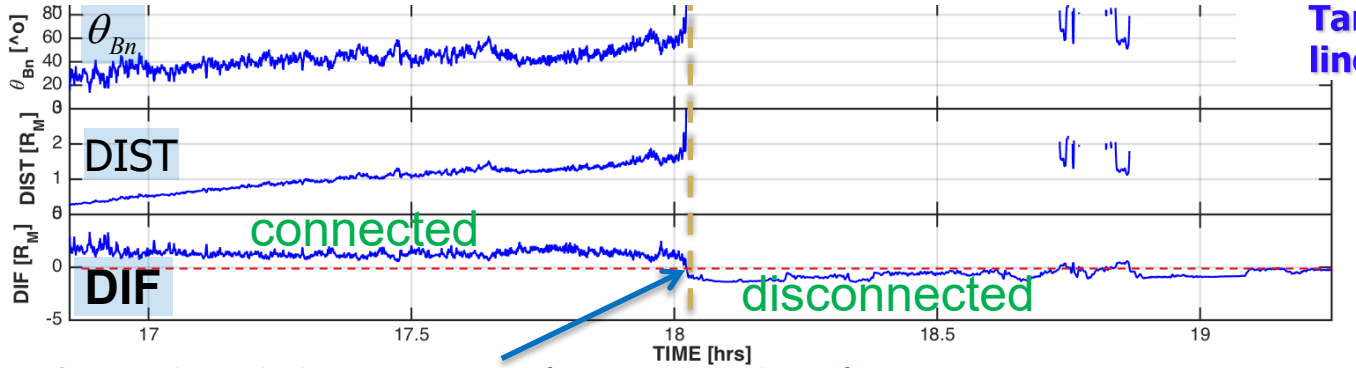

Electron foreshock boundary (tangent line)

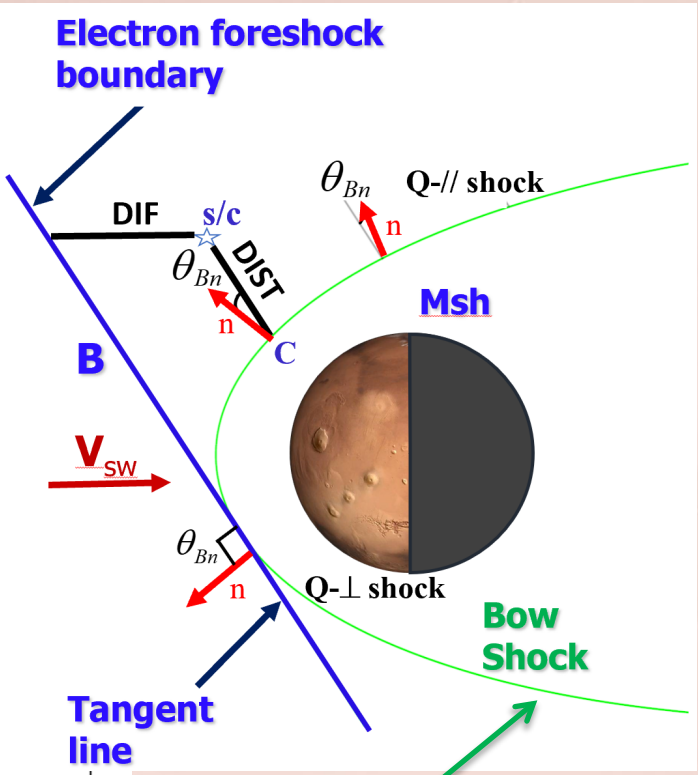

Bow shock model (fit):
Vignes+ 2000;
Trotignon+ 2006;
Gruesbeck+ 2018

after Meziane, Mazelle+ 2017

Ion distributions upstream from the Shock ramp: Earth

Gyrophase-bunched

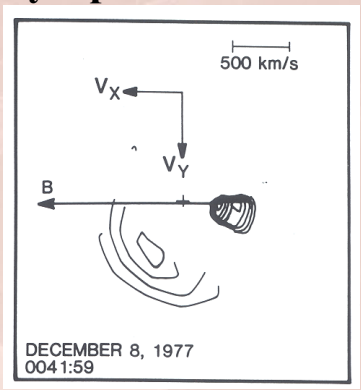

'Intermediate' distribution

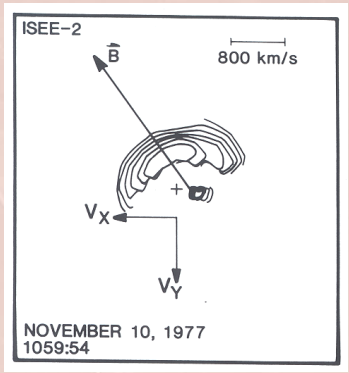

Field-aligned beam

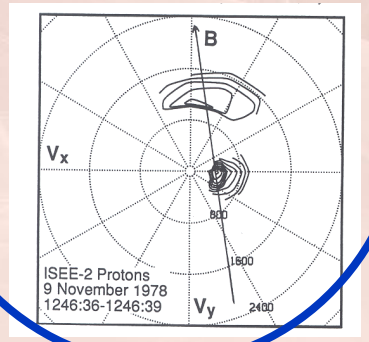

Quasi-perpendicular

Quasi-parallel

Gyrotropic distribution

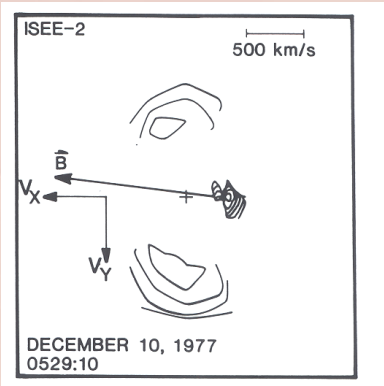

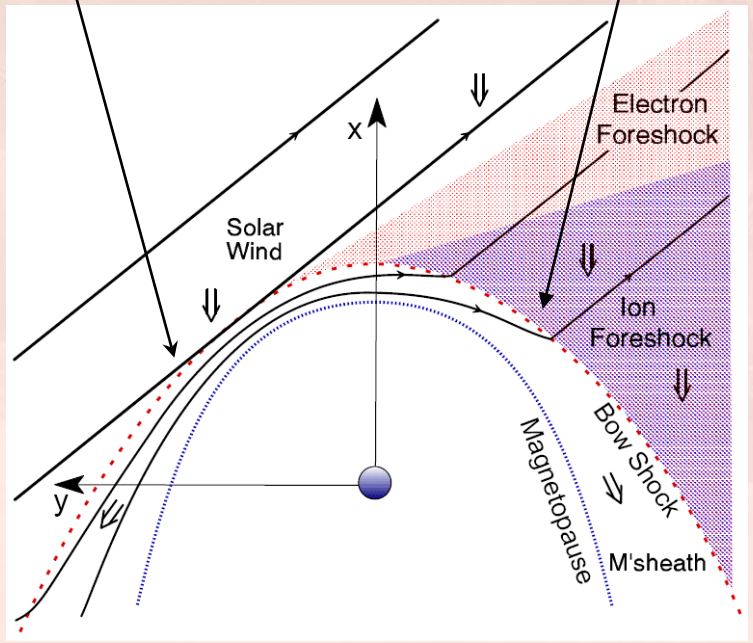

Specularly reflected ions

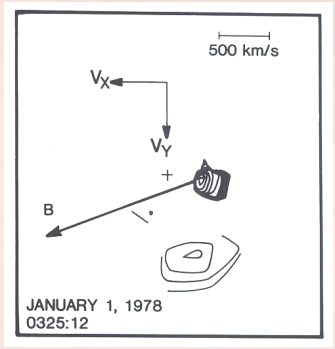

diffuse distribution

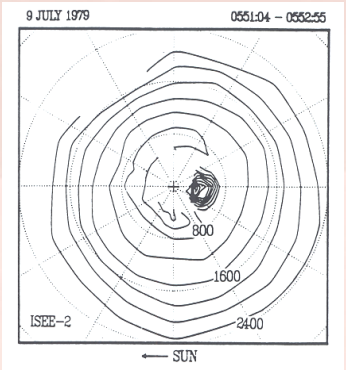

Foreshock Field-Aligned Beams: terrestrial 'paradigm'

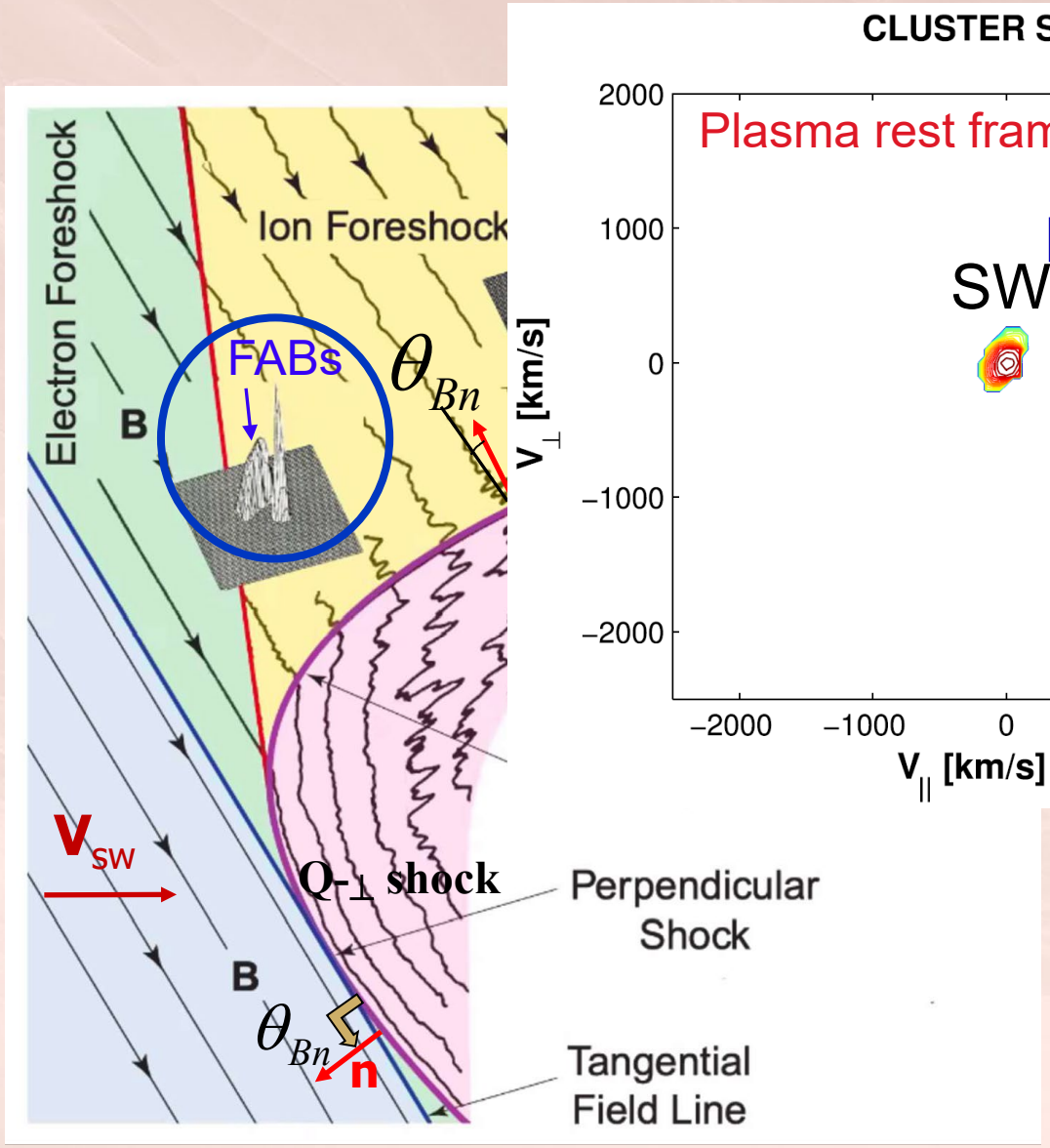

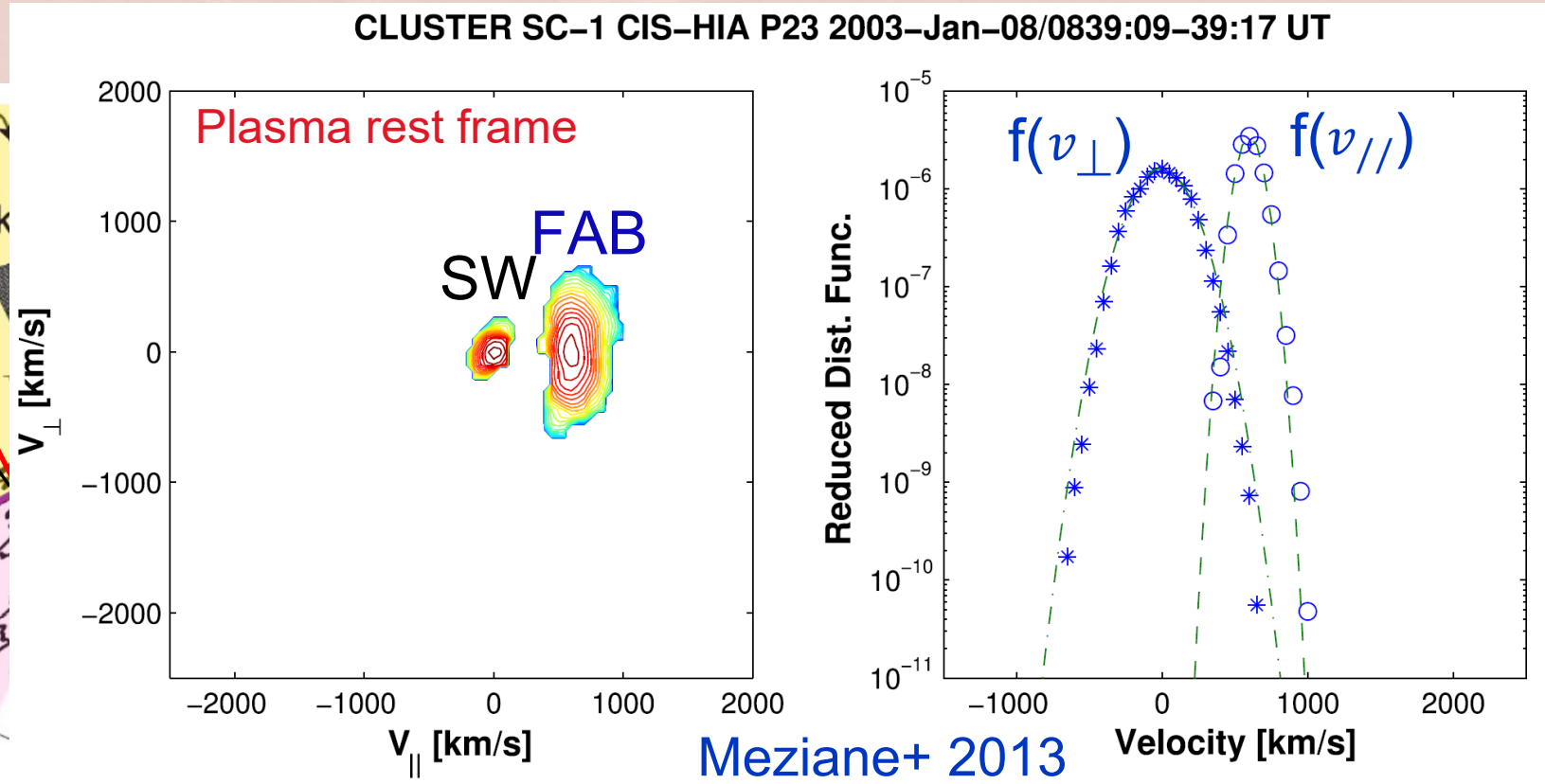

Foreshock Field-Aligned Beams: terrestrial 'paradigm'

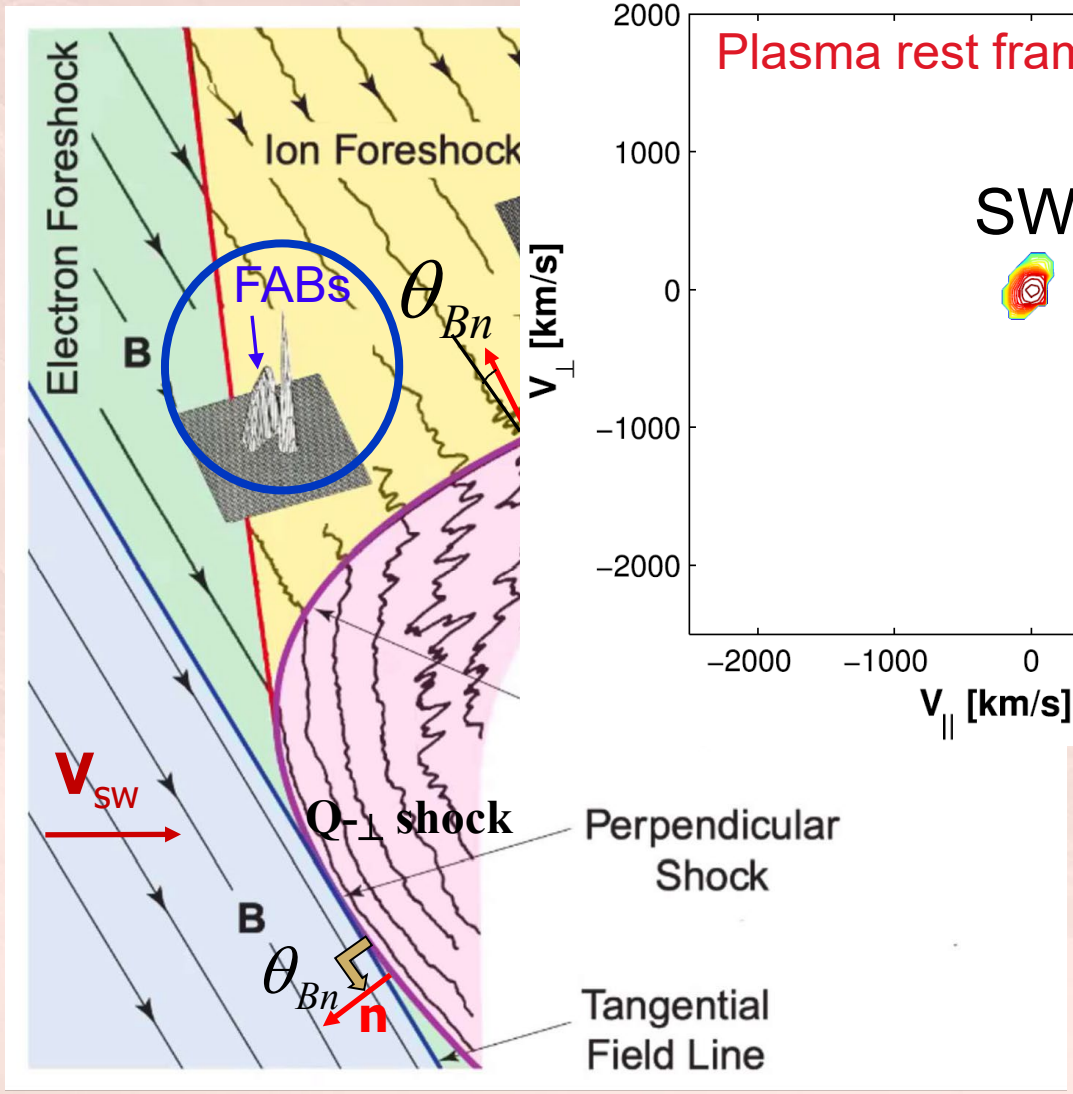

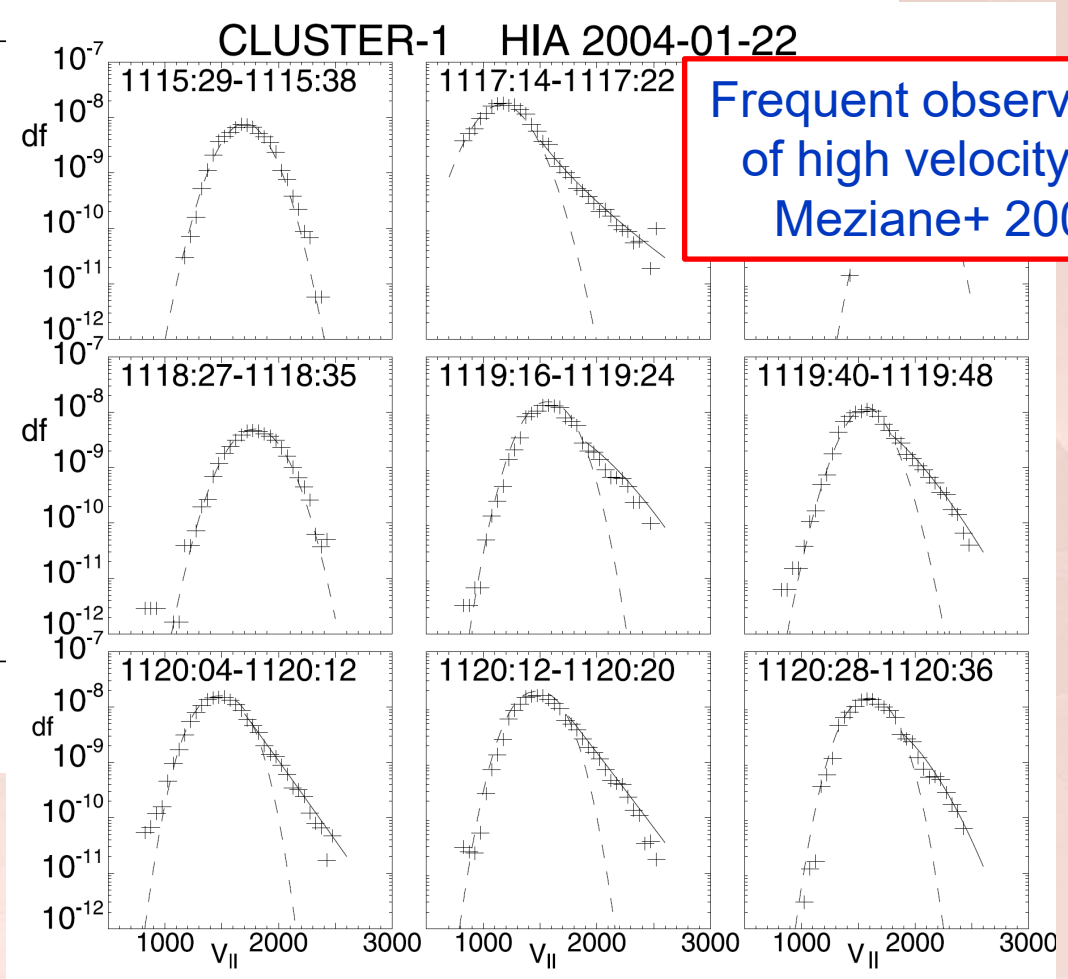

Frequent observation of high velocity tail Meziane+ 2007

Foreshock Field-Aligned Beams: terrestrial 'paradigm'

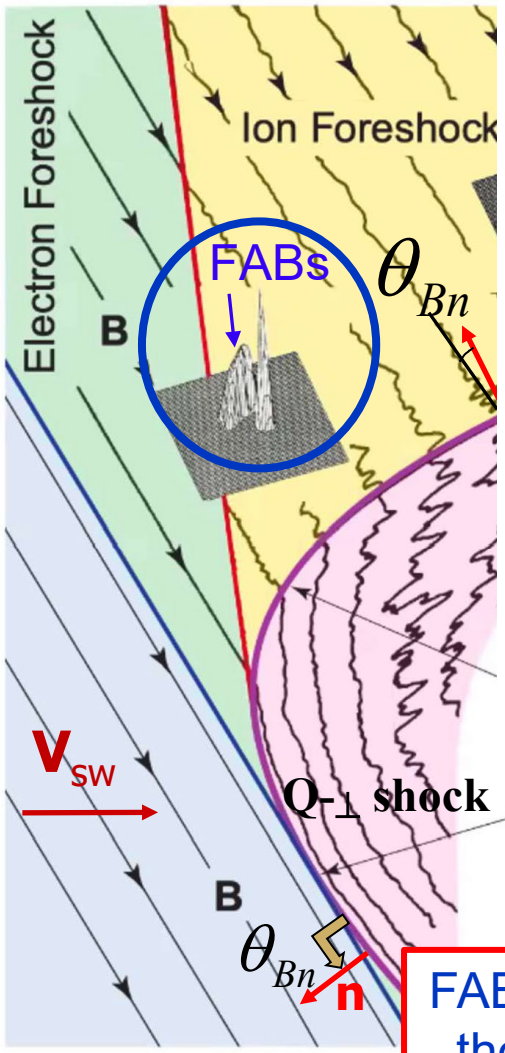

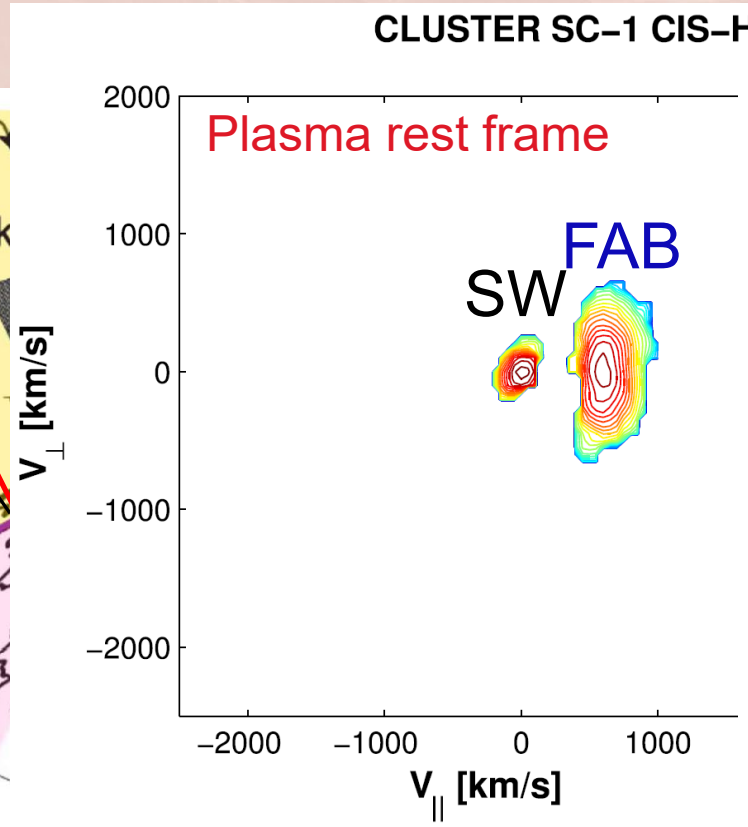

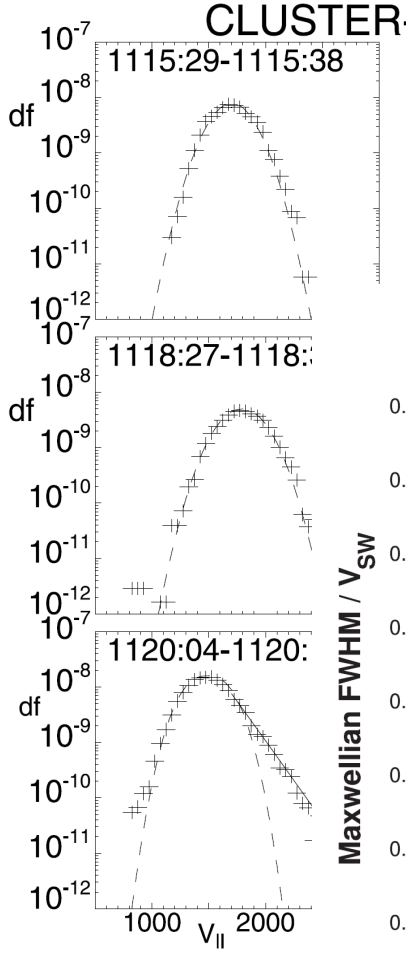

Frequent observation of high velocity tail Meziane+ 2007

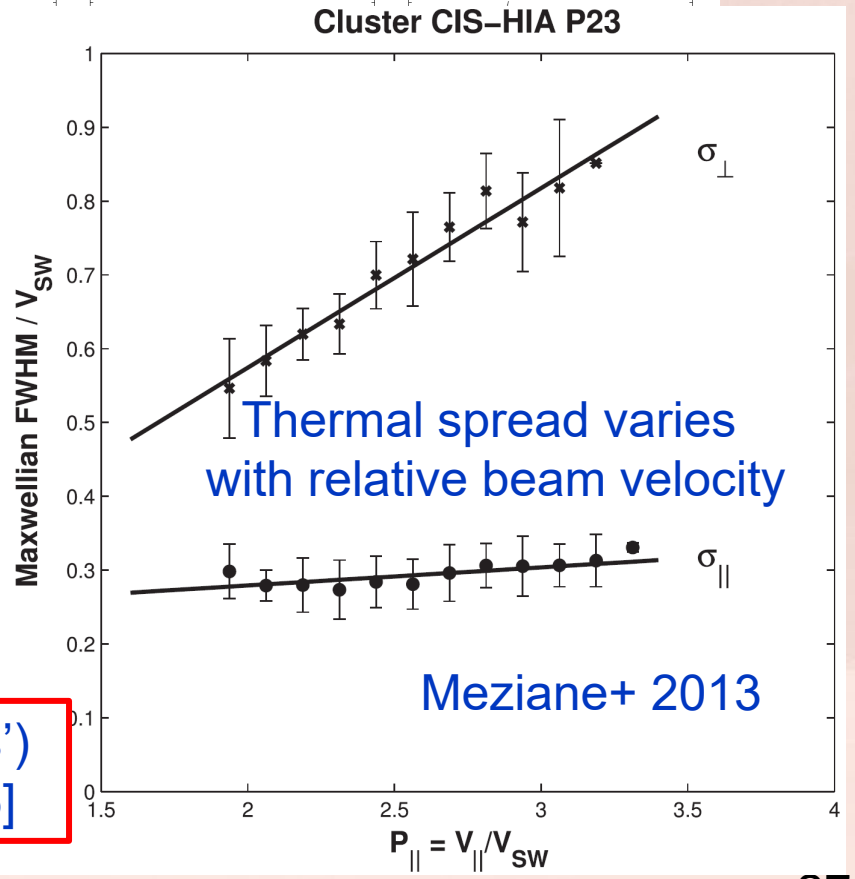

FABs: sources of ULF waves (so-called '30s waves') though cyclotron resonance [Mazelle+ 2003; 2005]

About Martian Pickup Ions

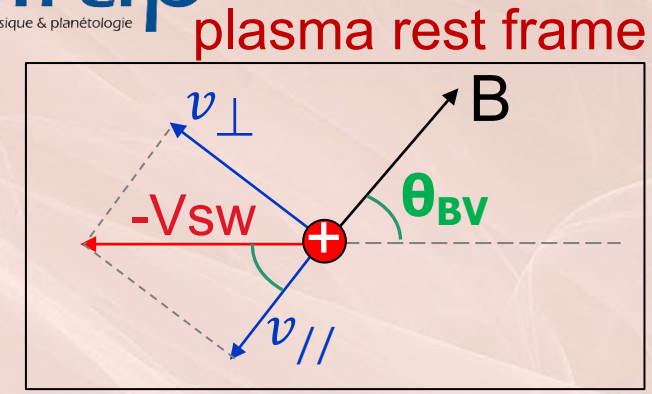

$$v_\perp = V_{sw} \sin(\pi - \theta_{BV})$$

$$v_{//} = V_{sw} \cos(\pi - \theta_{BV})$$

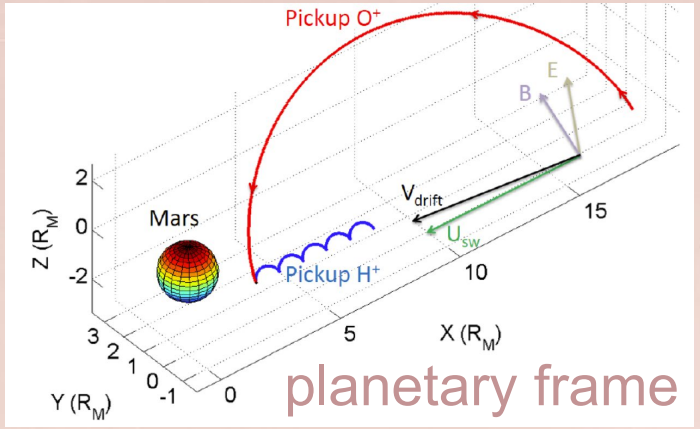

acceleration by convective electric field

Adapted from Ali Rahmati

- Newly created ions: initial ring-beam velocity distribution in the plasma rest frame (SW)
- **Initial pitch-angle = π-θ_{BV}** ; θ_{BV} : local angle between the flow velocity and B (cone angle).
- Initial energy E_0 in the SW frame for protons : $E_0 \leq E_{sw}$ where $E_{sw} = {}^1/_2 m_p V_{sw}^2$
- Not yet significant scattering in energy and pitch angle through wave-particle interaction (on longer characteristic time scales, *e.g.*, Yoon+ 1991)
- Inside the **foreshock**, **solar wind ions, shock-reflected ions, and pickup ions** must be differentiated.

First in-depth study of the Martian Ion Foreshock

Meziane, Mazelle+ GRL 2025

MAVEN location

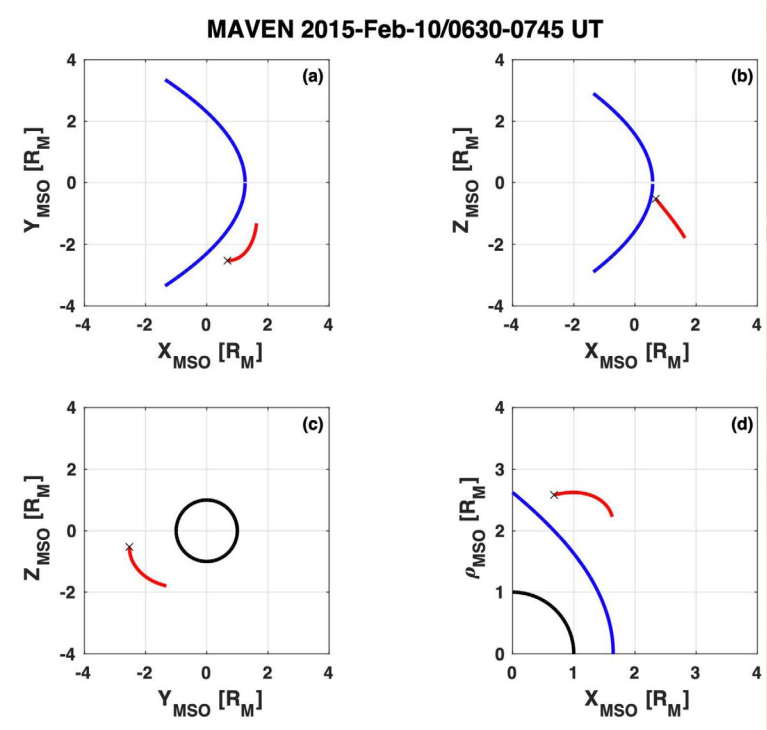

Field-Aligned Beams

Pitch-angle distributions in the solar wind rest frame

Pickup protons

Superimposed black line is the local π-θ_{BV} (here between 50 and 90 deg.)

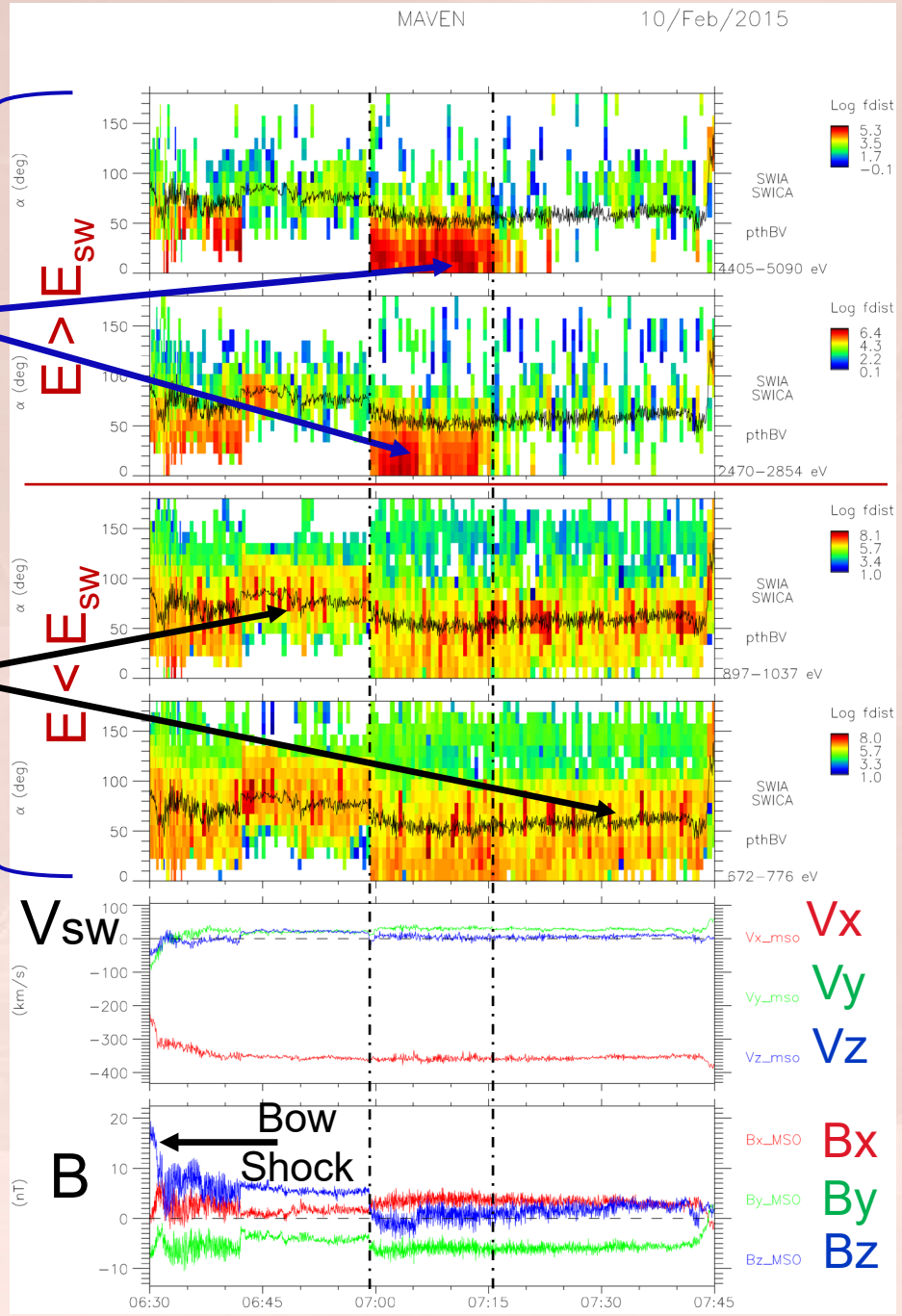

PADs reveal that newly pickup protons are always present with maxima around the theoretical value and with their associated waves (PCWs).

Another population is observed with lower pitch-angles and for higher energies than E_{sw} inside a specific time interval.

Shock connection analysis results

θ_{BV} values reveal non field-aligned pickup protons (pitch-angle around 50 deg.) during the time of interest.

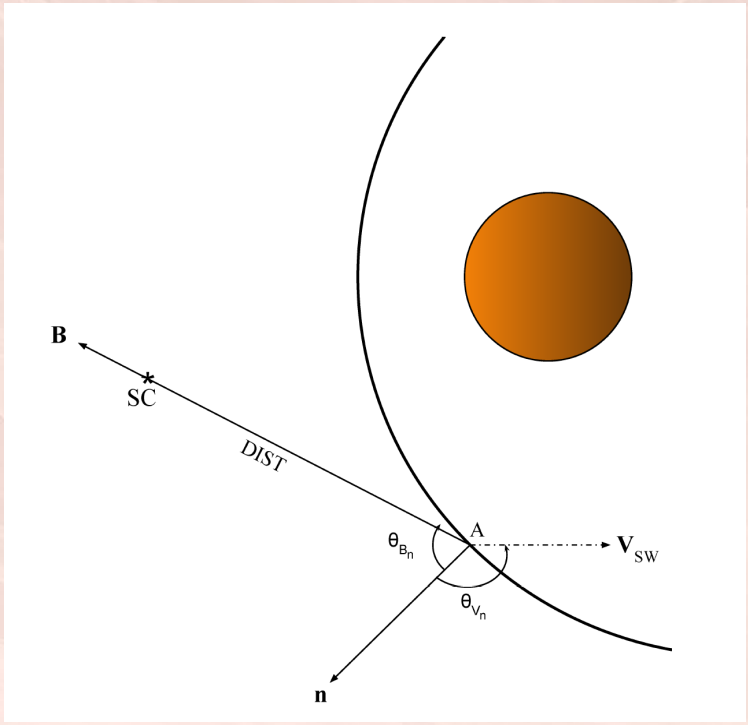

Connection Parameters (model: Vignes+ 2000)

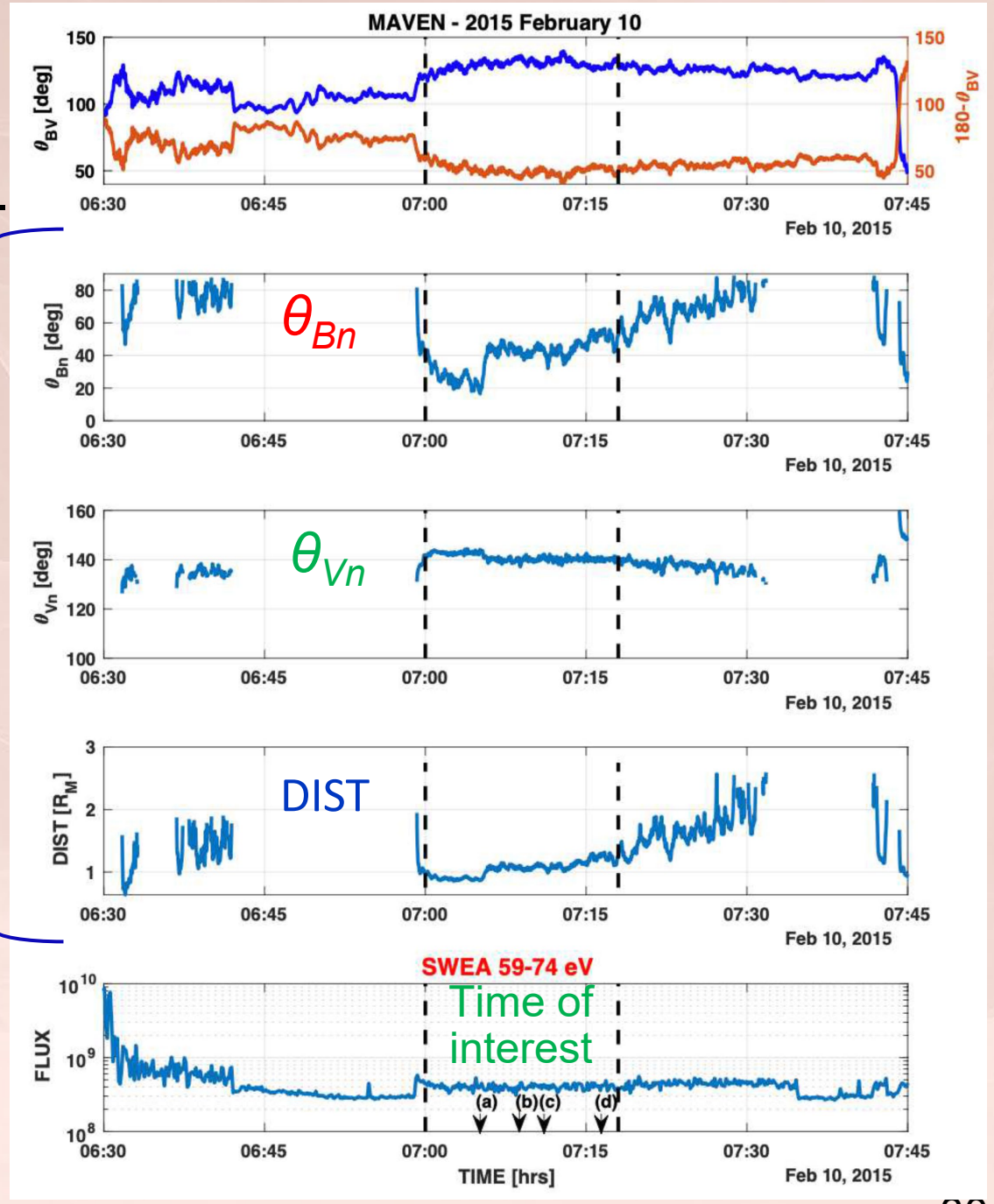

Superthermal electrons reveal magnetic connection to the shock during the time of interest for the FABs

Ion velocity distributions: plasma rest frame

2D $v_{//}$ $v_{\perp}$ distributions

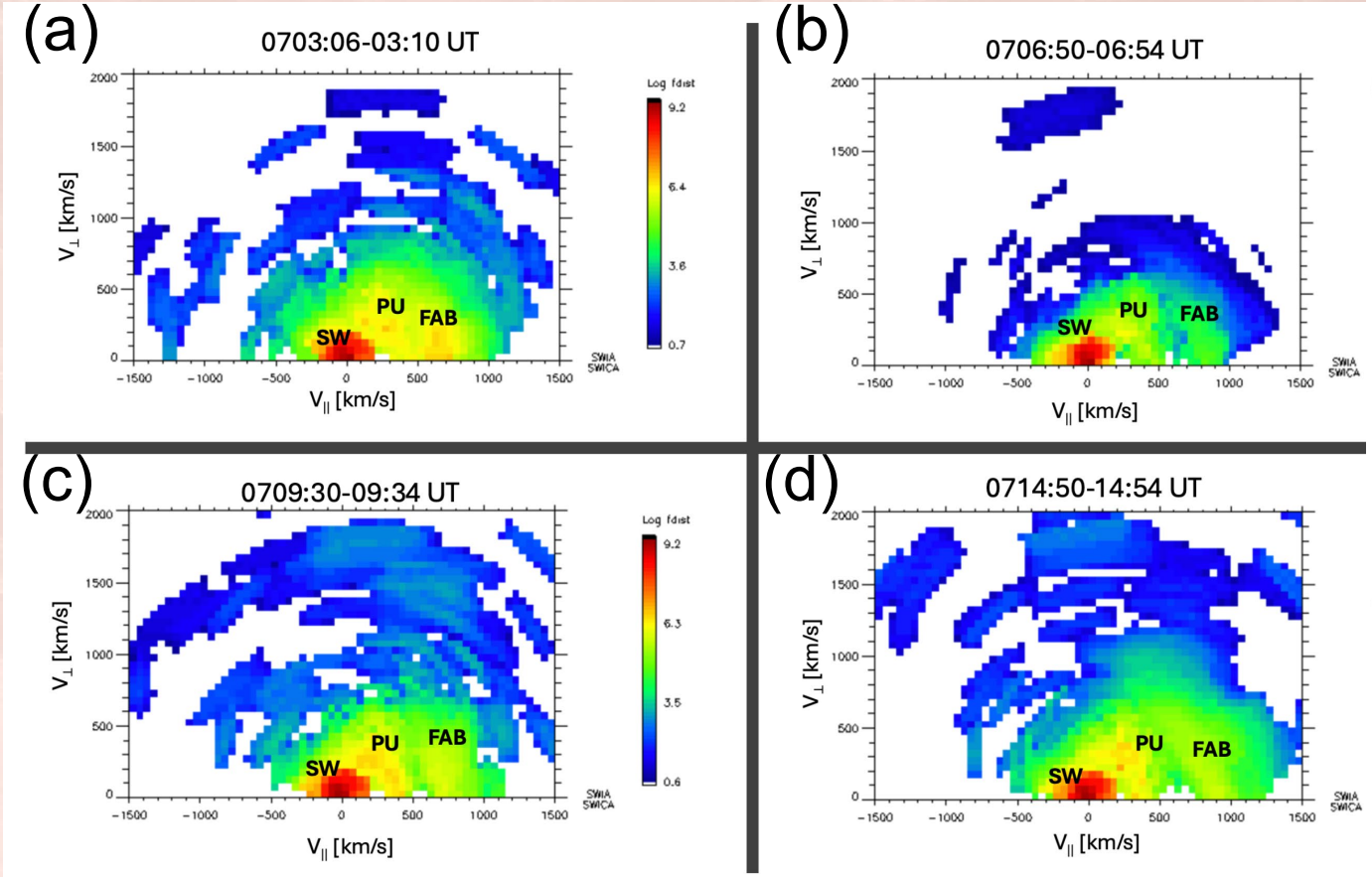

reduced distributions f($v_{//}$)

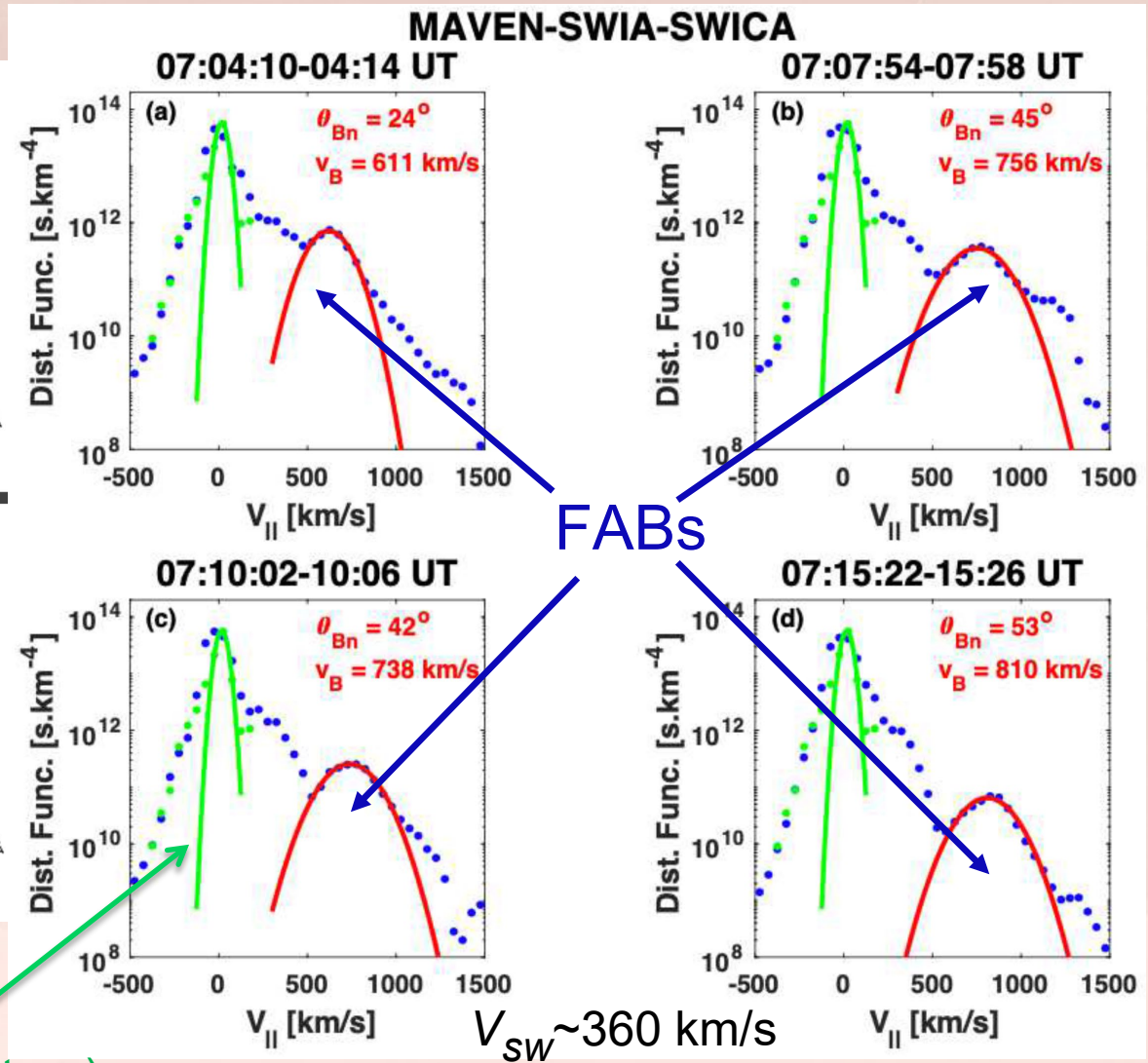

Core SW proton dist. fitted from specific high-angular resolution product (more representative of real SW temperature)

V_{sw}~360 km/s

Mechanism of particle reflection?

- ✓ Specular Reflection: Inversion of the incident particle velocity (in the deHoffmann-Teller frame): $V_{||} = -2(\mathbf{Vi}\cdot\mathbf{n})\cos(\theta_{Bn})$

- ✓ Escape [Shock] Speed $V_S = \mathbf{Vi}\cdot\mathbf{n}/\cos(\theta_{Bn})$

Specular reflection of a portion of the solar wind accounts for backstreaming ion distributions seen in the quasi-parallel terrestrial foreshock (Gosling+, 1982).

This mechanism produces ion distributions that are field-aligned only for a parallel shock geometry ($\theta_{Bn} \sim 0$).

In addition, the post-encounter parallel ion velocity decreases when the shock θ_{Bn} increases.

Consequently, the observations **rule out specular reflection as the mechanism responsible for the production of FABs.**

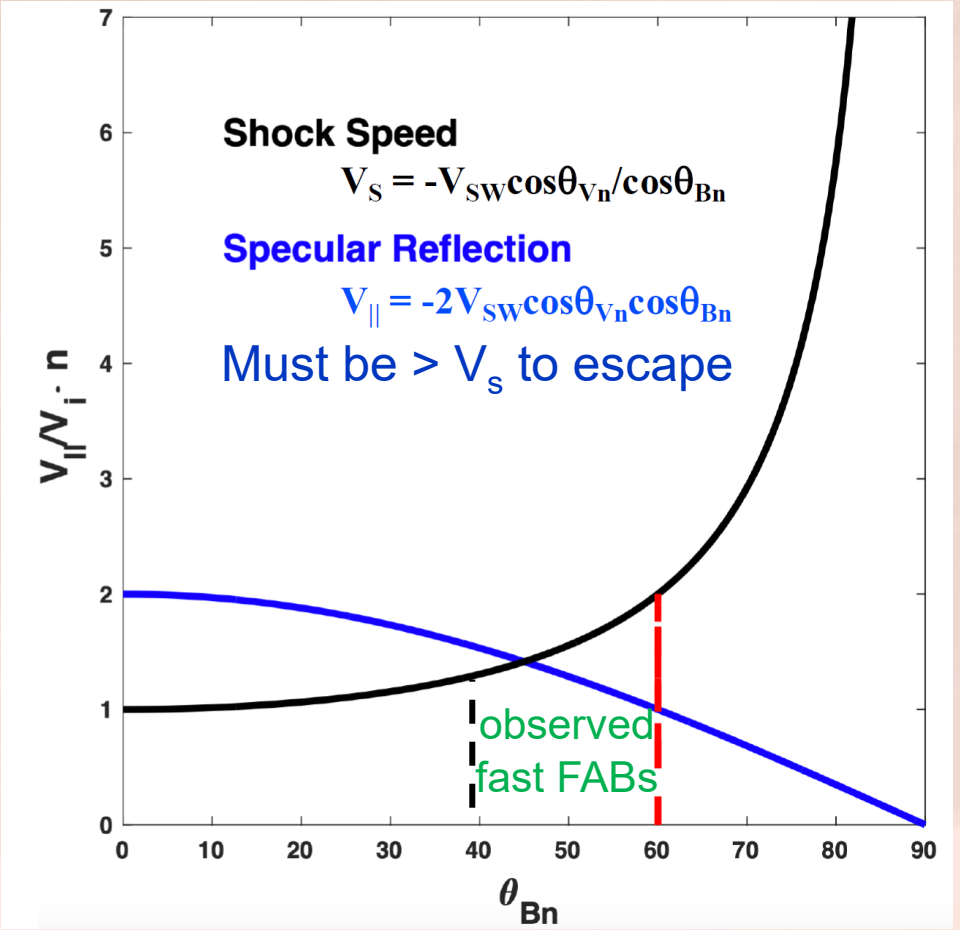

Mechanism of particle reflection

Quasi-adiabatic reflection:

$$p = -(1+\delta)p_s$$

$$0 < \delta \leq 1$$

Meziane+,2004

Adiabatic: δ = 1

Earth: δ = 0.85-1

Paschmann+,1980

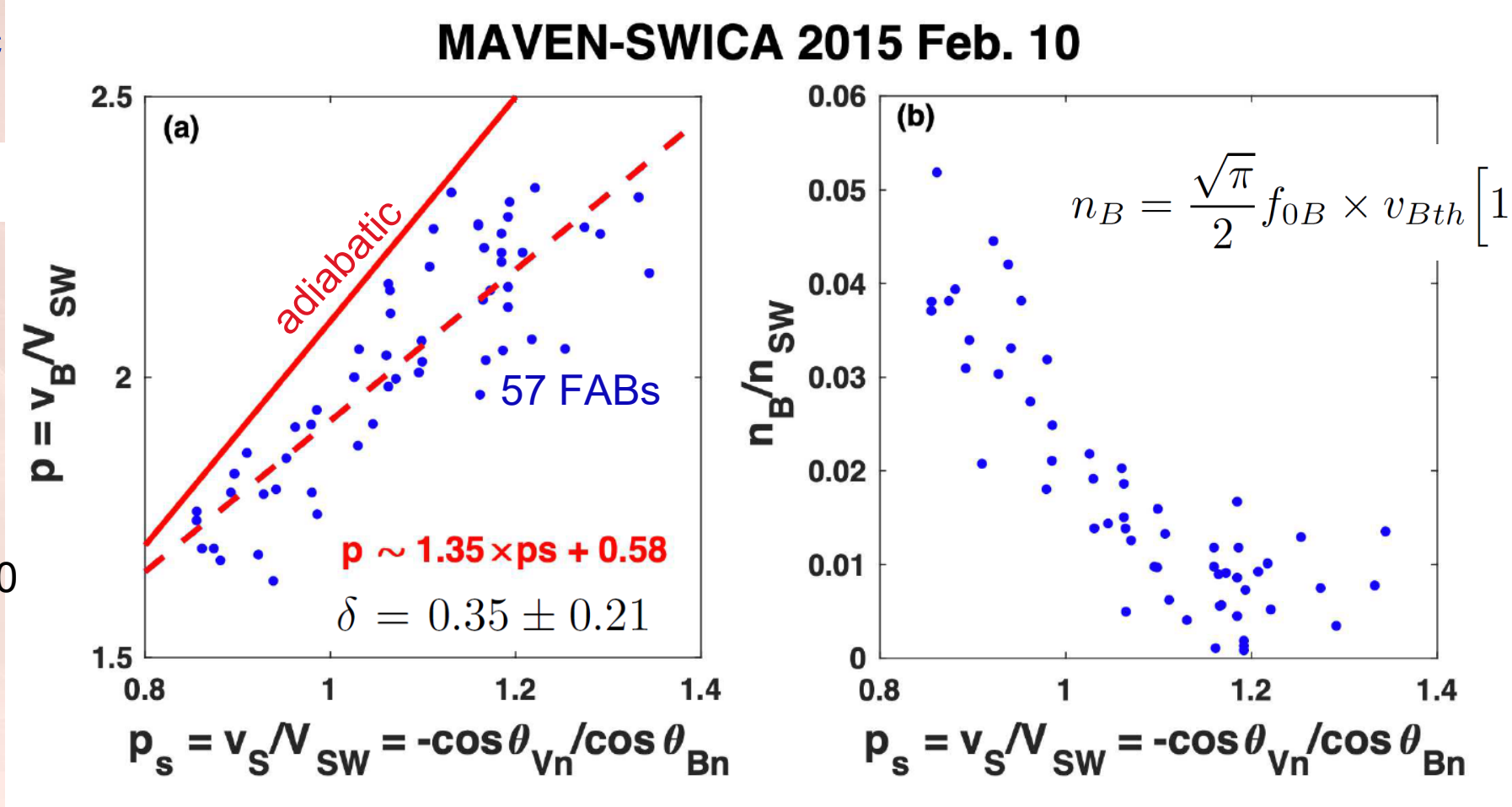

$$n_B = \frac{\sqrt{\pi}}{2} f_{0B} \times v_{Bth}\left[1 + erf\left(\frac{v_B}{v_{Bth}}\right)\right]$$

In all cases, the Martian FABs speed appears significantly smaller than their terrestrial counterpart. The agreement with the reflection model indicates that the Martian FABs agree well with the known characteristics of the terrestrial foreshock counterparts.

ULF Foreshock waves: frequency vs magnetic field

- ULF foreshock waves associated with backstreaming ions have been reported in several planetary foreshocks (*Hoppe & Russell, 1982; Gosling +, 1982; Mazelle + 2003; Andrés +, 2015; Romanelli +, 2020*)
- Different wave types (quasi-monochromatic 30 s, steepended waves, '1 Hz' waves,…) have been associated with different backstreaming ion distributions at the Earth (*Hoppe & Russell, 1983*).
- Narrow frequency bandwith waves (so-called 'quasi-monochromatic') generated through cyclotron resonance with backstreaming FABs (protons).
- **Therefore, can these waves exist at Mars?**

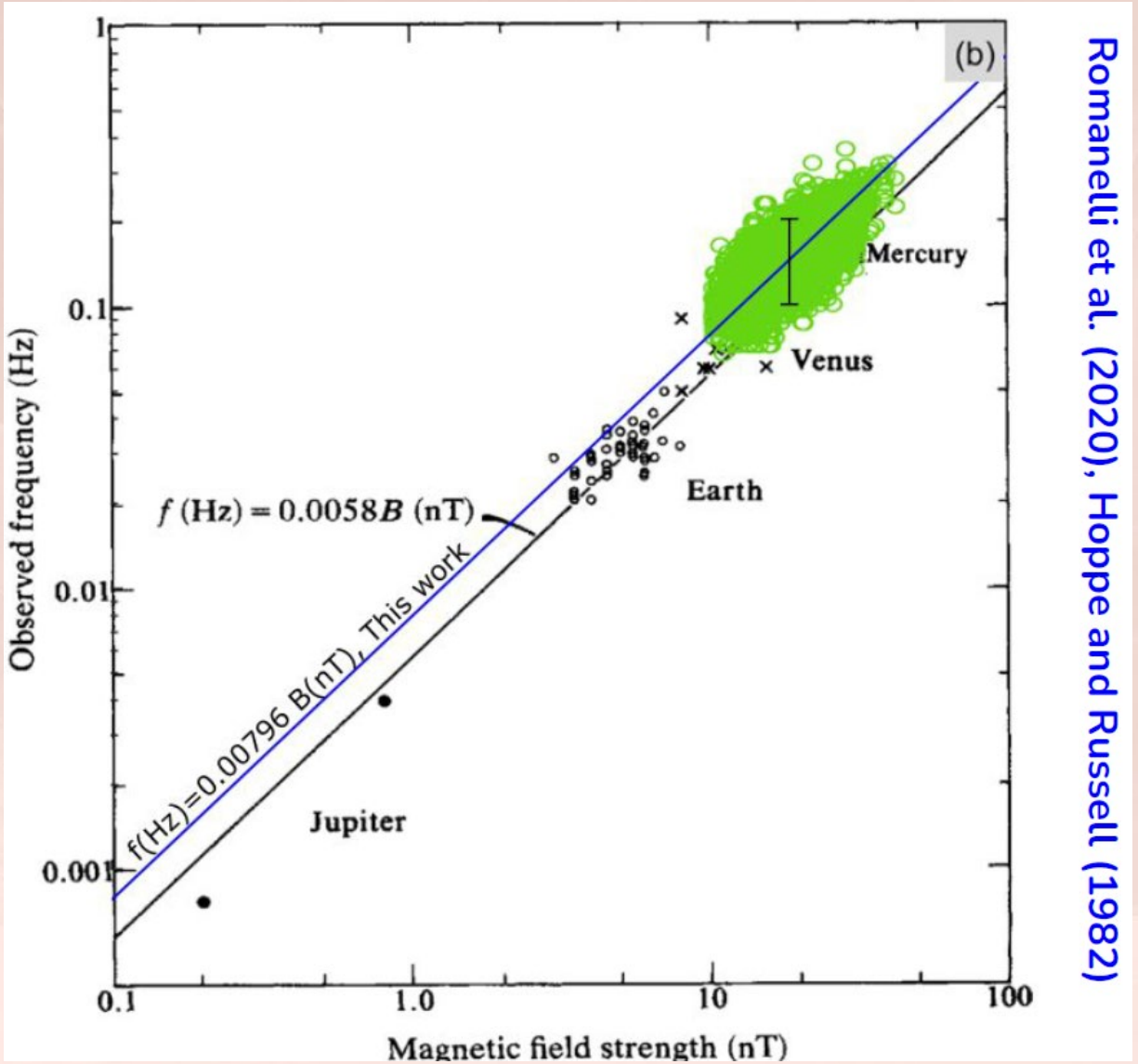

ULF Foreshock waves are present at Mars

One case study times series and PSD:

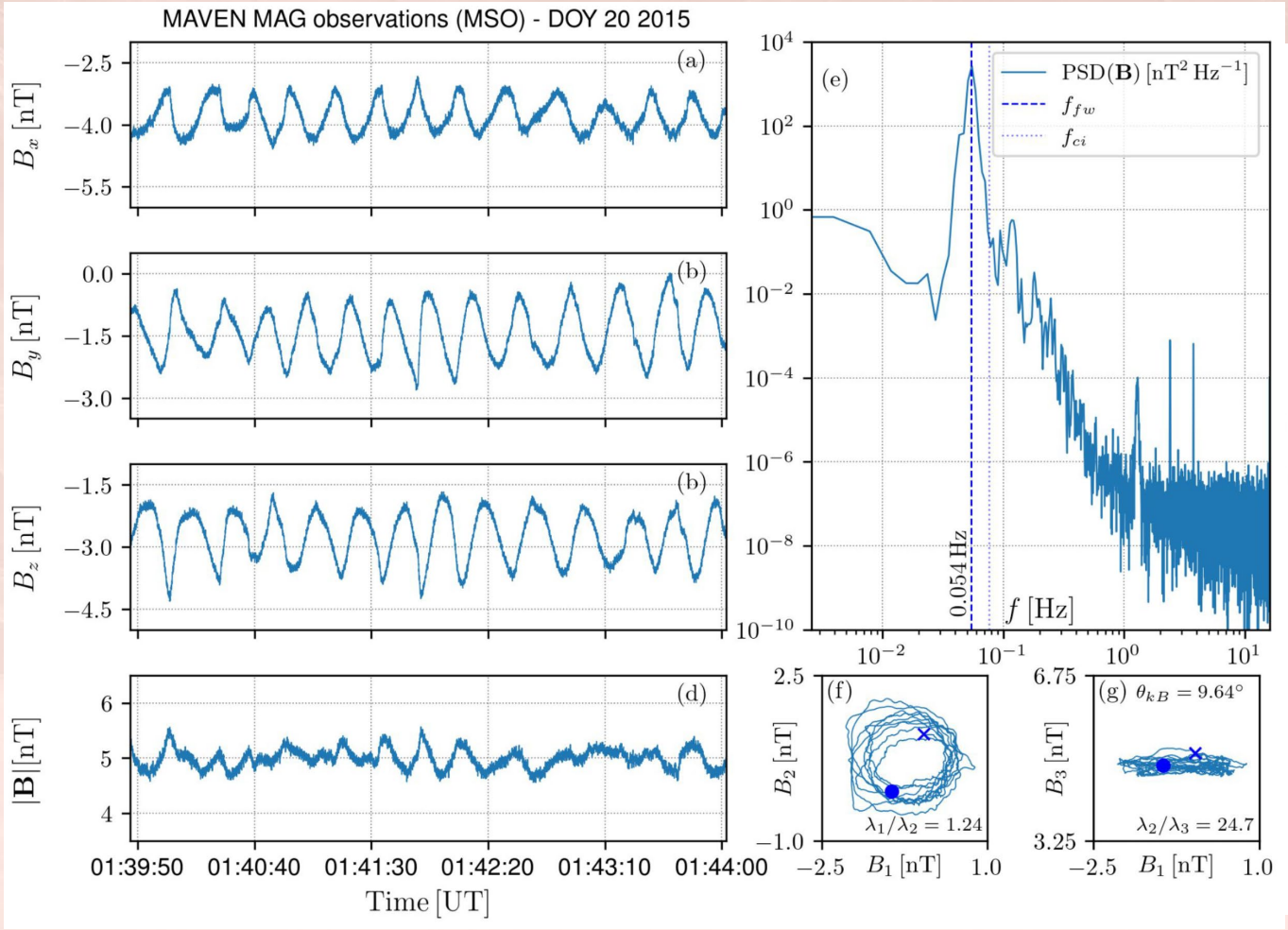

Statistics: All upstream waves:

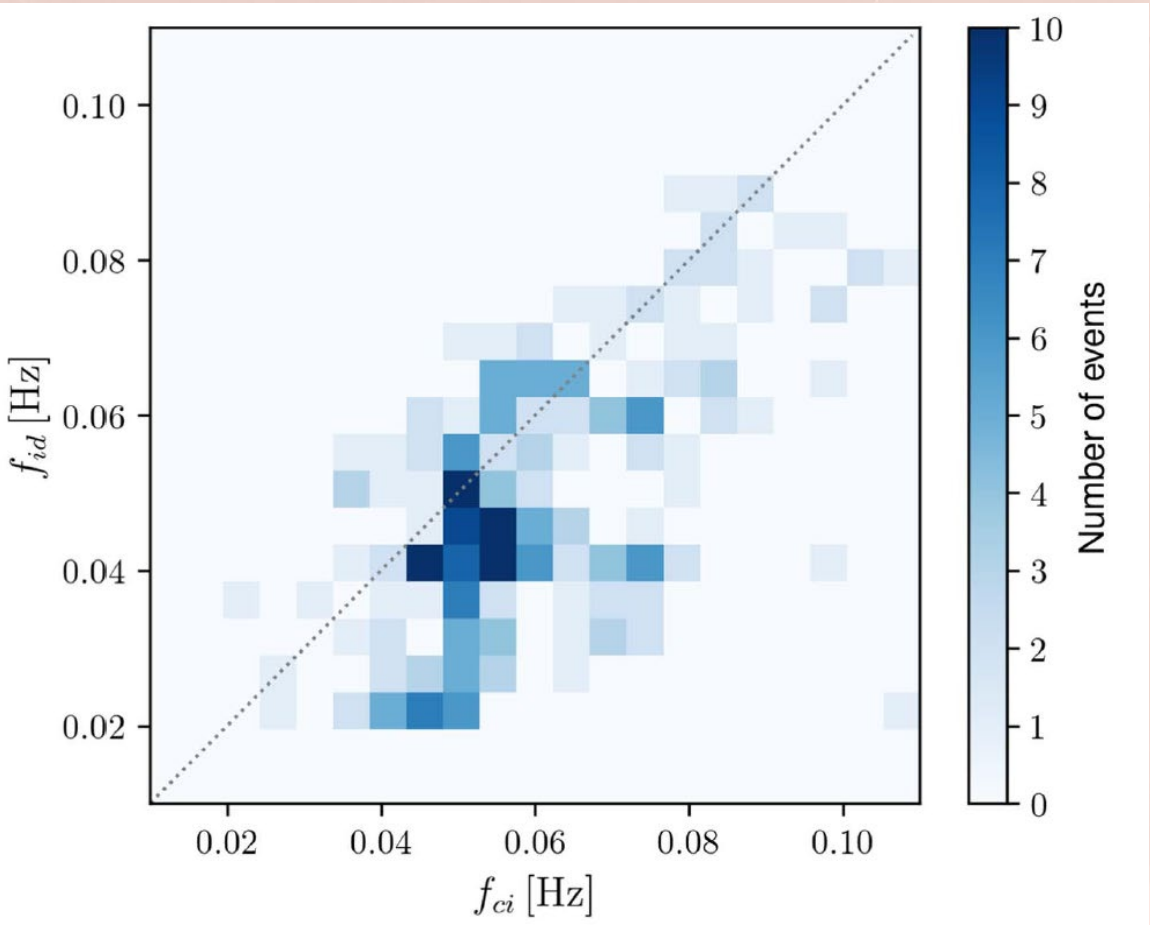

Andrés, Romanelli, Mazelle+, ApJ, 2025

ULF Foreshock waves are present at Mars

One case study times series and PSD:

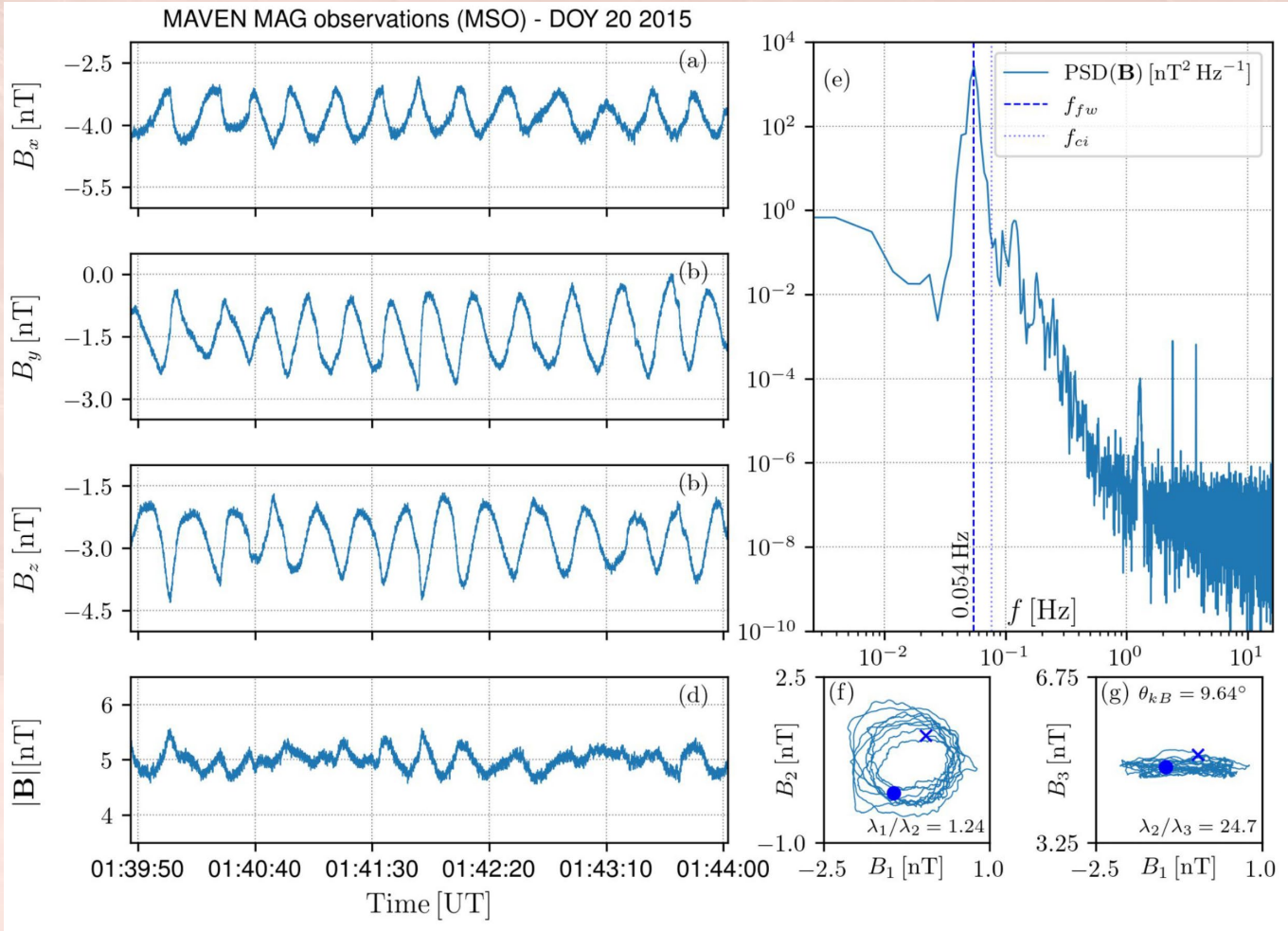

ULF Foreshock waves (removing PCWs):

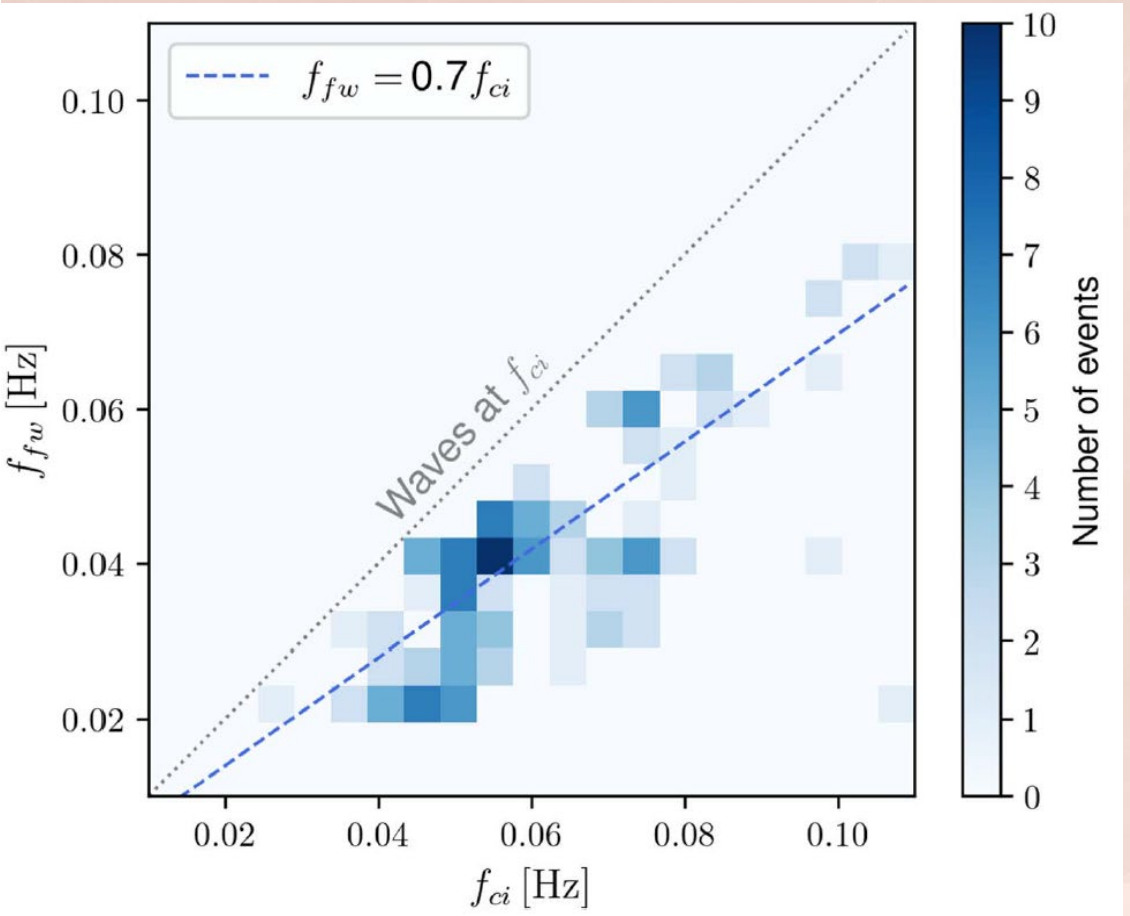

$f_{fw} = 0.5237 * f_{ci}$ Romanelli et al. (2020) Mercury

$f_{fw} = 0.6697 * f_{ci}$ Our work Mars

Andrés, Romanelli, Mazelle+, ApJ, 2025

ULF Foreshock waves are present at Mars

One case study times series and PSD:

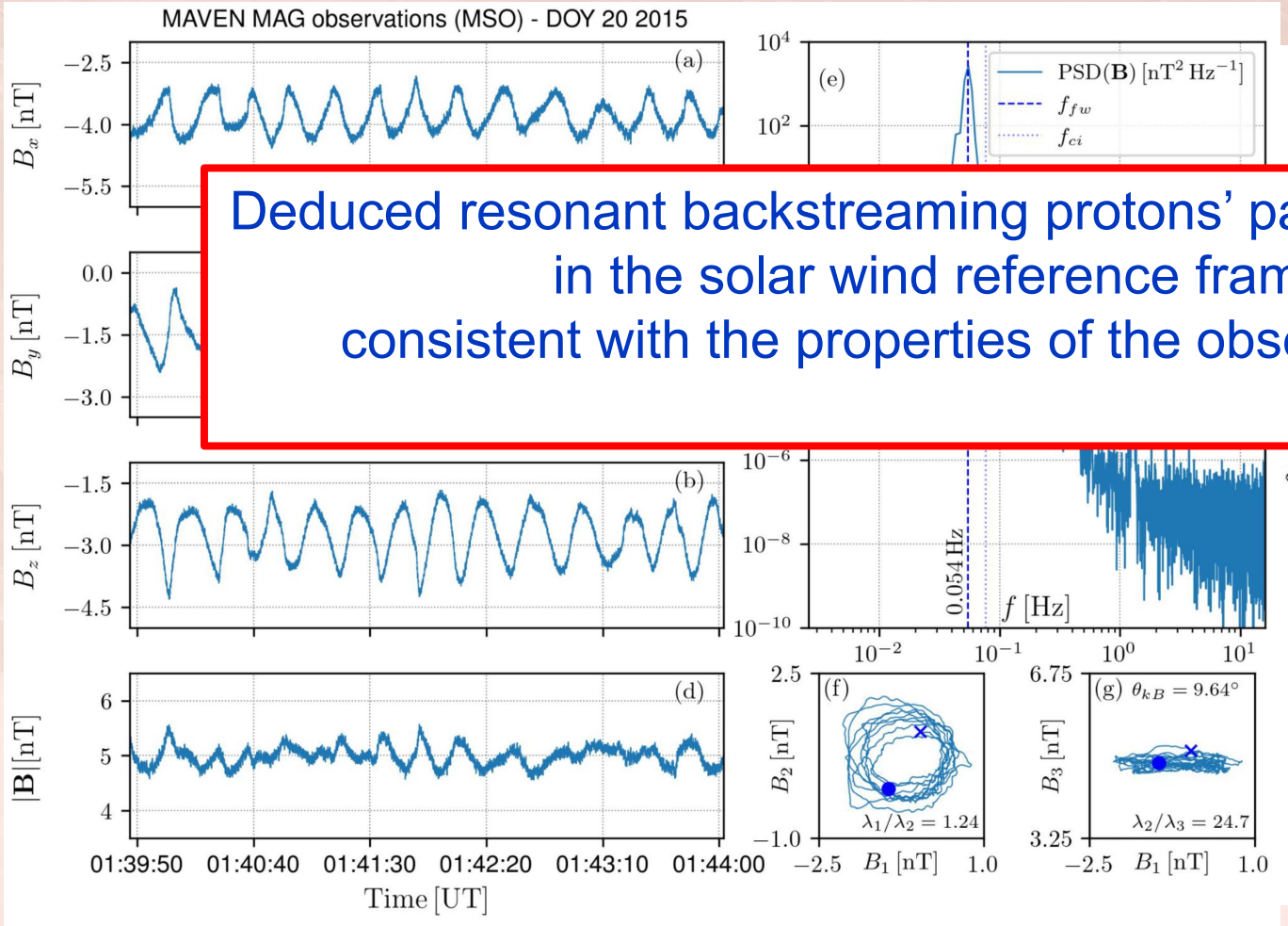

Deduced resonant backstreaming protons' parallel velocities
in the solar wind reference frame
consistent with the properties of the observed FABs

ULF Foreshock waves (removing PCWs):

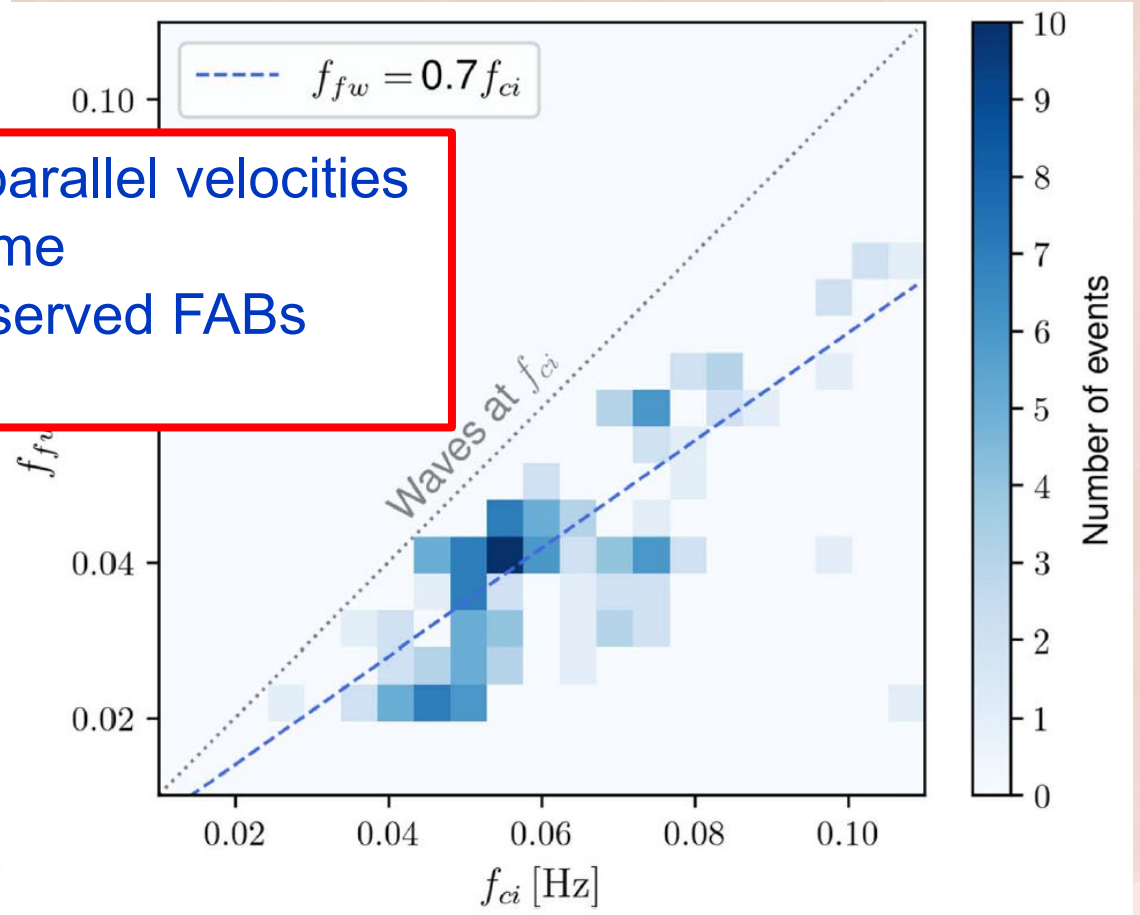

f_{fw} = 0.5237*f_{ci} Romanelli et al. (2020) Mercury

f_{fw} = 0.6697*f_{ci} Our work Mars

Andrés, Romanelli, Mazelle+, ApJ, 2025

Electron Acceleration at Qperp Shocks

- Fast Fermi by mirror reflection [Wu, 1984; Leroy and Mangeney, 1984]
- Highest energies (but lowest efficiency) at close to perpendicular

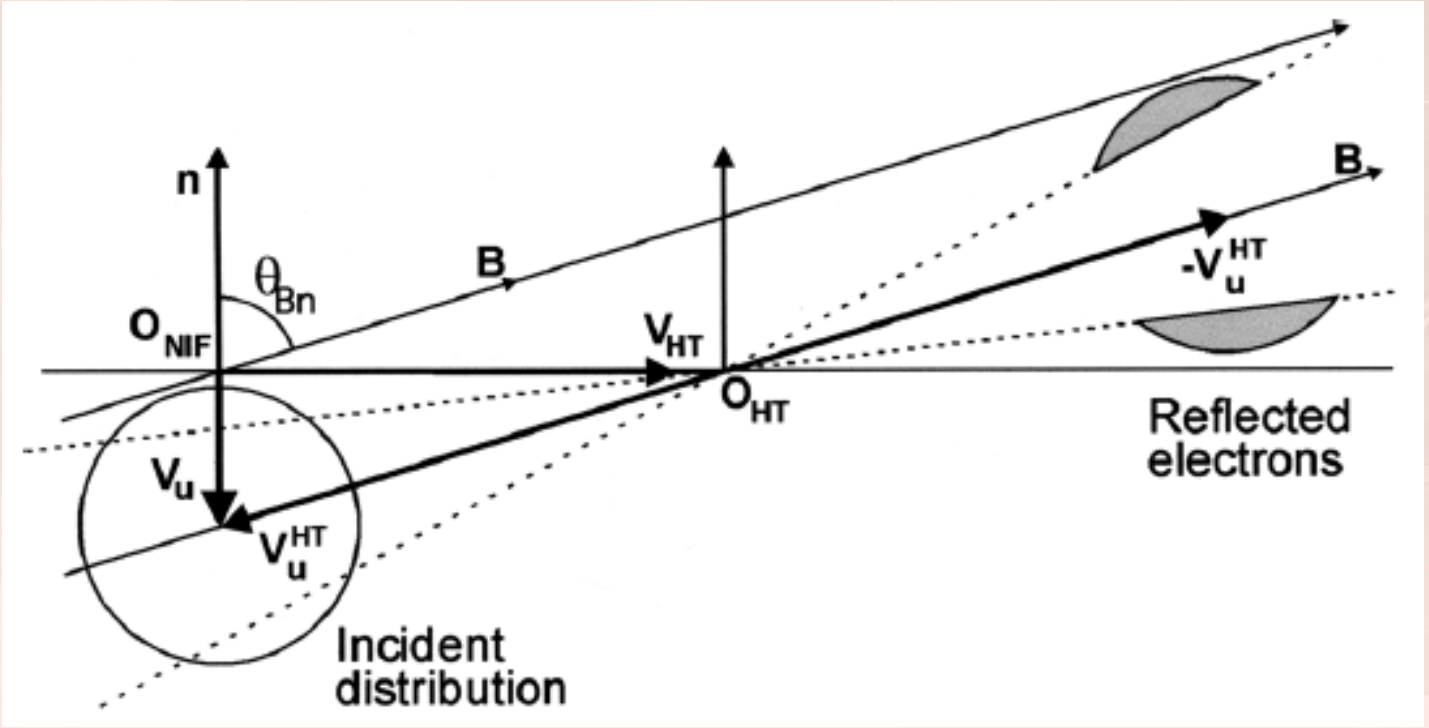

MAVEN reveals the unusual properties of Martian electron foreshock populations

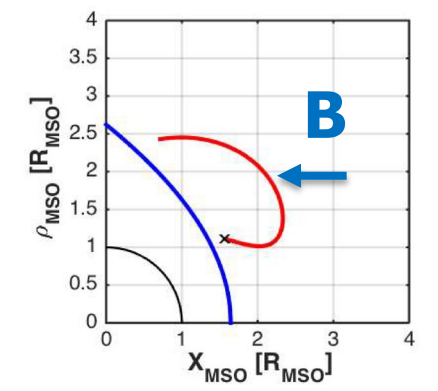

IMF ~ radial

Population 1:
Backstreaming e⁻
observed **from Q-// to Q-⊥**
~20 to 90°
Totally different from the terrestrial case: only ~90°

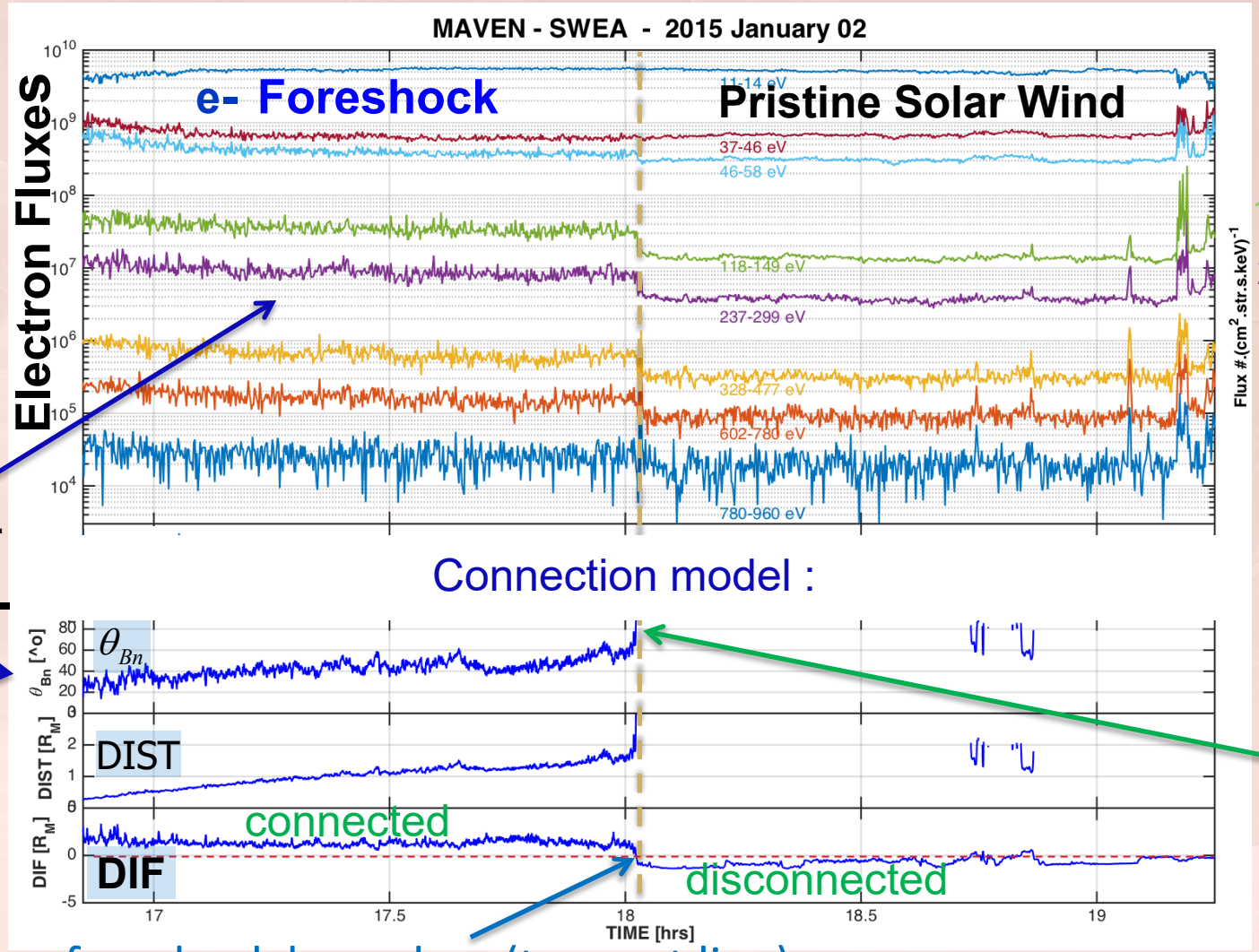

after Meziane, Mazelle +, 2017

MAVEN reveals the unusual properties of Martian electron foreshock populations

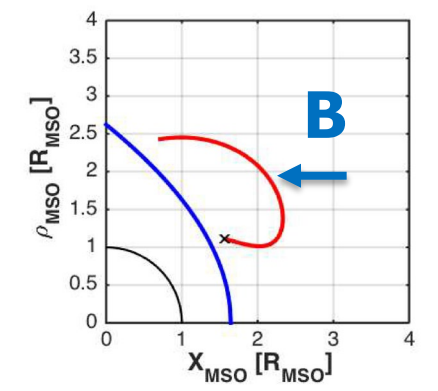

IMF ~ radial

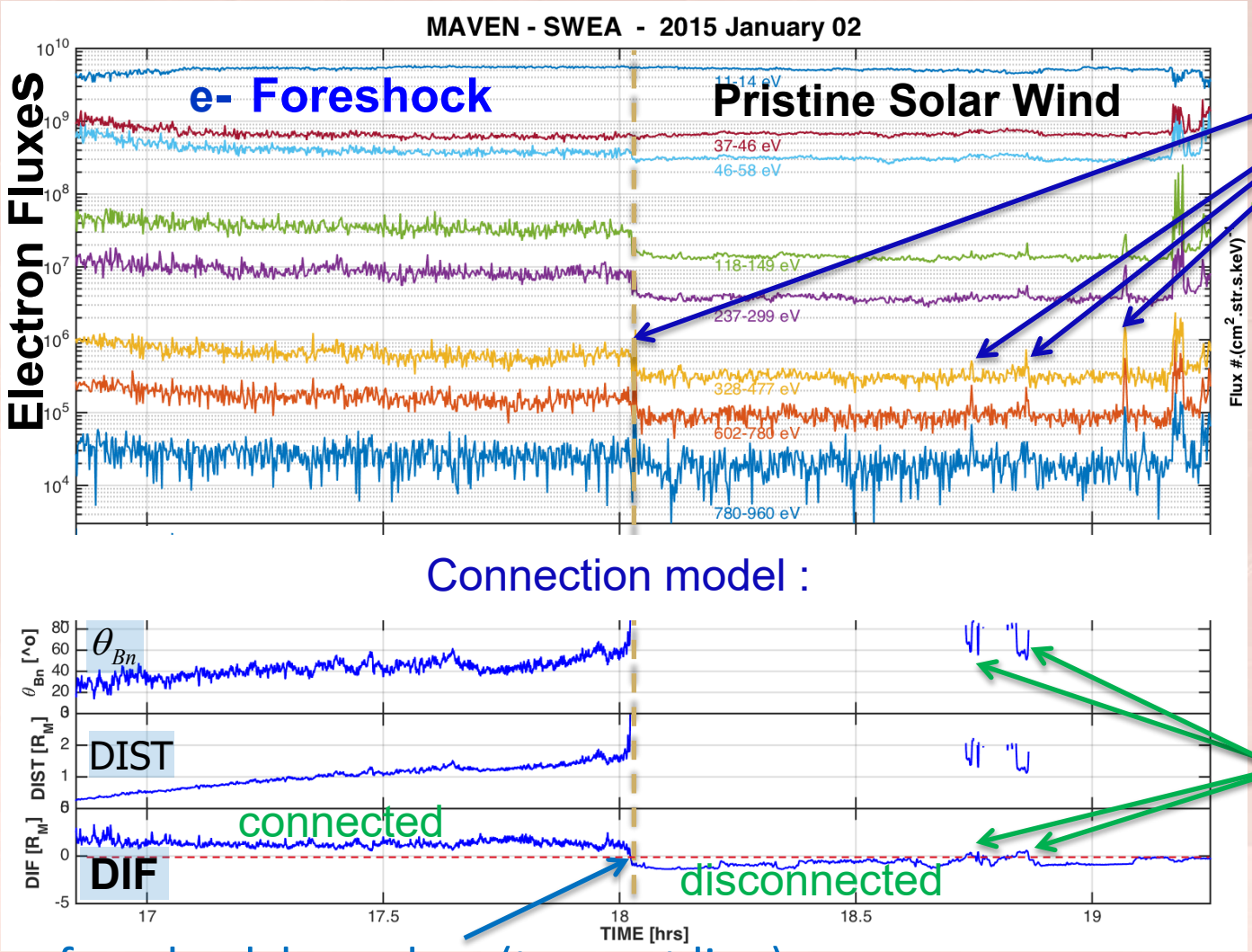

12 eV
42 eV
52 eV
132 eV
266 eV
396 eV
685 eV
865 eV

Population 2: High energy Electron Spikes

Sporadic connections with θ_{Bn} ~ 90 deg.

Electron foreshock boundary (tangent line)

after Meziane, Mazelle +, 2017

e^- spikes are produced by Fast Fermi accel.

Meziane, Mazelle +, 2019

Isolated Spikes

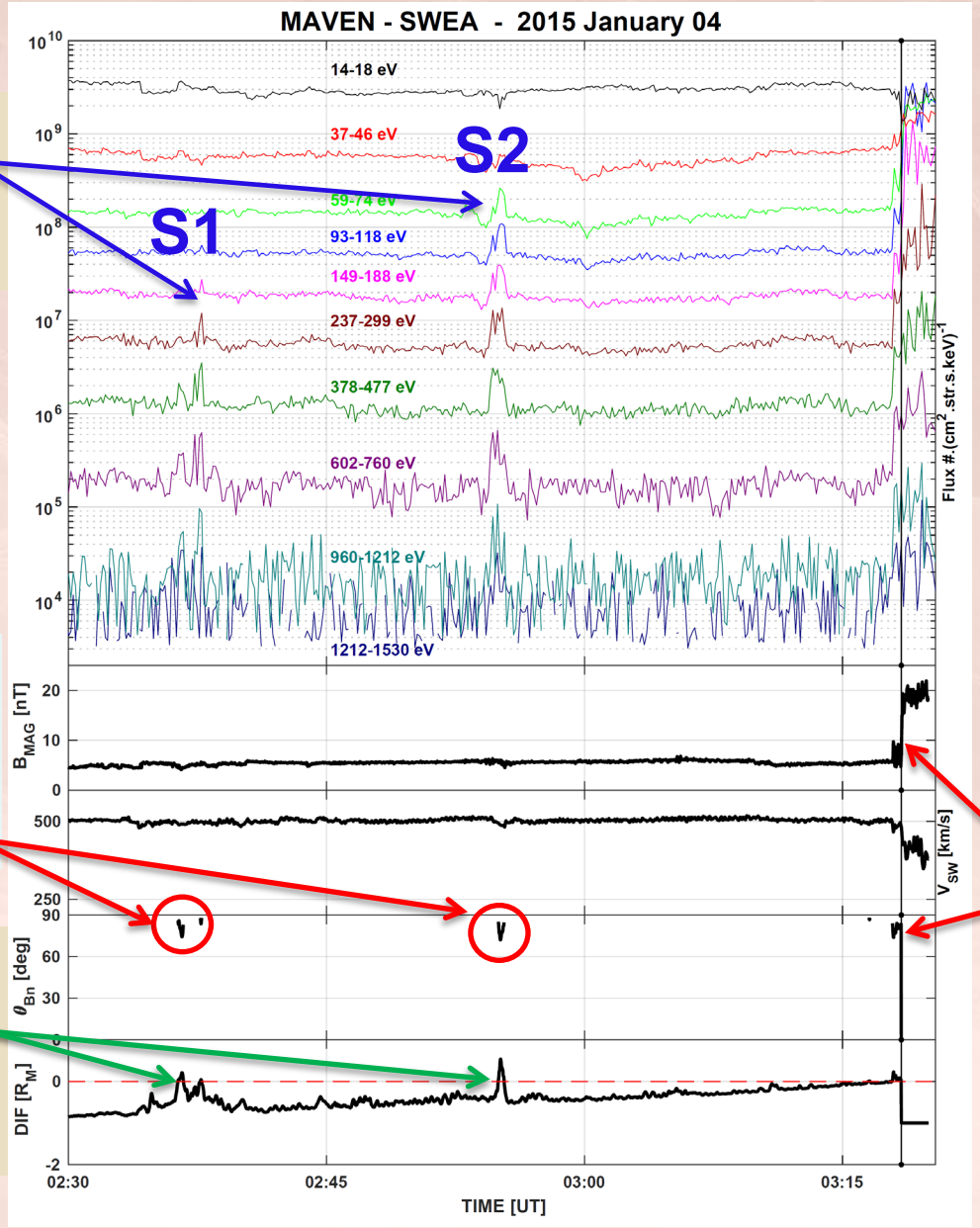

θ_{Bn} close to 90 deg.

Sporadic Connection (DIF > 0)

Nearly Perpendicular Shock

e^- spikes are produced by Fast Fermi accel.

Meziane, Mazelle +, 2019

Isolated Spikes

θ_{Bn} close to 90 deg.

Sporadic Connection (DIF > 0)

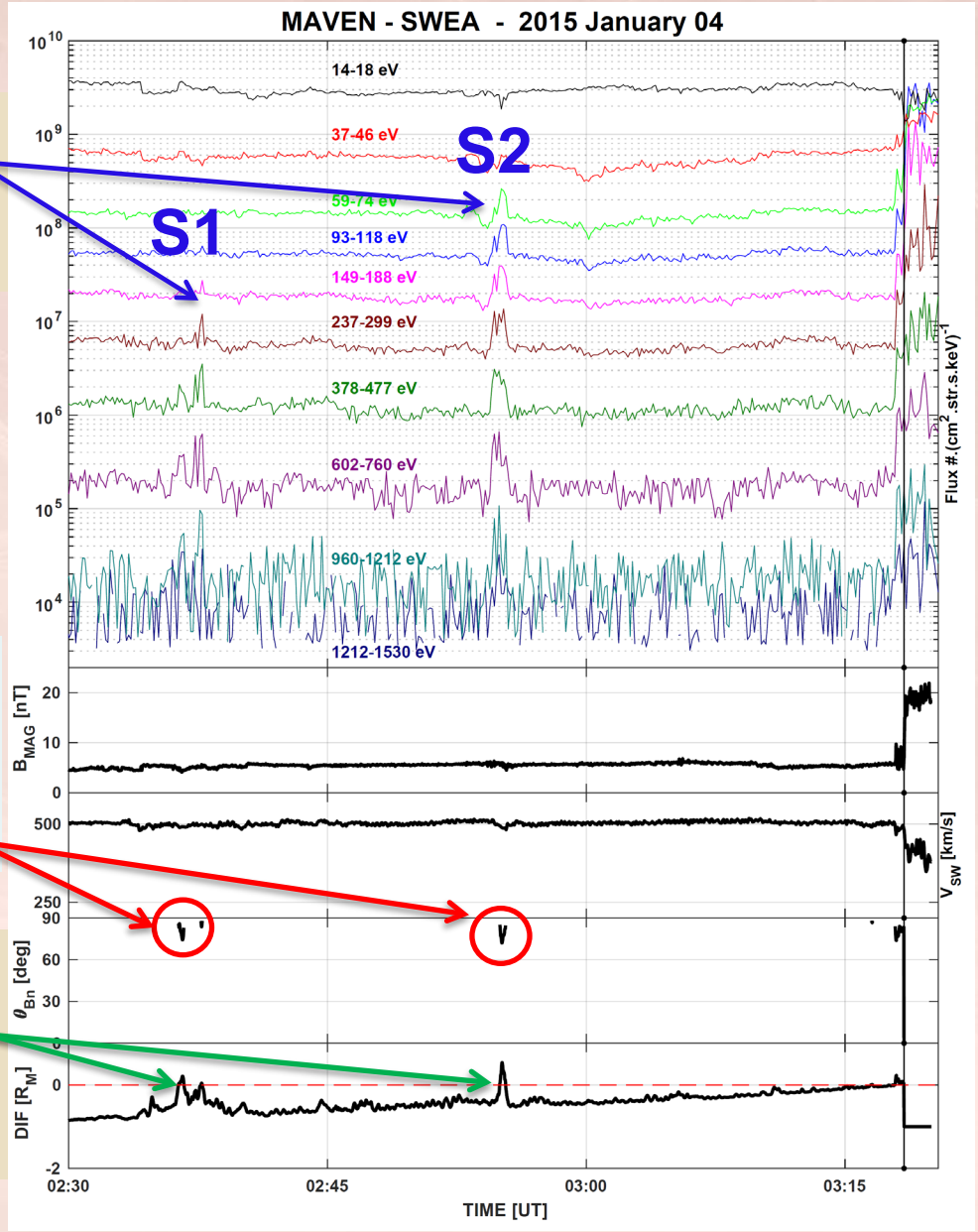

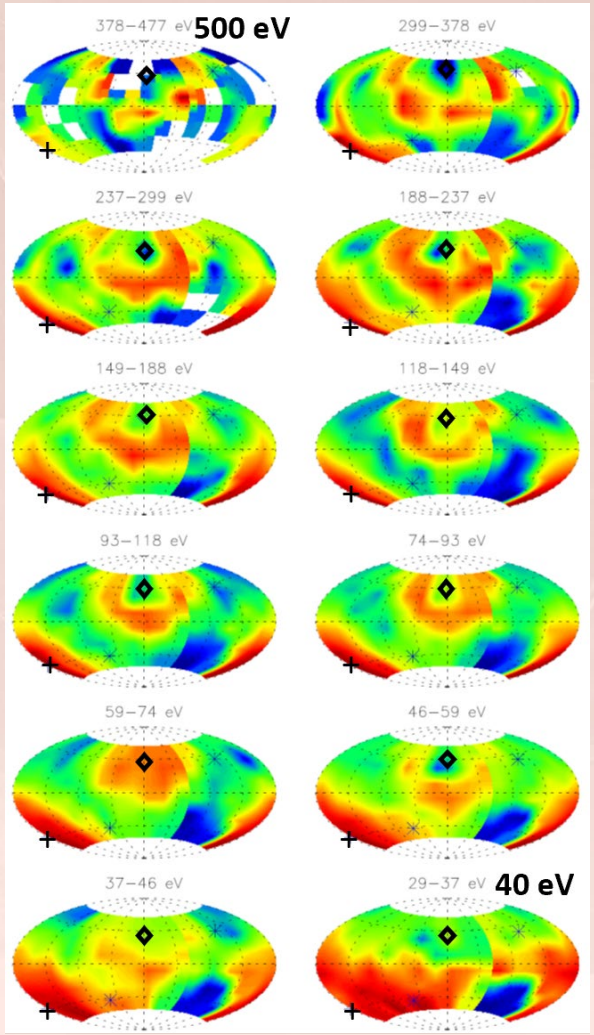

Analysis from the 3-D and pitch-angle distributions (loss cones).

Particle gains a large energy by a single reflection (adiabatic magnetic mirror) [Leroy & Mangeney, 1984; Wu, 1984]

First evidence for another planet than Earth

Wrap up

- The problem of shocks is multi-scale and needs multi-point observations.
- Shocks display universal mechanisms such as particle acceleration and dissipation at the kinetic scale.
- Most effort made on the ion dynamics up to now: need for better understanding of electron acceleration and heating.

BACKUP slides

Dispersion: creation of lower scales

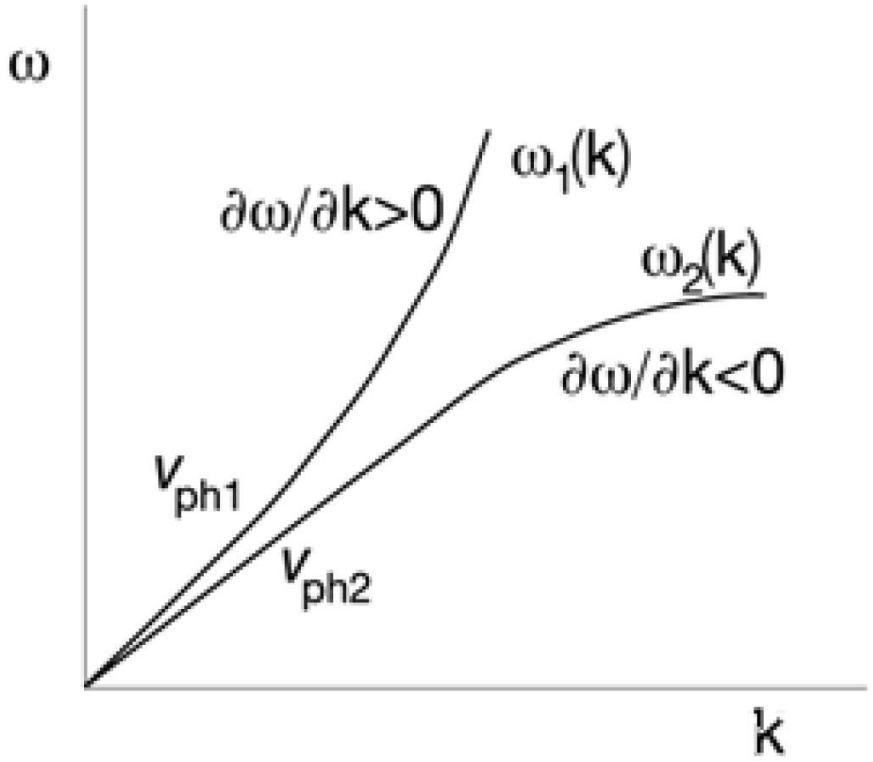

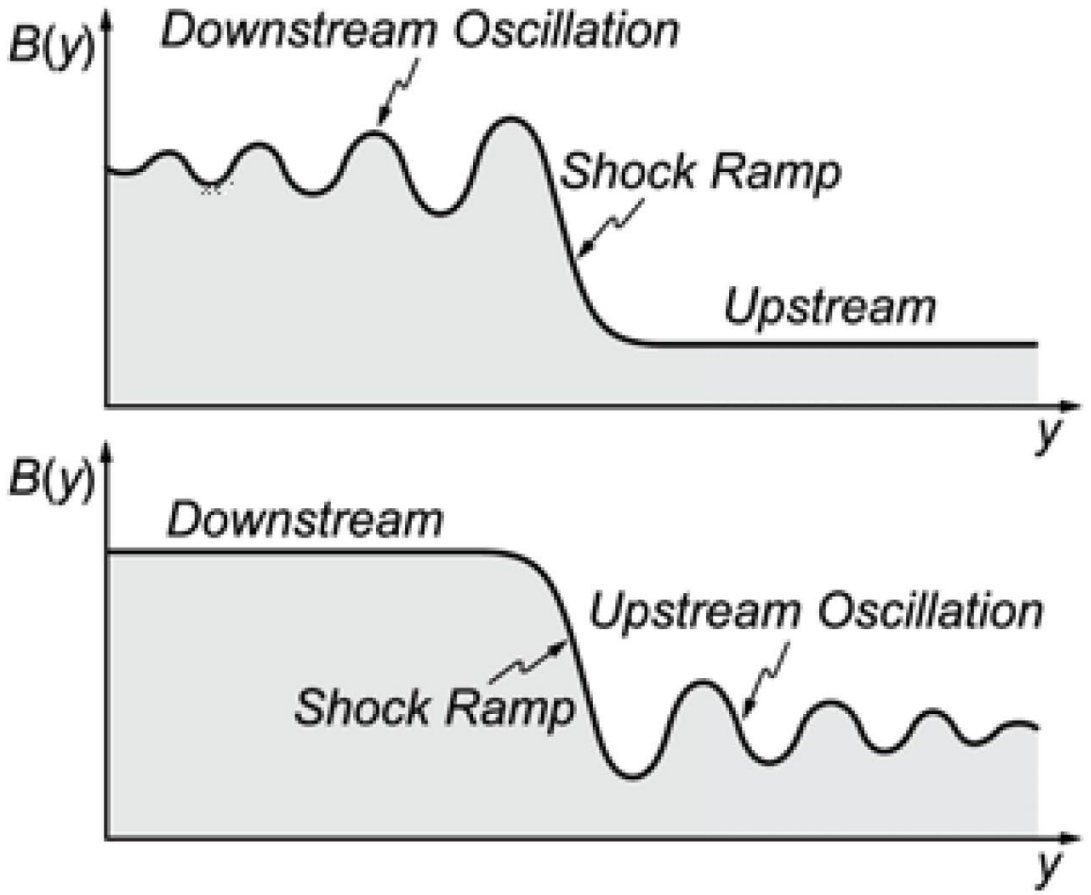

Rankine-Hugoniot jump conditions (MHD)

From integration of MHD eqs.

$$\nabla X \rightarrow \hat{\mathbf{n}}\frac{\partial}{\partial n} \rightarrow \hat{\mathbf{n}}\frac{[X]}{\delta}$$

$$[X] = X_2 - X_1$$

δ is the shock width

$$\hat{\mathbf{n}} \cdot [n\mathbf{v}] = 0,$$

$$\hat{\mathbf{n}} \cdot [nm\mathbf{v}\mathbf{v}] + \hat{\mathbf{n}}\left[p + \frac{B^2}{2\mu_0}\right] - \frac{\hat{\mathbf{n}} \cdot [\mathbf{B}\mathbf{B}]}{\mu_0} = 0,$$

$$\hat{\mathbf{n}} \times [\mathbf{v} \times \mathbf{B}] = 0,$$

$$\hat{\mathbf{n}} \cdot [\mathbf{B}] = 0,$$

$$nm\hat{\mathbf{n}} \cdot \mathbf{v}\left[\frac{v^2}{2} + w + \frac{1}{nm}\left(p + \frac{B^2}{\mu_0}\right)\right] - \frac{1}{\mu_0}(\mathbf{v} \cdot \mathbf{B})\,\hat{\mathbf{n}} \cdot \mathbf{B} = 0.$$

Just conservation laws between the upstream and downstream states.
The shock is simply a black box here. No structure. No particles.

Kinetic approach: Maxwell-Vlasov theory

Evolution of the velocity distribution function (vdf) of species ‘s’

$$\frac{\partial f_s}{\partial t} + \mathbf{v}\cdot\nabla f_s + \frac{e_s}{m_s}(\mathbf{E} + \mathbf{v}\times\mathbf{B})\cdot\nabla_{\mathbf{v}} f_s = 0$$

+ Maxwell equations

$$\mathbf{j} = \sum_s e_s \int \mathbf{v} f_s d\mathbf{v} \qquad \rho = \sum_s e_s \int f_s d\mathbf{v} \qquad f_s = f_{s0} + \delta f_s \qquad f_{s0} = \langle f_s \rangle \qquad \langle \delta f_s \rangle = 0$$

Linear theory: micro-instabilities + N.L. evolution

anomalous collision frequency $\nu \simeq \frac{W_{sat}}{NT_e}\omega_{pe}$

W_{sat}: Enery wave at saturation

The wave-particle interactions plays the role of collisions.

Fermi acceleration at shocks: 1st order (or DSA)

Diffusive shock acceleration

Shocks: convergent flows with frozen-in magnetic turbulence.
Gain by cycles on both sides of the shock.

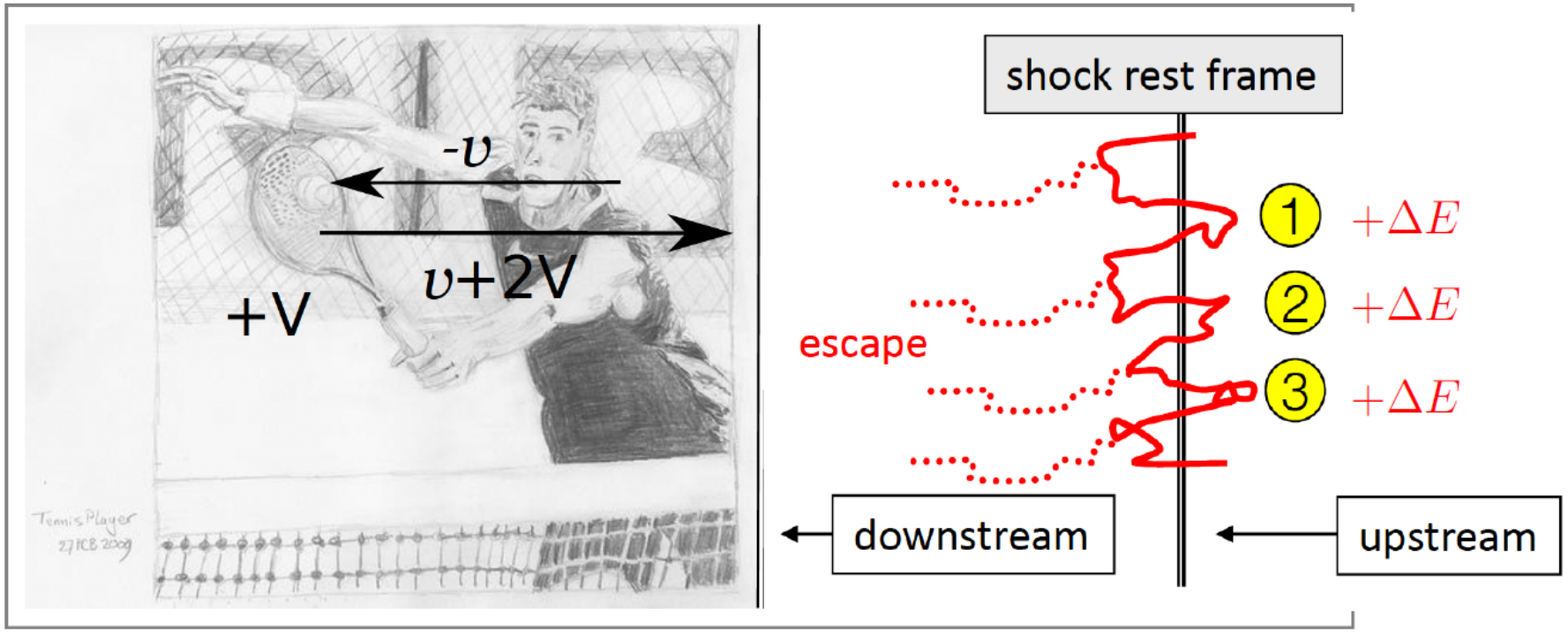

Credits: M. Lemoine

Mostly for quasi-parallel shocks

Acceleration mechanisms for Q-perp shocks

1. shock drift acceleration (SDA)

shock rest frame

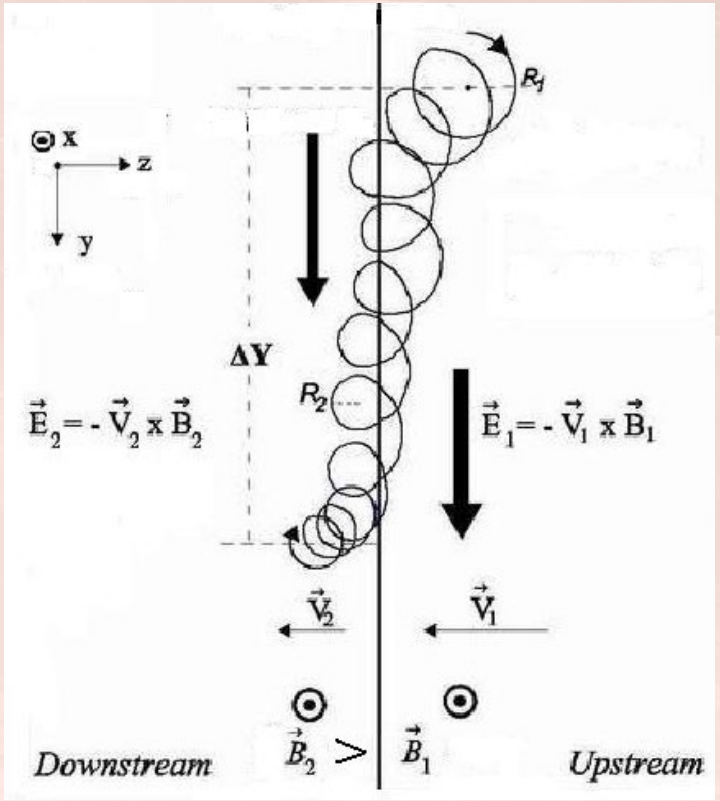

Definition: Zank, 1996

$m d\mathbf{v}/dt = e(\cancel{\mathbf{E}} + \mathbf{v} \times \mathbf{B}/c)$

Shapiro and Ucer, 2003; Lever et al. 2001; Yang et al. 2009

Webb et al. 1982; Decker, 1988; etc.

2. shock surfing acceleration (SSA)

shock rest frame

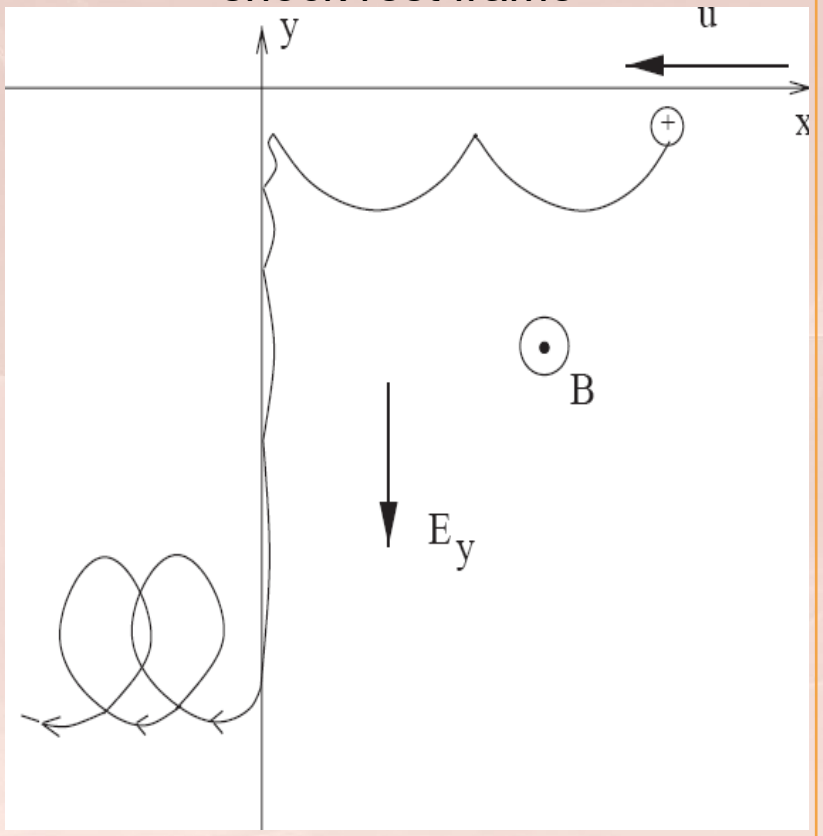

Definition:

$m d\mathbf{v}/dt = e(\mathbf{E} + \mathbf{v} \times \mathbf{B}/c)$

Shapiro and Ucer, 2003; Lever et al. 2001; Yang et al. 2009

Lee et al. 1996; Zank et al. 1996; Shapiro & Ucer, 2003

Fast Fermi Acceleration

In the case of an **adiabatic magnetic mirror reflection** of a particle off the shock, the reflected distribution is peaked at a pitch-angle α_C **in dHT frame of reference if NO cross shock potential :**

(no motional Electric field: energy conserved)

$$cos\alpha_C = \sqrt{1 - \frac{1}{N}}$$ where $N = B_2/B_1 = B_{down}/B_{ups}$ shock compression ratio $\mathbf{V}_{dHT} = \mathbf{n}\times(\mathbf{V}_{SW}\times\mathbf{B}_1)/\mathbf{B}_1\cdot\mathbf{n}$

In the plasma rest frame of reference if NO cross shock potential $\Delta\Phi$ = 0:

$$cos\alpha_C = \left(\frac{1}{N}\right)\left(\eta + \sqrt{(N-1)(N-\eta^2)}\right)$$ [Decker, 1983]

where $\eta^2 = E_S/E$ (<1) **Energy-dependent**

E = particle energy (in the plasma rest frame)

E_S (energy corresponding to shock speed or **dHT** velocity with respect to the plasma frame):

$$\mathbf{V}_S = \mathbf{V}_{SW} - \mathbf{V}_{dHT} \qquad V_S = V_{SW} \times \cos\theta_{Vn} / \cos\theta_{Bn}$$

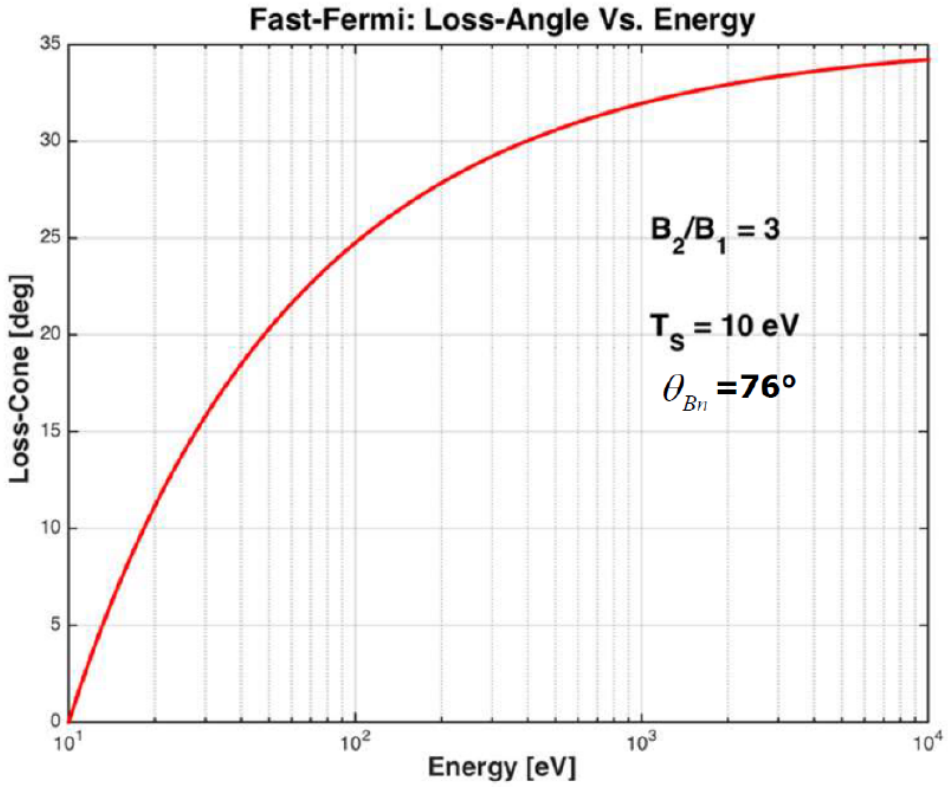

Fast Fermi Acceleration

Wu,1984; Leroy & Mangeney,1984

In the case of an adiabatic magnetic mirror reflection of a particle off the shock, the reflected particle gets a parallel velocity $v_{//r} = -v_{//i}$ **in dHT frame of reference** while the perpendicular velocity $v_{\perp}$ remains unchanged ('elastic encounter') by conservation of the magnetic moment:

$$\mathbf{V}_{dHT} = \mathbf{n}\times(\mathbf{V}_{SW}\times\mathbf{B}_1)/\mathbf{B}_1\cdot\mathbf{n}$$

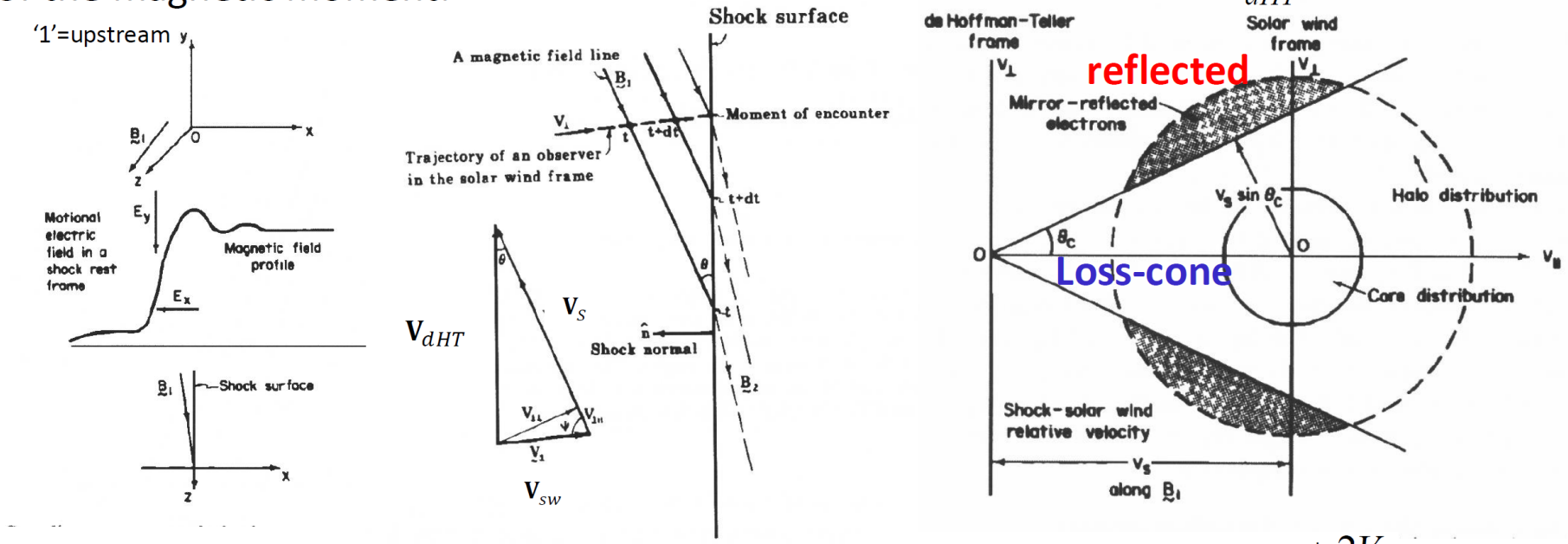

In the plasma rest frame, the particle gets a parallel velocity $v_{//r} = -v_{//i} + 2V_S$

where V_S is the 'shock speed' such as $\mathbf{V}_S = \mathbf{V}_{SW} - \mathbf{V}_{dHT}$ or $V_S = V_{SW} \times \cos\theta_{Vn} / \cos\theta_{Bn}$

➡ **For large θ_{Bn} the particle can gain a large energy by a single reflection:**

Fast Fermi Acceleration

Reformation of an oblique shock observed by Cluster:

[Lefebvre *et al.*, 2009]

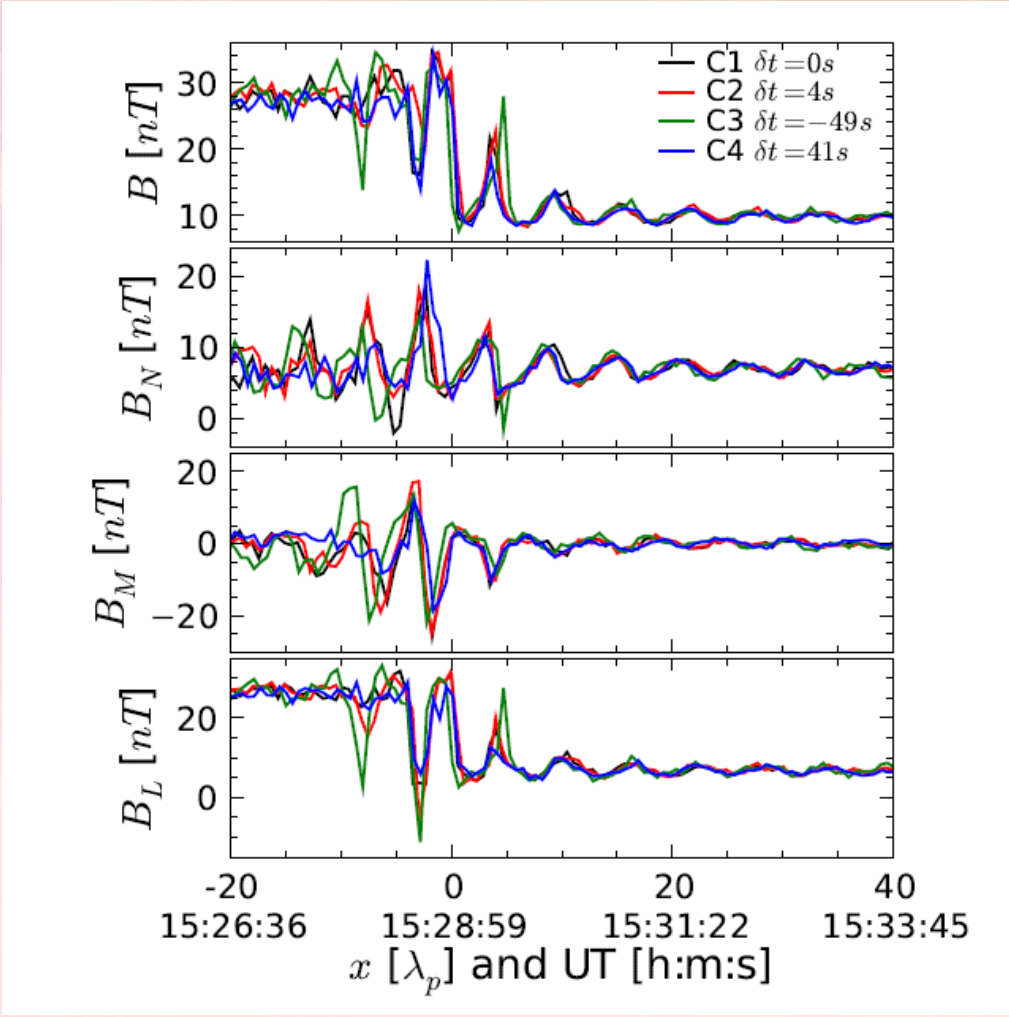

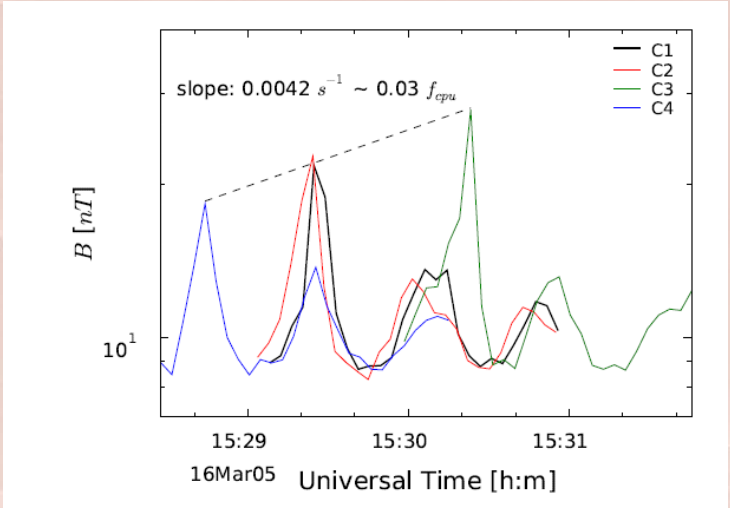

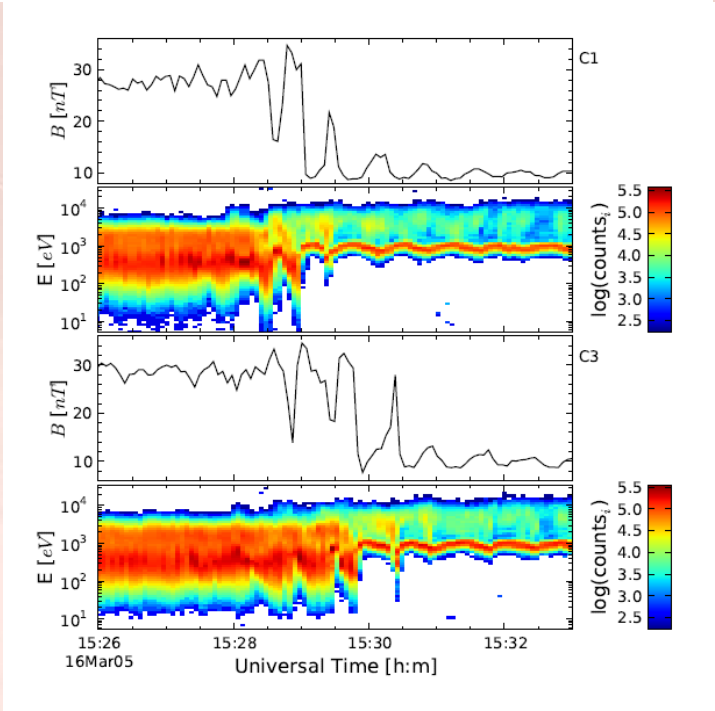

$\theta_{Bn} = 47°$

M_A=5.5